Second Order Sliding Modes: Theory and Applications

PHD Thesis

Author: Alessandro PISANO

Advisor: Prof. Giorgio BARTOLINI

Dipartimento di Ingegneria Elettrica ed Elettronica (DIEE)
Universitá degli Studi di Cagliari

December 2000

INDEX

Ai miei Genitori

A Irene

Acknowledgements

This work contains some results attained during my PhD (from 1998 to 2000) at the Department of Electrical and Electronic Engineering (DIEE) of the University of Cagliari.

The research presented here would not have been possible without the unvaluable support and teachings of Giorgio Bartolini, the advisor of the present work, and Elio Usai, co-worker and co-advisor.

I own an immense debt of gratitude to Giorgio Bartolini, for having given me the curiosity, that later became passion, about research in Automatic Control, and for being advisor and good friend at the same time.

Thesis' overview

In the Introduction, some motivations for the sliding mode approach are discussed to state the framework within which this work is developed.

This thesis is divided in two fundamental parts, namely, the **Part I**, in which the theoretical background of the second-order sliding mode approach is discussed, and a collection of algorithms is presented, and the **Part II**, where some important applicative problems are addressed and solved by means of the proposed approaches.

More specifically, as for the Part I, in *Chapter 1* the fundamentals regarding the variable structure control approach are recalled. In the subsequent *Chapter 2* the attention is focused on the second order sliding mode (2-sliding) approach, and its main features are described. *Chapter 3* the so-called "sub-optimal 2-sliding algorithm" is presented in its original formulation, and a novel continuous-time version, enjoying some better properties, is proposed. *Chapter 4* refers to the problem of the discrete-time implementation of 2-sliding control, while in *Chapter 5* a new 2-sliding control algorithm is proposed, which enjoys global convergence features similar to those of the conventional first-order sliding mode approach.

In the Part II the control problems of robotic manipulators, induction motors and overhead container cranes are addressed and solved, using the 2-sliding mode approach, in *Chapters 6, 7 and 8* respectively.

Introduction and Motivations

In recent years the availability of powerful low-cost microprocessors has made actually implementable complex, and very efficient, nonlinear control strategies.

In particular, motivated by a large amount of important practical problems, the control of uncertain nonlinear systems has become an important subject of research. As a result, considerable progresses in nonlinear robust control techniques, such as nonlinear adaptive control, geometric-approach based control, backstepping, sliding mode control and others, that explicitly account for an imprecise description of the model of the controlled plant, guaranteeing the attainment of the relevant control objectives in the face of modeling error and/or parameter uncertainties, have been attained.

Sliding mode control is generally recognized as very robust and simple to implement, but the so-called " chattering phenomenon" (the effects of the discontinuous nature of the control), and the high control activity, have originated a certain skepticism about such an approach.

This work analyzes a quite recent development of sliding mode control, namely the second order sliding mode approach, which is encountering a growing attention in the control research community.

The objective of this thesis is to survey the theoretical background of the second order sliding mode control, mainly developed in the last years, to present some new results, and to show that the second order sliding mode approach, is an effective solution to the above-cited drawbacks, and may constitute a good candidate for solving a wide range of important practical problems.

Part I

Theory

1 Variable Structure Systems and Sliding Modes

1.1 Preliminaries

This work deals with a special class of systems, called "VARIABLE STRUCTURE SYSTEMS" (VSSs), that are of great importance in systems and control theory.

The concept of VSS, and its applications to the control theory, were originated mainly by the work of researchers from the former Russia, starting from the sixties [Emel'yanov and Taran '62, Emel'yanov ed '70, Utkin '78, Ytkis '92]. Nowadays, the VSS theory involves a wide research community, and it is one of the most promising control methodologies [Young et al. 1999, Young et al. 1999, Utkin '00].

In principle, VSSs can be represented by the parallel connection of several different continuous subsystems (called "STRUCTURES") that act one at a time in the input-output path (see Fig. 1). A certain switching logic schedules in time the relevant structures, that can be either controlled or autonomous plants.

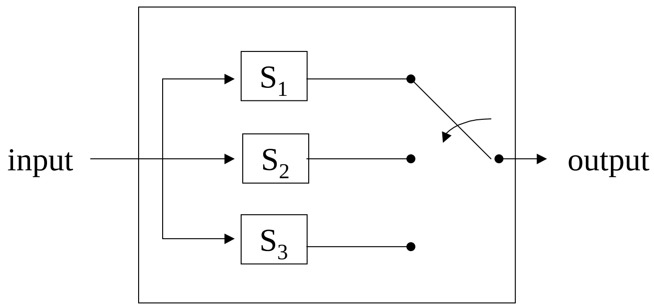

Figure 1: The representation of a controlled VSS.

A possible mathematical description of the VSSs in figure can be the following

$$\dot{x} = \begin{cases} 4x + u & if\ x \leq -3 \\ 3 + u & if\ -3 < x < 2 \\ -6x + u & if\ x \geq 2 \end{cases} \tag{1}$$

System (1) is the inter-connection between three linear structures ($\dot{x} = 4x + u$, $\dot{x} = 3 + u$, $\dot{x} = -6x + u$), while the overall system is, off course, a nonlinear one.

It must be evidenced that the interconnection between stable plants can produce either stable or unstable plants, depending on the actual switching logic [Utkin '92].

In the context of the control theory, VSSs derive generally from the implementation of a discontinuous feedback control. Consider, for example, the integrator system $\dot{x} = u$. Under the action of the discontinuous feedback $u = -sign(x)$, the closed-loop system is an autonomuos VSS (see fig. 2), and this is the type of VSSs we will generally encounter during this work.

Nevertheless, there are physical systems that are intrinsically VSSs. The most known paradigm given in the literature is the unforced mass-spring system in the presence of Coulomb friction, which is described by the differential equation

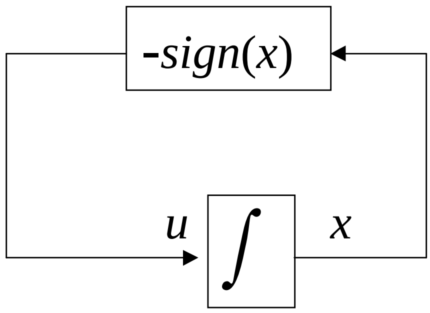

Figure 2: Integrator with discontinuous feedback.

$$m\ddot{x} + C_f(\dot{x}) + kx = 0 \tag{2}$$

where x is the displacement, m is the mass, k is the spring coefficient and $C_f(\dot{x})$ is the Coulomb friction term

$$C_f(\dot{x}) = \begin{cases} P_0 & if\ \dot{x} > 0 \\ -P_0 & if\ \dot{x} < 0 \end{cases} \tag{3}$$

P_0 being a positive constant. The friction term is *discontinuous across the manifold* $\dot{x} = 0$ (and also *undefined on the manifold*).

The reader is referred to [Utkin '92] for an analysis of the behaviour of such system, that points out the difficulty of describing the VSS's behaviour.

1.2 Sliding Modes, Invariance Principle and Order Reduction

A fundamental property of VSSs is that they often exhibit a peculiar behaviour (called "SLIDING MODE BEHAVIOUR" or "SLIDING MOTION"), characterized by the fact that the commutation between the different system structures takes place at infinite frequency.

From a geometrical point of view, this phenomenon occurs when the system trajectory converges towards the discontinuity surface on both its sides (see Fig. 3), where as "discontinuity surface" we mean the manifold across which the switching logic commutes between the system structures. The consequence is that the system state is constrained on the discontinuity surface, which is an *invariant set* after the sliding mode has been established.

Example 1.1

To clarify how the sliding mode behaviour can arise, consider system

$$\dot{x} = \begin{cases} 1 & if\ x \leq 0 \\ -1 & if\ x > 0 \end{cases} \tag{4}$$

Starting from a positive initial condition, the structure $\dot{x} = -1$ is first enabled, and x approaches zero until the discontinuity surface $x = 0$ is reached. The same is if the initial condition is

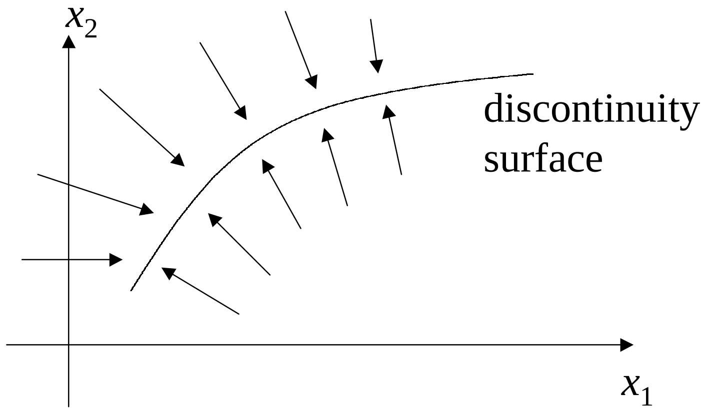

Figure 3: Attractiveness of the sliding manifold

negative. Once the point $x = 0$ is hitten, it is not difficult to see that as soon as x approaches 0^+, driven by the corresponding structure $\dot{x} = 1$, immediately the structure $\dot{x} = -1$ re-steer to zero the state, and this process is repeated infinitely fast for all the subsequent times.

Therefore, after the discontinuity point $x = 0$ has been reached, the two structures commute at infinite frequency, and the discontinuity surface $x = 0$ is an *invariant set* for the motion of the VSS. Such system is said to perform a *sliding mode on the manifold* $x = 0$.

The reader can verify by simulation that the sliding motion exhibited by the system (4) is robust against additive and multiplicative disturbances acting in the control channel. Referring to perturbations as in Fig. 4, the sliding mode is maintained if the exogenous disturbances Δ_a and Δ_m are s.t. $\Delta_m(t) > 0$, $|\Delta_a(t)/\Delta_m(t)| < 1$.

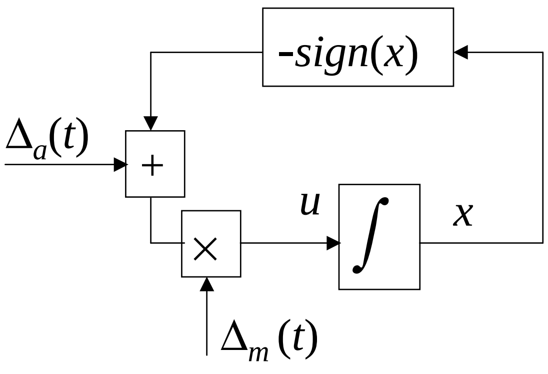

Figure 4: Robustness of VSS

The methodology generally referred as "SLIDING MODE CONTROL" (SMC) exploits for control purposes the properties of the sliding mode behaviour, which include *insensitivity to parameter variation* and complete *rejection of matched disturbances*.

The SMC approach consists of two steps:

The **first step** is the choice of a manifold in the state space such that, once the state trajectory is constrained on it, the controlled plant exhibits the desired performance.

The **second step** is represented by the design of a discontinuous state-feedback capable of forcing the system state to reach, in finite time, such a manifold (accordingly called "SLIDING MANIFOLD").

During the sliding motion, if the so-called "*invariance principle*" [Drazenovic '69], [Levant and Fridman '96] can be invoked, any system belonging to a certain set behaves in the same way (semigroup property). This motivates why this approach is well suited to deal with uncertain systems. In other words, different systems performing a sliding mode on the same manifold may exhibit the same behaviour, which depends only on the manifold on which the sliding mode occurs. In some sense, the sliding mode *erases* the original system's dynamics, and replace it with that proper of the sliding manifold.

Due to its robustness, variable structure controllers are always able to deal with classes of plants instead of specific systems. Unless other methodologies, in the context of SMC there is no 1-to-1 correspondence between controller and plant.

Moreover, another interesting peculiarity of the sliding mode behaviour is that, because of the geometrical constraint represented by the sliding manifold, **a system in sliding mode behaves as a system of reduced order respect to the original plant**.

To evidence such phenomena (invariance and order reduction) let us consider the following example

Example 1.1 - First part.

Consider the class of systems

$$\begin{cases} \dot{x}_1 = x_2 & \qquad a \in \Re \\ \dot{x}_2 = ax_2 + u \end{cases} \tag{5}$$

subjected to the discontinuous control

$$u = -\left[|(a+c)x_2| + k^2\right] sign(s) \qquad k \neq 0 \tag{6}$$

whose manifold of discontinuity is defined through the vanishing of the variable

$$s = x_2 + cx_1 \qquad c > 0 \tag{7}$$

where c and k are real coefficients.

By using the Lyapunov candidate function $V(s) = \frac{1}{2}s^2$, it is not difficult to show that the manifold $s = 0$ is an invariant set for system (5)-(7). Since the system dynamics is discontinuous across $s = 0$, a sliding mode behaviour on the manifold $s = 0$ turns out to be established.

The initial conditions are $x_1(0) = x_2(0) = 1$.

To evidence the invariance of the behaviour and the order reduction, let us compare the behaviour of two systems belonging to the class (5), setting $a = 1$ and $a = 3$ respectively. Both systems exhibit a transient phase while the sliding manifold is being approached (called the "*REACHING PHASE*"). During this phase the system behaviour depends on the dynamics of the controlled plant. On the contrary, after the sliding mode is established, the two system trajectories in the state plane coincide (see Fig. 5).

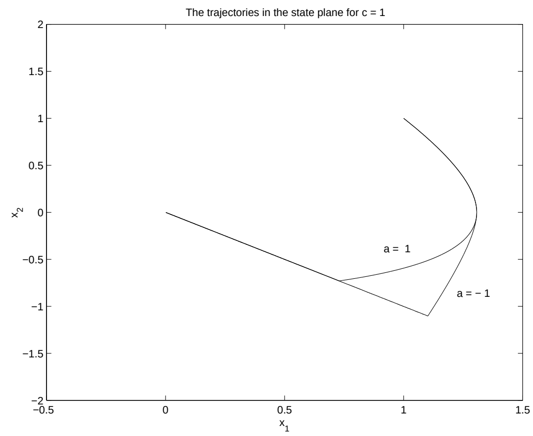

Figure 5: Example 1.2. Different systems ($a = 1$ and $a = -1$) with the same sliding manifold ($c = 1$). Phase-plane trajectories

Fig. 5 evidences the order reduction as well, since the straight line defined by the system trajectories correspond to the linear first-order system

$$\dot{x}_1 = -cx_1 \tag{8}$$

whose dynamics is defined through the equation of the sliding manifold $s = x_2 + cx_1 = 0$.

If we consider the system with $a = -1$, and we use two different values of c, the dependence of the sliding behavior from the actual sliding manifold is highlighted (see Fig. 6)

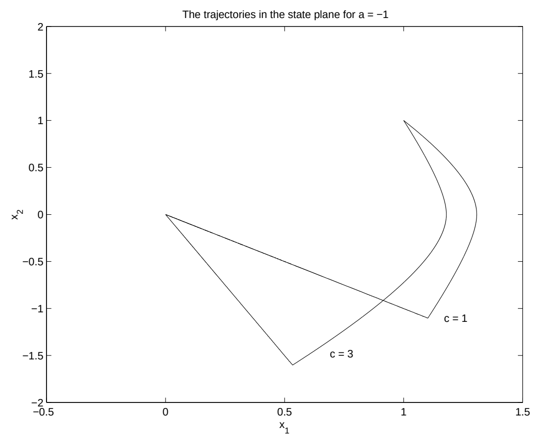

Figure 6: Example 1.2. The same system ($a = -1$) with different sliding manifolds ($c = 1$ and $c = 3$). Phase-plane trajectories

Whatever a and $c > 0$ are, the state converge asymptotically to the origin of the state plane with a linear stable dynamics assigned from the actual sliding manifold (see Fig. 7)

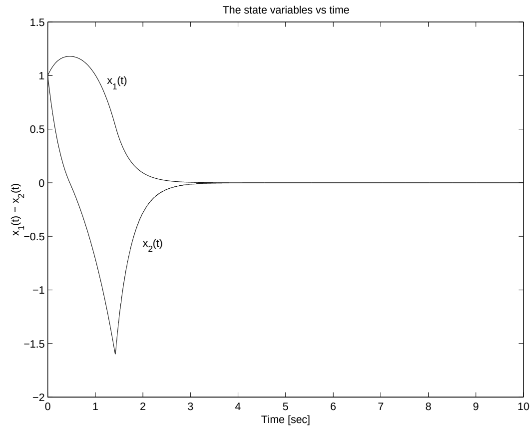

Figure 7: Example 1.2. The state trajectories vs time for $a = -1$, $c = 3$ and $k^2 = 1$

The robust convergence to zero of the state vector components encountered has not a general validity, and it is due, in the above example, to the chain-of-integrators normal form of system (5)-(7). More general classes of systems, even in sliding mode on the same manifold, could be unstable. The reader can easily verify through simulation that the system

$$\begin{cases} \dot{x}_1 = x_2 + b x_1^2 \\ \dot{x}_2 = a x_2 + u \end{cases} \qquad a, b \in \Re \tag{9}$$

with a feedback control

$$u = -\left[|(a+c)x_2| + |bc| x_1^2 k^2 \right] sign(s) \tag{10}$$

evolves in sliding mode on the manifold $x_2 + cx_1 = 0$ and its state variables may escape to infinity (in finite time !) if the initial conditions are not sufficiently close to zero (set, for example, $k^2 = c = a = 1$ and $x_1(0) = 2, x_2(0) = -2$).

The analysis of the behaviour of non-trivial classes of VSSs (borrowing the terminology introduced by Isidori [Isidori '89], we can refer to the sliding mode dynamics as the "zero dynamics respect to the output variable s") is a challenging task. The next subsection is devoted to give some fundamental results about this topic, and the unstable behaviour of system (9)-(10) will be justified.

1.3 VSS Analysis. The Filippov continuation method and the equivalent control method.

If some uncertainties affect the description of the controlled system, as always happens in real-life application, it is worth noting that a control ensuring the fulfillment of the ideal sliding mode objective is intrinsically discontinuous and with infinite switching frequency, having to instantaneously react to any deviation of the system trajectory from the sliding manifold.

The following question arises spontaneously:

"*What's the behaviour of a dynamical system subjected to a discontinuous control action characterized by infinite switching frequency?*"

In other words: how to define the system trajectories during a sliding mode on a manifold ?

The reply is not straightforward, neither from a mathematical point of view nor from a " practical" one, since the VSS behaviour is quite far from the typical one to which the control engineer is get used (except from few exceptions, alike electrical engineers involved in PWM-based power electronics applications).

The problem of the VSS analysis leads to the solution of a differential equation with discontinuous right-hand side, that was first addressed and solved in the sixties by the Russian mathematician Filippov, in a purely mathematical framework of research [Filippov '88]

More precisely, consider the dynamic system

$$\dot{\mathbf{x}} = f(\mathbf{x}, t, \mathbf{u}) \qquad \mathbf{x} \in R^n \quad \mathbf{u} \in R^m \tag{11}$$

subjected to the discontinuous feedback

$$u_i = \begin{cases} u_i^+(\mathbf{x}, t) & if\ s_i(\mathbf{x}, t) > 0 \\ u_i^-(\mathbf{x}, t) & if\ s_i(\mathbf{x}, t) < 0 \end{cases} \qquad i = 1, 2, \dots, m \tag{12}$$

where $\mathbf{u}$=$[u_1(\mathbf{x}, t), u_2(\mathbf{x}, t), \dots, u_m(\mathbf{x}, t)]^T$.

Under suitable assumptions, the closed-loop system (11)-(12) may exhibit a sliding behaviour on the m-dimensional manifold $\mathbf{s}(\mathbf{x}, t) = 0$, where $\mathbf{s}$=$[s_1(\mathbf{x}, t), s_2(\mathbf{x}, t), \dots, s_m(\mathbf{x}, t)]^T$

The regularity assumptions that ensure the existence of a solution in the *classical* sense are not verified on the discontinuity manifold $\mathbf{s} = 0$.

Skipping more complex technicalities (for which the reader is referred to [Filippov '88] and, for shorter discussions, to [Utkin '92, Levant '93]), Filippov demonstrated that *the solution of the equation* (11),(12) *onto the discontinuity surface satisfies the differential inclusion*

$$\dot{\mathbf{x}} \in V(\mathbf{x}, t) \tag{13}$$

where the set $V(\mathbf{x}, t)$ is the *minimal convex closure containing all values of* $f(\mathbf{x}, t, \mathbf{u}(\mathbf{x}, t))$ when $\mathbf{x}$ covers the *entire* δ-neighbourhood of the manifold (possibly except from a zero-measure set).

Once defined the set $V(\mathbf{x}, t)$, the velocity vector $f_0(\mathbf{x}, t)$ describing the sliding mode behaviour is taken, within the set $V(\mathbf{x}, t)$, as that *tangent to the manifold of discontinuity.*

The above-defined solution is called "*solution in the Filippov sense*".

In order to clarify the above procedure,let us consider the single input case with $n = 3$, so that a graphical representation can be obtained.

Referring to Figure 8, the convex set $V(\mathbf{x}, t)$ is constituted by all the velocity vectors starting from the point of interest, P, and with the corresponding vertex along the straight line that connects the vertexes of vectors $f(\mathbf{x}, t, \mathbf{u}^+)$ and $f(\mathbf{x}, t, \mathbf{u}^-)$ (dashed line in figure), where $\mathbf{u}^+ = [u_1^+, u_2^+, \dots, u_m^+]^T$ and $\mathbf{u}^- = [u_1^-, u_2^-, \dots, u_m^-]^T$.

The velocity vector f_0, that defines the sliding behaviour, has its vertex on the intersection between the dashed straight line and the plane tangential in P to the manifold.

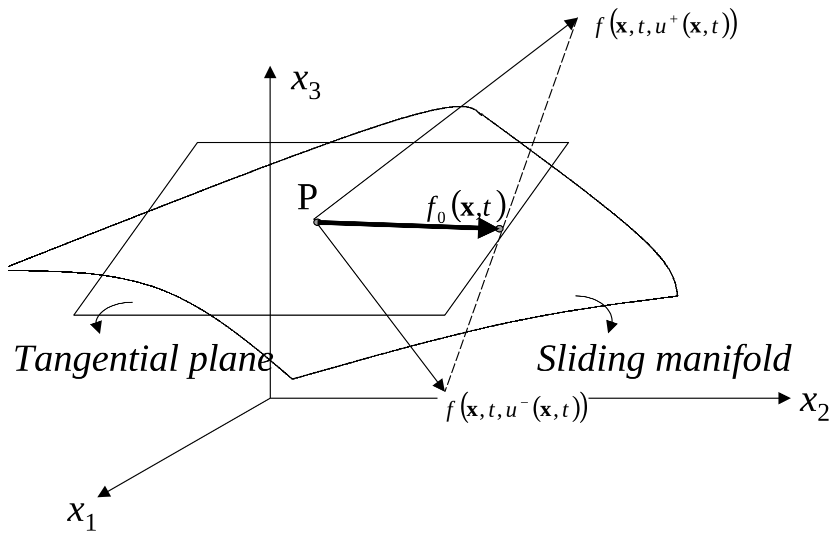

Figure 8: The application of the Filippov continuation method to a third-order plant.

This procedure for obtaining a solution is called the "FILIPPOV CONTINUATION METHOD", yielding an elegant description of the sliding mode dynamics. However, its essentially geometric nature makes its practical relevance quite limited.

In the following a different method is presented, called the "EQUIVALENT CONTROL METHOD", developed by V. Utkin [Utkin '92]. The analytical nature of such method makes it a powerful tool for both analysis and design purposes, and in the next subsection will be detailed the implications of such methodology, that allows one to go deep inside the core of the VSS theory.

It will be shown that the equivalent control method produces the same solution of the Filippov continuation method if the controlled system is affine in the control input, while the two solution may differ in more general cases. Finally, such ambiguity is discussed and motivated.

Consider system (11) with discontinuous control (12), and assume that a sliding mode on the manifold $s = 0$ occurs.

Essentially, the equivalent control method establishes that the solution of system (11),(12) on the manifold $\mathbf{s} = 0$, can be defined as

$$\dot{\mathbf{x}} = f(\mathbf{x}, t, \mathbf{u}_{eq}) \tag{14}$$

where $\mathbf{u}_{eq}(\mathbf{x}, t)$ is a continuous control action, called *"EQUIVALENT CONTROL"*, which is the solution of the equation

$$\dot{s} = \mathbf{J}(s) f(\mathbf{x}, t, \mathbf{u}) = 0 \tag{15}$$

where $\mathbf{J}(s)$ is the m×n Jacobian matrix associated to the sliding manifold.

The above definition is reasonable, because of under the action of the equivalent control any trajectory starting from the manifold $\mathbf{s} = \mathbf{0}$ remains on it, since $\dot{s}$ is null and s remains constant (ion other words, the sliding manifold $s = 0$ is an invariant set)

Example 1.1 - Second part.

Let us analyze the behaviour of systems (5)-(6) and (9)-(10), both in sliding mode on the manifold $s = x_2 + cx_1 = 0$.

Simulations results have shown that the state of the first system exhibit a stable behaviour, while the state of the second one escapes to infinity (in finite time!). Now we are able to justify the reasons for this difference.

As for system (5)-(6), applying the definition of the equivalent control yields

$$\dot{s} = \dot{x}_2 + cx_2 = ax_2 + u + cx_2 = 0 \Longleftrightarrow u = u_{eq} = -(a+c)x_2 \tag{16}$$

Substituting u_{eq} for u in the last equation of (5) one obtains

$$\dot{x}_2 = -cx_2 \tag{17}$$

Taking into account that $x_2 = -cx_1$, the dynamics of x_1 is stable as well.

Repeating the same procedure for system (9), one has

$$\dot{s} = \dot{x}_2 + cx_2 = ax_2 + u + cx_2 + bcx_1^2 \tag{18}$$

and the equivalent control turns out to be given by

$$u_{eq} = -(a+c)x_2 - bcx_1^2 \tag{19}$$

which, substituted in (9), after some manipulations, leads to

$$\dot{x}_2 = -cx_2 - \frac{b}{c}x_2^2 \tag{20}$$

which may be either stable or unstable depending on the initial condition.

From a geometrical point of view, the vertex of the velocity vector $f(\mathbf{x}, t, \mathbf{u}_{eq})$ is obtained intersecting the tangential plane with the *locus of* $f(\mathbf{x}, t, \mathbf{u})$ *for* u *varying between* u^- *and* u^+.

In the following figure 9, the equivalent control method is applied to a second-oder single-input system. The locus of $f(\mathbf{x}, t, \mathbf{u})$ is the dashed line, and its intersection with the straight line tangential to the manifold defines the vertex of the velocity vector $f(\mathbf{x}, t, \mathbf{u}_{eq})$ that describes the sliding mode behaviour.

It is apparent that the solution found by means of the equivalent control method is generally different from that obtained using the Filippov method. This is highlighted by analyzing the following figure 10, in which it is also described the very particular case in which the intersection occurs in the same point (locus of type B) and the two solutions coincide. In this latter case, $f_0(\mathbf{x}, t) \equiv f(\mathbf{x}, t, \mathbf{u}_{eq})$ would be the unambiguous solution to the problem.

It must be evidenced that there exists an important class of systems for which both the methods of analysis lead to the same solution. Such class is that of the the systems with *affine dependance on the control*, i.e. systems expressed as follows

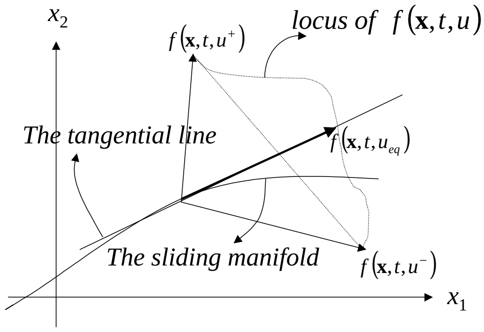

Figure 9: The application of the equivalent control method to a second-order plant.

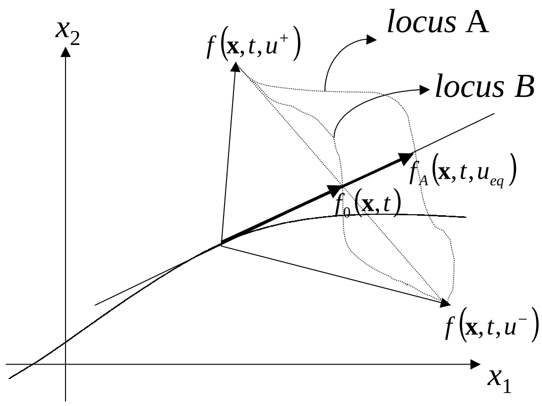

Figure 10: Comparison between the Filippov method and the equivalent control method.

$$\dot{\mathbf{x}} = a(\mathbf{x},t) + b(\mathbf{x},t)\mathbf{u} \qquad \mathbf{x} \in R^n \quad \mathbf{u} \in R^m \tag{21}$$

Indeed, in this case, it is easy to see that *the locus of* $f(\mathbf{x},t,\mathbf{u})(\triangleq a(\mathbf{x},t) + b(\mathbf{x},t)\mathbf{u})$ *coincides with the above defined minimal convex set* $V(\mathbf{x},t)$, and the correspondence of the solutions is the trivial consequence.

Some comments are needed about the non-uniqueness of the solution in the general case of nonlinear systems with arbitrary dependence on the control.

The conceptual difference between the two methods is that the Filippov method prescinds from the existence of a control action able to generate the velocity vector $f_0(\mathbf{x},t)$.

The equivalent control, on the contrary, searches the solution only within the "feasible set" of velocity vector, i.e. there always exists a continuous control action that represents ("is equivalent to") the discontinuous control.

This difference originates a different capability of the two methods to capture the plant behaviour. In fact, it is noteworthy that a discontinuous infinite-frequency switching signal is physically meaningless, so that in real applications must be replaced by some approximation.

The Filippov method is devoted to deal with cases in which the actual control is discontinuous in a neighbour of the sliding manifold (i.e. when the switching control is implemented by means of a switch with an hysteresis).

On the other hand, the equivalent control method is well suited when the control law is implemented by means of continuous approximations of the sign function, i.e. when the motion in a neighbour of the manifold is smooth.

Summarizing, when the sliding mode behaviour of a system nonlinear in the control law is investigated, there is no "correct" or "uncorrect" solution, but the right way to understand the system behaviour depends on the actual implementation of the control law [Utkin '92].

1.4 Ideal and Real Sliding. Chattering, Identificability and Approximability.

In real-life applications, it is not reasonable to assume that the control signal time evolution can switch at infinite frequency, while it is more realistic, due to the inertias of the actuating and measuring devices, and to the presence of noise and/or exogenous disturbances, to assume that it commute at a very high (but finite) frequency. The control oscillation frequency turns out to be not only finite but also almost unpredictable.

The main consequence is that *the sliding mode takes place in a small neighbour of the sliding manifold*, whose dimension is inversely proportional to the control switching frequency.

We introduce the notions of "*IDEAL SLIDING MODE*" and "*REAL SLIDING MODE*" to distinguish the sliding motion that occurs *exactly* on the sliding manifold (analyzed in previous subsections assuming ideal control devices) from a sliding motion that, due to the non-idealities of the control law implementation, takes place in a vicinity of the sliding manifold, which is called "*BOUNDARY LAYER*".

The effects of the finite switching frequency of the control are referred in the literature as "*CHATTERING*". Basically, the high frequency components of the control propagate through the system, therefore exciting the unmodeled fast dynamics, and undesired oscillations affect the system output. Moreover, the term "chattering" has been also designated to indicate the bad effect, potentially disruptive, that a switching control force/torque can produce on the controlled mechanical plant.

Chattering and high control activity were the major drawbacks of the sliding mode approach in the practical realization of variable structure control (VSC) schemes [Utkin '92] [DeCarlo et al. '88].

In order to overcame these drawbacks, a research activity aimed at finding a continuous control action, robust against uncertainties and disturbances, guaranteeing the attainment of the same control objective of the standard sliding mode approach has been carried out in recent years [Bartolini et al. '96, Bartolini et al. '98b, Sira-Ramirez '92].

A possible way to reduce chattering, though maintaining a very high switching frequency, is based on the use of observers for the modeled part of the system [Utkin '92]. The sliding mode is generated in the observer state space with a motion which is close to the ideal one. The resulting high frequency control is filtered out by the fast dynamics of the plant so that a practical continuous control is fed to the slow dynamical subsystem (see Fig. 11). This approach, in the case of known nonlinear systems, has been proposed in [Sira-Ramirez '92], while it has been extended to uncertain systems in [Bartolini et al. '96].

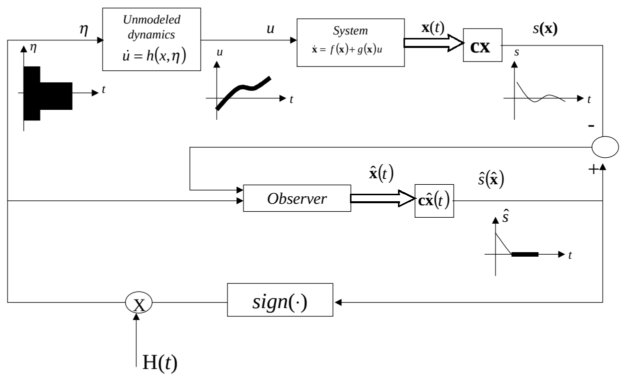

Figure 11: Elimination of chattering via the use of asymptotic observers

Another approach, probably the most used in practice, is based on the use of continuous approximations of the sign function (such as the $sat(\cdot)$ function, the $tanh(\cdot)$ function and so on) in the implementation of the control law. It was pointed out in [Slotine and Li '91] as this methodology is highly sensitive to the unmodeled fast dynamics, and in some cases can lead to unacceptable performance. An interesting class of smoothing functions, characterized by a time-varying parameters, was proposed in [Slotine and Li '91], attempting to find a compromise between the chattering elimination aim and the possible excitation of the unmodeled dynamics.

The most recent and interesting approach for the elimination of chattering is represented (at least in the authors' opinion) by the second order sliding mode methodology, that will be extensively detailed in the following of the present thesis.

1.4.1 Identificability: the on-line availability of the equivalent control

The invariance property establishes that different systems may exhibit the same behaviour when constrained to evolve on the same manifold.

Although any informations regarding the original plant seem to be "lost" during the sliding motion, V. Utkin theorized the possibility of recovering it through the analysis of the discontinuous plant input signal.

He observed that the response of a dynamic system is largely determined by the slow components of its input, while the fast components are often negligible. On the other hand, the equivalent control method requires the substitution of the actual discontinuous control with a continuous function which does not contain high-rate components.

On the basis of the above considerations, he argued that *the equivalent control coincides with the slow components of the input*, and was able to give a formal proof of this statement.

In [Utkin '92], Utkin succeeded in proving that, under certain assumptions on the system dynamics, if the system remains within a Δ-vicinity of the sliding manifold, *the output of the first-order filter*

$$\tau \dot{u}_{av}(t) + u_{av}(t) = u(t) \tag{22}$$

where u is the actual control input, *is close to the equivalent control* according to the following inequality

$$|u_{av}(t) - u_{eq}(t)| \leq k_0 |u_{av}(0) - u_{eq}(0)| e^{-t/\tau} + k_1 \tau + k_2 \Delta + k_3 \frac{\Delta}{\tau} \tag{23}$$

where k_0, k_1, k_2, k_3 are proper known constants.

This result is not valid for systems nonlinear in the control law, as in such systems the dynamic plant response to the high-frequency terms cannot generally be neglected.

The expression (23) contains useful informations on the criterion for properly choosing the filter time constant τ in order to achieve the best estimate.

It is apparent that the right-hand side of (23) can be minimized if the time constant τ of the filter is taken to be proportional to $\sqrt{\Delta}$, which leads to

$$|u_{av}(t) - u_{eq}(t)| \leq O\left(\sqrt{\Delta}\right) \tag{24}$$

The filter time constant, that must be *small enough* as compared with the slow components of the control yet *large enough* to filter out the high-rate components, is to be chosen suitably *matched with the size of the boundary layer.*

This property of "*identificability*" constitutes one of the most important structural property of sliding mode control. It has been successfully applied for design purposes in various works [Hsu *et al.*'89, Fu *et al.* '91], and also has been recently extended to the second order sliding mode control setting [Bartolini et al. '98a].

1.4.2 The Approximability Property

To validate the application of the sliding mode control methodology, which *always* gives rise to sliding modes on some vicinities of the relevant sliding manifold, it is crucial to understand if the description of the sliding mode behaviour is *regular* respect to small deviations from the manifold.

In other terms, are the *real* sliding mode trajectories close to the *ideal* ones obtained through the methods in Subsect. 1.3?

A first reply is contained in a fundamental Theorem, demonstrated in [Utkin '92], that basically states that under reasonable smoothness assumptions on the system dynamics, the above regularity property (called " APPROXIMABILITY PROPERTY") always holds in systems affine in the control.

The Utkin's Theorem sounds like follows:

Under certain assumptions there exists a constant M such that, for any $\Delta \geq 0$, the following correspondance occurs

$$\|s(t)\| \leq \Delta \qquad \Longleftrightarrow \qquad \|\mathbf{x}(t) - \mathbf{x}^*(t)\| \leq M\Delta \tag{25}$$

where s is the sliding variable, and $\mathbf{x}(t)$, $\mathbf{x}^*(t)$ *are the system trajectories in real and ideal sliding mode respecticively*

The analysis of the approximability for systems non-affine in the control law has been pioneered in [Bartolini et al. '86]. For more details the reader is referred to the above work (and references therein).

1.5 Considerations

The main advantages of the SMC approach are the simplicity (of both design and implementation), the high efficiency and the robustness. The basic properties are the order reduction, invariance principle and approximability.

Chattering and high control activity were the reasons that fomented a generalized criticism towards SMC. Nowadays, due to great advances in the research, a number of effective SMC-based control tools is available for practicing engineers that must address complex control problems involving nonlinearities and/or hard uncertainties [Young et al. 1999]

In the second part of this thesis, in which some applicative problems are addressed and solved by second order sliding mode technique, the superb theoretical properties of SMC are confirmed in applications.

Some performance indexes to compare different sliding mode control strategies could be the real $ACCURACY$ in implementation, the smoothness of the control law and the information demand. On the basis of *all* this criteria, second order sliding mode control reveals itself as an improvement respect to previous methodologies.

It is the objective of this thesis to detail a collection of tools, based on second order sliding modes, whose effectiveness cover a large number of practical cases, ranging from discrete-time (or sampled-data) systems to continuous ones, and encompassing important physical plants (even underactuated, see Chapter 8), hoping that this work will attract attention (as well as stimulate experimental activities) about this novel class of algorithms.

References

[Drazenovic '69] B. Drazenovic, "The invariance condition in variable structure systems", *Automatica*, vol. 5, pp. 287–295, 1969.

[Bartolini et al. '86] G. Bartolini and T. Zolezzi, "Control of Nonlinear Variable Structure Systems", *J. Math. Analysis Appl.*, vol.118, pp. 42–62, 1986.

[Bartolini et al. '96] G. Bartolini, P. Pydynowski, "An improved chattering free VSC scheme for uncertain dynamical systems", *IEEE Trans. on Automatic Control*, vol. 41, pp. 1220–1226, 1996.

[Bartolini et al. ‘97] G. Bartolini, A. Ferrara, E. Usai, “Applications of a sub–optimal discontinuous control algorithm for uncertain second order systems”, *Int. J. of Robust and Nonlinear Control*, vol. 7, no.4, pp. 299–319, 1997.

[Bartolini et al. ‘98a] G. Bartolini, A. Ferrara, A. Pisano and E. Usai “Adaptive reduction of the control effort in chattering-free sliding mode control of uncertain nonlinear plants”, *J. Appl. Math. and Comp. Sc.*, vol. 8, no. 1, pp. 51–71, 1998.

[Bartolini et al. ‘98b] G. Bartolini, A. Ferrara, E. Usai, “Chattering Avoidance by Second Order Sliding Mode Control”, *IEEE Trans. on Automatic Control*, vol. 43, no. 2, pp. 241–246, 1998.

[DeCarlo et al. ‘88] R.A. De Carlo, S.H. Zak, G.P. Matthews “Variable Structure Control of Nonlinear Multivariable Systems: A Tutorial”, *Proceedings of the IEEE*, vol. 76, no. 3, pp. 212–232, 1988.

[Emel’yanov and Taran ‘62] S.V. Emel’yanov and V.A. Taran “On a class of Variable Structure Control Systems ”, *Proc. of USSR Academy of Sciences, Energy and Automation*, No. 3, 1962 (in russian).

[Emel’yanov ed ‘70] “Theory of Variable Structure Systems ”, S.V. Emel’yanov ed., Nauka, Moscow, 1970 (in russian).

[Fu *et al.* ‘91] L.C. Fu, “A robust model reference adaptive control using variable structure adaptation for a class of plants”, *Int. J. Contr.*, vol.53, pp. 1359–1375, 1991.

[Hsu *et al.*‘89] L. Hsu and R.R. Costa “Variable structure model reference adaptive control using only input and output measurement: Part 1 ”, *Int. J. Contr.*, vol.49, no. 2, pp. 399–419, 1989.

[Filippov ‘88] A.F. Filippov *Differential Equations with Discontinuous Right–Hand Side*, Kluwer, Dordrecht, Netherlands, 1988.

[Isidori ‘89] A. Isidori *Non Linear Control Systems*, Springer Verlag, Berlin, 1989.

[Levant ‘93] A. Levant “Sliding order and sliding accuracy in sliding mode control”, *International Journal of Control*, vol. 58, pp. 1247–1263, 1993.

[Levant and Fridman ‘96] A. Levant, L. Fridman “Higher order sliding modes as a natural phenomenon in control theory” in *Robust control via variable structure and Lyapunov techniques*, F. Garofalo and L. Glielmo Eds., Lecture Notes in Control and Information Sciences, vol. 217, pp. 107–133, Springer–Verlag, London, 1996.

[Sira-Ramirez ‘92] H. Sira–Ramirez “On the sliding mode control of nonlinear systems,” *Syst. Contr. Lett.*, vol. 19, pp. 303–312, 1992.

[Slotine and Li ‘91] J.J.E.Slotine, W. Li *Applied Nonlinear Control*, Prentice–Hall International, Englewood Cliffs, New Jersey, 1991.

[Utkin ‘78] V.I. Utkin *Sliding Modes and their Applications in Variable Structure Systems*, Mir, Moscow, 1978 (in russian).

[Utkin ‘92] V.I. Utkin *Sliding Modes in Control and Optimization*, Springer Verlag, Berlin, 1992.

[Utkin ‘99] V.I. Utkin et al. *Sliding Modes Control in Electromechanical Systems*, Taylor and Francis, London, 1999.

[Utkin '00] V.I. Utkin "VSS Premise in XX Century: Evidence of a Witness", *Proc. of the 6th IEEE Int. Workshop on Variable Structure Systems*, Coolangatta, Australia, Dec. 2000, pp. 1- 32.

[Young and Ozguner eds., '99] K.D. Young and U. Ozguner (eds.) "Variable Structure Systems, Sliding Mode and Nonlinear Control", Lecture Notes in Control and Information Sciences, Springer-Verlag, 1999, in press.

[Young et al. 1999] D. Young, U. Ozguner and V. Utkin, "A control engineers guide to sliding mode control", *IEEE Trans. Contr. Syst. Tech.*, vol 7, pp. 328–342, 1999.

[Ytkis '92] U. Ytkis *Control Systems of Variable Structure*, Wiley, New York, 1976.

[Zinober '94] A.S.I. Zinober (Ed.), *Variable Structure and Lyapunov Control*, Lecture Notes in Control and Information Sciences, **193**, Springer–Verlag, London, 1994.

2 Sliding Order in Sliding Mode Control

2.1 Sliding Order and Sliding Sets

We have defined in Chapter 1 a sliding mode on a manifold as a particular type of constrained motion that is peculiar of variable structure systems. Such a motion is enforced by some discontinuity of the system dynamics across the manifold.

The concept of sliding order will be more clear after some considerations about the meaning, and different types, of "*discontinous dynamics*" will be given.

It is well known the meaning of the statement "*a function f is of class C^k*", i.e. *f is continuous with its derivatives up to the order k.* For instance, a function of class C^0 is a function whose first derivative is discontinuous, a function of class C^1 is continuous with its first derivative, while the second one is discontinuous, and so on. In some sense, the class of continuity k represents the smoothness degree of the corresponding function.

If we try to apply this concept to system motions, instead of considering abstract functions, the smoothness order of a state trajectory can be defined in a similar manner, keeping in mind that, due to the own *discontinuous* nature of variable structure systems' dynamics, the corresponding motions are always of $finite$ class C^k.

If the sliding variable $\sigma(x,t)$ is of class C^k, then the sliding mode on $\sigma(x,t) = 0$ is referred as $k-1$-*th order sliding mode.* Note that the sliding mode of order one corresponds to a sliding variable of class C^0, i.e. with discontinuous derivative. The order of a sliding mode represents the smoothness degree associated to the motion constrained on the sliding manifold, and it can be defined as follows

***Definition* 2.1** *The sliding order r is the number of* continuous *total derivatives (including the zero one) of the function $\sigma = \sigma(x,t)$ whose vanishing defines the equations of the sliding manifold.*

Note that the constrained motions generated by other manifold-based control methodologies (geometric approach [Isidori '89] and others) are generally of infinite smoothness order. Moreover, note also that the sliding order does not depend on the characteristic of the system's zero dynamics (i.e. the state behaviour when constrained on the manifold) but it is associated only to the characteristic of the constrained motion.

REMARK: If we consider the real sliding behaviour (see sect. 1.4), the sliding order establishes, in some sense, the velocity of the system motion around the sliding manifold. It is not difficult to argue that the switching imperfections cause the system trajectories to lie on a boundary layer of the sliding manifold whose size is smaller and smaller as the sliding order increases.

Example 2.1

Consider system

$$\dot{x} = u \tag{26}$$

$$u = -\text{sign}(x) \tag{27}$$

It has been shown in previous Chapter (see (4)) that the above system exhibits a sliding mode on the manifold $\sigma(x) = x = 0$. According to the above definition, such mode is of order one, because of the total time derivative of the "constraint function" σ, that is given by

$$\dot{\sigma} = \dot{x} \tag{28}$$

turns out to be a *discontinuous function of the state.*

Examples of sliding modes of order higher than one are found in real control systems when some fast dynamic actuator is used to implement the switching control law [Levant and Fridman '96].

Example 2.2

Consider the integrator system, and assume that a dynamic actuator, represented by an high-bandwidth filter having as its input the switching control, is placed at the input side, i.e.

$$\begin{aligned} &\dot{x} = u \\ &\tau\dot{u} + u = z \\ &z = -\text{sign}(x) \end{aligned} \tag{29}$$

It can be verified that, with sufficiently small τ, a stable sliding mode is established on the manifold $x = 0$. Such mode is of order *two*, as the switching term acts on the *second* derivative of the constraint function, and the first total derivative of $\sigma(x) = x$ is a *continuous function of time.*

According to the above remark, one can observe also that the actual size of the residual set to which x is confined is here much smaller than that attained in Ex 2.1, confirming the higher real accuracy of second order sliding mode control as compared with first order SMC.

Higher order sliding modes (HOSM) behaviours may occur also when the relative degree r between the desired constraint function (i.e. the sliding variable) and the control is higher than one, so that the switching term turns out to be "hidden" in the higher derivatives of the constraint function. In this case, if the sliding mode is established (a non-trivial control task if $r > 1$!), the sliding order equals the relative degree.

The reader is referred to [Levant and Fridman '96] for a detailed discussion about these topics.

Before to give some formal definitions, we try to derive some properties of HOSM from the analysis of the behaviour of system (29).

Making reference to system (29), one can observe that *both x and $\dot{x}$ are steered to zero.*

It isn't a fortuity, while it is the consequence of a general property of HOSM's,. that can be derived through a generalization of the well known Barbalat's Lemma [Slotine and Li '91] (one of the most important Lemmas in adaptive control), that may be understood as follows:

If some function (signal) converges to a constant value then all its continuous derivatives converge to zero.

On the basis of this very intuitive statement, by combining the above definition of HOSM (number of continuous derivatives) with the fact that the sliding variable converges to zero (convergence to a constant value) then it can be claimed that an HOSM is characterized by the fact that *the derivatives of the sliding variable converge to zero up to a certain order.*

This property can be suitably formulated introducing a new type of manifold, called "SLIDING SET", on which an HOSM turns out to be established by definition.

***Definition* 2.2 SLIDING SET**

The sliding set of order r-th associated to the manifold $\sigma(x,t) = 0$ *is defined by the equalities*

$$\sigma(\cdot) = \dot{\sigma}(\cdot) = \ldots = \sigma^{(r-1)} = 0 \tag{30}$$

Note that (30) represents an **r-dimensional condition** on the state of the corresponding dynamic system; keeping in mind what happened in first order sliding modes (reduction of one in the system order) it can be argued that the order reduction corresponding to an r-th order sliding mode will be of order r. This means that, for example, a system of the fourth order performing a sliding mode of order three will behave as a first order system !

Now let us give a more precise definition of higher order sliding modes. .

***Definition* 2.3** [Levant and Fridman '96]

Let the r-th oder sliding set (30) *be non-empty, and assume that it is locally an integral set in Filippov's sense (i.e. it consists of Filippov's trajectories of the discontinuous dynamic system). Then, the corresponding motion satisfying* (30) *is called an r-th oder sliding mode with respect to the manifold* $\sigma = 0$

As for the geometric conditions for the HOSM to exists, there must exist of a non-empty intersection between the Filippov's convex set and the tangential space to (30).

The importance of HOSM's will be clear after that the benefits introduced by enforcing them in controlled systems will be detailed (among them, the possible elimination of chattering and/or the capability of controlling high-relative-two plants using only output measurements).

2.2 Differential Inequalities in Sliding Mode Control Design

The first step of the sliding mode control design methodology (and of other manifold-based control techniques [Isidori '89]) is to define a suitable manifold in the state space such that the associated zero-dynamics is stable and satisfies the control objectives.

This step is the most difficult of the whole design procedure, especially for non-trivial classes of systems, since there is no systematic way to perform it for nonlinear systems in the general form

$$\dot{x} = f(x,t,u) \tag{31}$$

In order to make the problem to admit a solution, it is usually assumed the existence of a change of variables that transforms the system in a normal form such that the manifold design is simplified.

Here we are mainly interested in the second phase, i.e., given a desired manifold $\sigma(\mathbf{x}, t) = 0$, whose corresponding zero-dynamics enjoys all properties we can desire, the problem is to find a control action that **forces the system to evolve on such a manifold**.

It is shown that the main mathematical tool used for the second step of the SMC design is constituted by ***differential inequalities***.

In particular, **first order SMC is based on differential inequalities of order one, while second order SMC relies on differential inequalities of order two**, much more difficult to manage.

We consider now for the sake of simplicity systems single-input with affine dependence on the control, and generalizations are postponed to successive Chapters.

Consider system

$$\dot{\mathbf{x}} = \mathbf{a}(\mathbf{x}, t) + \mathbf{b}(\mathbf{x}, t)u(t) \tag{32}$$

where $\mathbf{x} \in X$ is the state variable, X is a smooth finite-dimensional manifold, t is the time, $u \in R$ is the control and $\mathbf{a}$, $\mathbf{b}$ are uncertain vector fields.

Let $\sigma(t, \mathbf{x}) = 0$ be the manifold on which we want to drive the system state. Our goal is to force the constraint function $\sigma(\cdot)$ to vanish in finite time.

Using the traditional way to indicate the partial derivatives, $\dot{\sigma}(t)$ may be expressed in the form

$$\begin{aligned} \dot{\sigma}(t) &= \sigma_t^{'}(\mathbf{x}, t) + \sigma_x^{'}(\mathbf{x}, t)\mathbf{a}(\mathbf{x}, t) + \sigma_x^{'}(\mathbf{x}, t)\mathbf{b}(\mathbf{x}, t)u(t) = \\ &= \alpha(\mathbf{x}, t) + \beta(\mathbf{x}, t)u(t) \end{aligned} \tag{33}$$

where

$$\alpha(\mathbf{x}, t) = \sigma_t^{'}(\mathbf{x}, t) + \sigma_x^{'}(\mathbf{x}, t)\mathbf{a}(\mathbf{x}, t) \tag{34}$$

$$\beta(\mathbf{x}, t) = \sigma_x^{'}(\mathbf{x}, t)\mathbf{b}(\mathbf{x}, t) \tag{35}$$

Make the following assumption

A1.

$$\beta(\mathbf{x}, t) \neq 0 \quad \forall \mathbf{x} \in X \tag{36}$$

Assumption A1 means that system (32) has *uniform relative degree one* with respect to the output variable σ.

If the system dynamics were perfectly known, the control $u(t)$ could be designed to assign the desired stable dynamics to the variable σ. Indeed, under suitable minimum-phase assumptions (stability of the inverse dynamics), the feedback-linearizing control

$$u(t) = [\beta(\mathbf{x}, t)]^{-1} [v(t) - \alpha(\mathbf{x}, t)] \tag{37}$$

transforms the expression for $\dot{\sigma}$ in the form

$$\dot{\sigma}(t) = v(t) \tag{38}$$

and the signal $v(t)$ may be used to assign the desired dynamics, for instance

$$v(t) = -k\sigma(t) \qquad k > 0 \tag{39}$$

would assign a linear first-order stable dynamics to the σ variable.

In the presence of uncertainties, the perfect "cancellation" of the nonlinearities is no more feasible, and it is not possible to assign a pre-specified dynamics to the σ variable.

*At the price of additional assumptions, one can define a control law that makes σ satisfying a proper **differential inequality** of order one.*

We are interested in *differential inequalities whose all possible solutions globally converge to zero.*

The most known (and used in control design) is the so-called "*REACHING CONDITION*"

$$\sigma\dot{\sigma} \leq k^2|\sigma| \tag{40}$$

It is not difficult to see that, independently from the initial condition, *any solution of* (40) *converges to zero in finite time.*

If we are able to guarantee that the sliding variable σ satisfies the above condition, then the finite-time reaching of the sliding manifold turns out to be ensured.

Making reference to (33), we assume that two positive functions $\alpha_M(\mathbf{x}, t)$ and $\beta_m(\mathbf{x}, t)$ exist, and are known, such that

A2.

$$|\alpha(\mathbf{x}, t)| \leq \alpha_M(\mathbf{x}, t) \quad \forall \mathbf{x} \in X \tag{41}$$

A3.

$$0 < \beta_m(\mathbf{x}, t) \leq \beta(\mathbf{x}, t) \quad \forall \mathbf{x} \in X \tag{42}$$

The traditional First Order Sliding Mode Control approach is summarized by the following Proposition, whose proof is trivial and is omitted.

Proposition 2.1 Given the uncertain system (32), satisfying assumptions **A2** and **A3**, then the feedback control law

$$u(t) = -\frac{\alpha_M(\mathbf{x}, t) + k^2}{\beta_m(\mathbf{x}, t)} \text{sign}(\sigma(\mathbf{x}, t)) \tag{43}$$

provides satisfaction of (40), and therefore, at the same time, the invariance and the global attractiveness of the manifold $\sigma(\mathbf{x}, t) = 0$

Basically, in FOSMC the *first derivative* of the sliding variable is *discontinuously* modified by the control signal in order to guarantee that the reaching condition (40), a first-order differential inequality (FODI) whose solutions globally converge to zero, holds.

2.2.1 Second order differential inequalities

As previously mentioned, the second order SMC approach is based on steering σ to zero through the fulfillment of a differential inequality of order two (second order differential inequality, SODI).

Differential inequalities (DIs) of order higher than one are not trivial to analyze. To apply the SOSMC methodology, we have first to design a stable SODI, and then a control action must be found such that the sliding variable σ is forced to satisfy the relevant stable SODI.

It is easy to prove that conditions of the type

$$\ddot{\sigma}\sigma \leq -\xi(t)|\sigma| \qquad \xi(t) \geq \xi_1 > 0 \tag{44}$$

always give rise to a sequence of singular points

$$\{\sigma_{M_i} = \sigma(t_{M_i})\} \quad t_{M_i} \,:\, \dot{\sigma}(t_{M_i}) = 0 \quad i = 1, 2, \ldots \tag{45}$$

and, accordingly, to a sequence of time intervals between two successive singular points

$$\left\{\Delta_{t_{M_i}}\right\} = \left(t_{M_{i+1}} - t_{M_i}\right) \tag{46}$$

Any possible behaviour of σ, ranging from explosion and persistent oscillations to asymptotic or finite-time vanishing transients, can arise, depending on the characteristics of the aforesaid sequences (see Fig. 12)

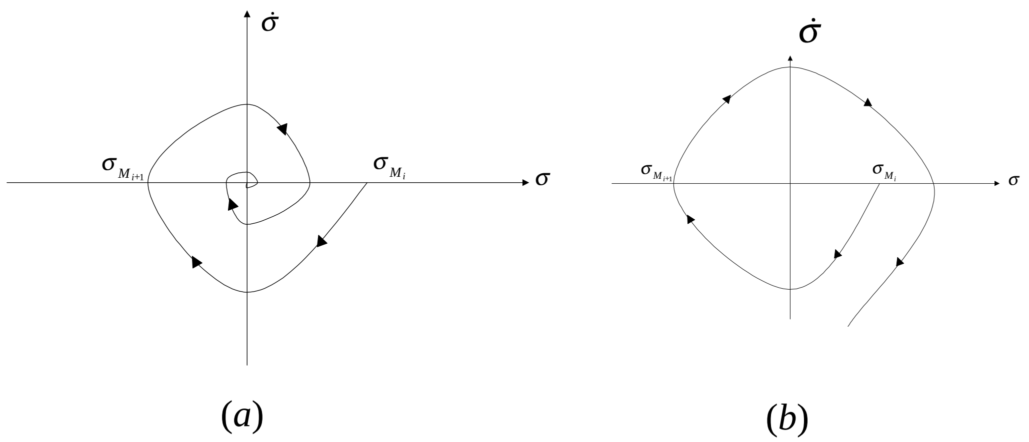

Figure 12: Stable and unstable solutions for the SODI (44).

The desired behaviour involves that both σ and $\dot{\sigma}$ are steered to zero in a finite time, and a sufficient condition to achieve the control goal is the simultaneous fulfillment of the two contraction properties

$$\begin{cases} \left|\frac{\sigma_{M_{i+1}}}{\sigma_{M_i}}\right| \leq \nu^2 < 1 \\ \\ \left|\frac{\Delta_{t_{M_{i+1}}}}{\Delta_{t_{M_i}}}\right| \leq \varepsilon^2 < 1 \end{cases} \tag{47}$$

the first ensuring the contraction of the state trajectory toward the origin of the $\sigma - \dot{\sigma}$ plane, and the second ensuring the finite transient time.

As the considered system has a relative degree equal to two, no Lyapunov-based approach can be used directly to ensure convergence. Some specific control algorithms that guarantee (47) have been presented in the literature, and were briefly surveyed in [Bartolini et al. '99].

In [Levant '93] it was proved that, by guaranteeing

$$\begin{cases} \xi(t) \leq \xi^*(t) & \sigma\dot{\sigma} < 0 \\ \xi(t) \geq \alpha\xi^*(t) & \sigma\dot{\sigma} > 0 \end{cases} \tag{48}$$

with $\xi^*(t) > \xi_1 > 0$ and $\alpha \geq 1$, the contraction properties (47) are satisfied.

The typical trajectories in the $\sigma - \dot{\sigma}$ plane corresponding to (44-(48 are of the type in Fig. 12(a), i.e. the trajectories *twist* around the origin, converging to it in finite time. Due to this peculiar behaviour, the control algorithm based on this DI is called *"TWISTING ALGORITHM"*, [Levant '93, Bartolini et al. '99].

A different approach is characterized by a different contraction principle, based on the time-optimal bang-bang control method. It lies in anticipating the commutation of the sign of $\ddot{\sigma}$ at the time instant at which $\sigma = \frac{1}{2}\sigma_{M_i}$, σ_{M_i} being the last singular point of σ

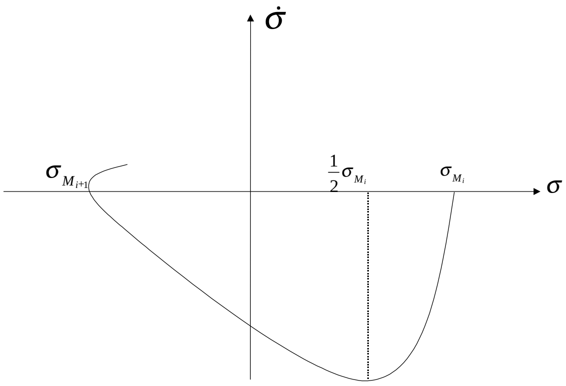

Figure 13: Anticipation of commutation.

More precisely, in [Bartolini et al. '98b] it was proved that choosing

$$\begin{cases} \xi(t) \leq \xi^*(t) & \left(\sigma(t) - \frac{1}{2}\sigma(t_{M_i})\right) > 0 \\ \xi(t) \geq \alpha\xi^*(t) & otherwise > 0 \end{cases} \tag{49}$$

with $\xi^*(t) > \xi_1 > 0$ and $\alpha \geq 1$, the contraction properties (47) are also satisfied.

The 2-SMC algorithm based on this contraction principle is called "SUBOPTIMAL ALGORITHM", to put in evidence that its switching logic is derived from the time-optimal control philosophy. The typical trajectories are different from that of the twisting algorithm, due to the anticipated commutation, and take one of the forms in Fig. 14. Depending on the actual value of ξ_1 and α *it is possible to enforce a monotonic convergence of* σ *to zero*, eliminating undesired transient oscillations. Moreover, it features less convergence time and control effort as compared with the twisting 2-sliding algorithm.

Note that the suboptimal algorithm requires the availability of the singular points of σ, i.e. it must be detected the sequence of the time instants at which $\dot{\sigma}$ is zero. This in not a particular drawback, as high-bandwidth peak detectors can be easily developed both in continuous and discrete time.

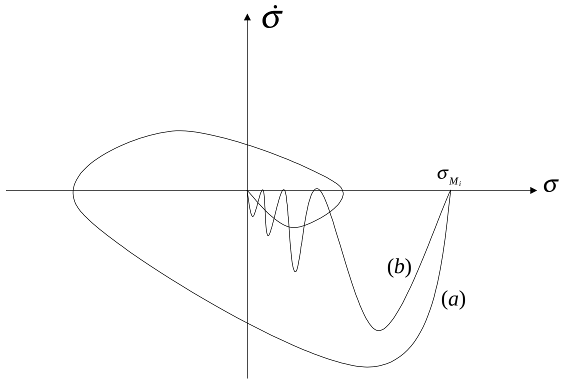

Figure 14: The two possible transient behaviours of the sub-optimal SOSMC algorithm.

2.2.2 Second order sliding mode algorithms

Once described some stable SODI's, the subsequent step is to define a control action that, given the controlled plant and given the desired sliding manifold, provides the fulfillment of the above-defined stable differential inequalities.

First of all, from the analysis of the SODI one can derive that *the relevant control acts discontinuously on* $\ddot{\sigma}$.

Defining SOSMC algorithms simply as those guaranteeing that both the sliding variable and its derivative are steered to zero may be (and has been !) source of misunderstandings about the nature of SOSMC.

In fact, a possible way to attain the relevant control objective could be that of using an observer to estimate $\dot{\sigma}$, and then redefining a new sliding quantity, $\sigma_1 = \dot{\sigma} + k\dot{\sigma}^{\frac{p}{q}}$, $(p/q \leq 1)$, to be steered to zero by a suitable control discontinuous on $\sigma_1 = 0$.

Guaranteeing $\dot{\sigma}_1\sigma_1 < -k^2|\sigma_1|$ yields that both σ and $\dot{\sigma}$ will be steered to zero (asymptotically if $\frac{p}{q} = 1$, in a finite time if $\frac{p}{q} < 1$, which is much more involved).

In the literature, these approaches have often been referred to as Second-Order Sliding-Mode Control (2-SMC) [Elmali and Olgac '92], Dynamical Sliding-Mode Control (DSMC)

[Sira-Ramirez '92] or Terminal Sliding-Mode Control (TMSC) [Yu and Zihong '96] [Venkataraman et al. '89].

In our opinion, **as the reaching condition is of the type (40), they actually belong to the class of 1-SMC algorithms. The kernel of "true" 2-SMC is a differential inequality of order two.**

It would be desirable to solve the control problem with no need for observation and/or estimation of $\dot{\sigma}$.

In 2-SMC, the actual control signal affects the sign and the amplitude of $\ddot{\sigma}$, and a suitable switching logic, based on s and, at most, on the sign of $\dot{s}$, guarantees the finite-time convergence of the state to the 2-sliding manifold $s = \dot{s} = 0$ through the fulfillment of the stable SODI's (44)-(48) or (44)-(49).

Making reference to system (32), let us analyze the second-order dynamics of σ.

The system dynamics, and the first order dynamics of σ, are recalled for the sake of clarity.

$$\dot{\mathbf{x}} = \mathbf{a}(\mathbf{x}, t) + \mathbf{b}(\mathbf{x}, t)u(t) \tag{50}$$

$$\dot{\sigma}(t) = \alpha(\mathbf{x}, t) + \beta(\mathbf{x}, t)u(t) \tag{51}$$

Two different cases must be distinguished, namely, the case A (assumption A1 still holds) and case B (assumption A1 is not verified). Note that *in case A the FOSMC approach is no more feasible.*

More precisely:

- Case A: $\beta(\mathbf{x}, t) \neq 0 \ \forall \ \mathbf{x} \in X$
- Case B: $\beta(\mathbf{x}, t) = 0 \ \forall \ \mathbf{x} \in X$

We first deal with separately the two cases A and B, and then we show that the resulting control problems are suitable to be formalized in the same way.

Case A.

Considering the second derivative of σ yields

$$\ddot{\sigma}(t) = \varphi_A(\mathbf{x}, u, t) + \beta(\mathbf{x}, t)\dot{u}(t) \tag{52}$$

where

$$\begin{aligned} \varphi_A(\mathbf{x}, u, t) \;=\; & \alpha_t^{'}(\mathbf{x}, t) + \alpha_x^{'}(\mathbf{x}, t)\mathbf{a}(\mathbf{x}, t) \\ & +[\alpha_x^{'}(\mathbf{x}, t)\mathbf{b}(\mathbf{x}, t) + \beta_t^{'}(\mathbf{x}, t) + \beta_x^{'}(\mathbf{x}, t)\left(\mathbf{a}(\mathbf{x}, t) + \mathbf{b}(\mathbf{x}, t)u(t)\right)] \end{aligned} \tag{53}$$

The main difference with respect to the case A is that the control time derivative $\dot{u}$ affects the $\ddot{\sigma}$ dynamics. u is understood as an unknown disturbance affecting the drift term $\alpha_B(\mathbf{x}, u, t)$.

The control derivative $\dot{u}$ can be used as an auxiliary control variable to be designed in order to satisfy the control objective of steering σ and $\dot{\sigma}$ to zero.

Case B.

The control does not affect directly the dynamics of $\dot{\sigma}$, which is given by

$$\dot{\sigma}(t) = \alpha(\mathbf{x}, t) \tag{54}$$

The second total derivative of $\sigma(t)$ may be expressed in the form

$$\ddot{\sigma}(t) = \varphi_B(\mathbf{x}, t) + \gamma_B(\mathbf{x}, t)u(t) \tag{55}$$

where

$$\varphi_B(\mathbf{x}, t) = \alpha_t^{'}(\mathbf{x}, t) + \alpha_x^{'}(\mathbf{x}, t)\mathbf{a}(\mathbf{x}, t) \tag{56}$$

$$\gamma_B(\mathbf{x}, t) = \alpha_x^{'}(\mathbf{x}, t)\mathbf{b}(\mathbf{x}, t) \tag{57}$$

It must be assumed that

$$\gamma_A(\mathbf{x}, t) \neq 0 \qquad \forall \mathbf{x} \in X \tag{58}$$

i.e. the sliding variable, understood as a system's output, must have $uniformrelativedegreetwo$.

The stabilization problem for system (55)-(58) must be addressed and solved under the basic assumption that $\dot{\sigma}$ **is not available for measurements**.

This fact, together with the presence of model uncertainties, makes the problem not easily solvable. The existence of a solution is obviously critically related to the relevant assumptions on the uncertain dynamics.

Both cases A and B can be dealt with in an unified treatment, as the structure of the system to be stabilized is is exactly the same: a second-order uncertain system with affine dependence on the relevant control signal (the control derivative $\dot{u}$ in case A, the actual control u in case B).

For this reason, in the next chapter it will be addressed and solved the stabilization problem for the system

$$\begin{cases} y_1(t) &= \sigma(x, t) \\ \dot{y}_1(t) &= y_2(t) \\ \dot{y}_2(t) &= \varphi(\cdot) + \gamma(\mathbf{x}, t)v(t) \end{cases} \tag{59}$$

As for the terms $\varphi(\cdot)$, $\gamma(\cdot)$ and $v(t)$ they have different meaning and structure in cases A and B.

More precisely :

$$\begin{array}{cc} Case A & Case B \\ \left\{\begin{array}{rcl} \varphi(\cdot) & = & \varphi(\mathbf{x}, u, t) \\ v(t) & = & \dot{u}(t) \end{array}\right. & \left\{\begin{array}{rcl} \varphi(\cdot) & = & \varphi(\mathbf{x}, t) \\ v(t) & = & u(t) \end{array}\right. \end{array} \tag{60}$$

Relying on the above presented stable SODI, a control action $v(t)$ must be defined such that the dynamics of σ satisfies (44)-(48) or (44)-(49).

We will concentrate our analysis on the second one; the resulting algorithm is referred as "SUB-OPTIMAL SECOND ORDER SLIDING MODE CONTROL ALGORITHM", and will be detailed in the following chapter.

In case A, called the "ANTICHATTERING CASE", the SOSMC approach satisfies the control objective by means of a continuous control input. In fact, the actual discontinuous control signal $v(t)$ is the derivative of the plant input $u(t)$, which, obtained by integrating the discontinuous derivative, turns out to be continuous. The first order SMC leads to the discontinuous relay control (43).

In case B (that is called “RELATIVE DEGREE TWO CASE”) the actual control is discontinuous. Note that the traditional first order SMC methodology, if not properly coupled to state observers, fails to solve this problem.

References

[Bartolini et al. ‘96] G. Bartolini and P. Pydynowski “An improved chattering free VSC scheme for uncertain dynamical systems”, *IEEE Trans. on Automatic Control*, vol. 41, pp. 1220–1226, 1996.

[Bartolini et al. ‘97] G. Bartolini, A. Ferrara and E. Usai “Applications of a sub–optimal discontinuous control algorithm for uncertain second order systems”, *Int. J. of Robust and Nonlinear Control*, vol. 7, no.4, pp. 299–319, 1997.

[Bartolini et al. ‘98a] G. Bartolini, A. Ferrara, A. Pisano and E. Usai “Adaptive reduction of the control effort in chattering-free sliding mode control of uncertain nonlinear plants”, *J. Appl. Math. and Comp. Sc.*, vol. 8, no. 1, pp. 51–71, 1998.

[Bartolini et al. ‘98b] G. Bartolini, A. Ferrara and E. Usai “Chattering Avoidance by Second Order Sliding Mode Control”, *IEEE Trans. on Automatic Control*, vol. 43, no. 2, pp. 241–246, 1998.

[Bartolini et al. 2000] G. Bartolini, A. Ferrara, A. Pisano, E. Usai “On the convergence properties of a 2-sliding control algorithm for nonlinear uncertain systems”, *Int. J. of Control*, in press.

[Bartolini et al. ‘99] G. Bartolini, A. Ferrara, A. Levant, E. Usai “On Second Order Sliding Mode Controllers”, in “Variable Structure Systems, Sliding Mode and Nonlinear Control”, K.D. Young and U. Ozguner eds., Lecture Notes in Control and Information Sciences, Springer-Verlag, 1999, in press.

[Young and Ozguner (eds.)‘99] K.D. Young and U. Ozguner (eds.) “Variable Structure Systems, Sliding Mode and Nonlinear Control”, Lecture Notes in Control and Information Sciences, Springer-Verlag, 1999, in press.

[DeCarlo et al. ‘88] R.A. De Carlo, S.H. Zak, G.P. Matthews “Variable Structure Control of Nonlinear Multivariable Systems: A Tutorial”, *Proceedings of the IEEE*, vol. 76, no. 3, pp. 212–232, 1988.

[Elmali and Olgac ‘92] H. Elmali H. and N. Olgac, “Robust Output Tracking Control of Nonlinear MIMO Systems via Sliding Mode Technique”, *Automatica*, vol. 28, pp. 145–151, 1992.

[Isidori ‘89] A. Isidori *Non Linear Control Systems*, Springer Verlag, Berlin, 1989.

[Levant ‘93] A. Levant “Sliding order and sliding accuracy in sliding mode control”, *International Journal of Control*, vol. 58, pp. 1247–1263, 1993.

[Levant and Fridman ‘96] A. Levant, L. Fridman “Higher order sliding modes as a natural phenomenon in control theory” in *Robust control via variable structure and Lyapunov techniques*, F. Garofalo and L. Glielmo Eds., Lecture Notes in Control and Information Sciences, vol. 217, pp. 107–133, Springer–Verlag, London, 1996.

[Sira-Ramirez ‘92] H. Sira–Ramirez “On the sliding mode control of nonlinear systems,” *Syst. Contr. Lett.*, vol. 19, pp. 303–312, 1992.

[Slotine and Li ‘91] J.J.E.Slotine, W. Li *Applied Nonlinear Control*, Prentice–Hall International, Englewood Cliffs, New Jersey, 1991.

[Yu and Zihong ‘96] X. Yu and M. Zihong, “Model Reference Adaptive Control Systems with Terminal Sliding Modes” *Int. J. Contr.*, vol. 64, pp. 1165–1176, 1996.

[Venkataraman et al. ‘89] S.T. Venkataraman and S. Gulati, “Control of Nonlinear Systems using Terminal Sliding Modes”, *ASME J. Dyn. Syst. Meas. Contr.*, vol. 115, pp. 554–560, 1989.

[Utkin ‘92] V.I. Utkin *Sliding Modes in Control and Optimization*, Springer Verlag, Berlin, 1992.

3 Second Order Sliding Mode Control - The sub-optimal Algorithm

3.1 Preliminaries

It has been shown in the previous Chapter that the Second Order Sliding Mode Control (2-SMC) problem for n-th order systems affine in the control is expressed in terms of the *stabilization of a proper second order system.*

In the first part of this chapter we solve the associated control problem under various assumptions, with increasing generality, about the system uncertainties. In this analysis it is assumed that the expression for the sliding manifold is known.

In the second part we consider the overall control problem, and we address also the problem of designing a suitable manifold on which to enforce the system motion to achieve the desired close-loop behaviour. In order to have a systematic procedure for defining the sliding manifold, systems expressed in the canonical Brunowsky form are considered.

3.2 The Sub-Optimal Second Order Sliding Mode Control Algorithm

According to previous chapter (see (59)) the 2-SMC problem for n-th order systems of the type

$$\dot{\mathbf{x}} = \mathbf{a}(\mathbf{x}, t) + \mathbf{b}(\mathbf{x}, t)u(t) \tag{61}$$

where $\mathbf{x} = [x_1 \dots x_n]$ is the state variable, t is the time, $u \in R$ is the control and $\mathbf{a}(\mathbf{x}, t)$, $\mathbf{b}(\mathbf{x}, t)$ are uncertain vector fields can be reduced to the stabilization problem for a second order uncertain system represented in the canonical Brunowsky form, i.e.

$$\begin{cases} \dot{y}_1(t) & = y_2(t) \\ \dot{y}_2(t) & = \varphi(\cdot) + g\left(\mathbf{x}(t)\right) v(t) \end{cases} \tag{62}$$

where y_1 and y_2 represent the actual sliding variable and its derivative, respectively, y_2 is not available, and $\varphi(\cdot)$, $g\left(\mathbf{x}(t)\right)$ are uncertain terms.

Depending on the relative degree r between the sliding variable and the actual control input, $v(t)$ may represent either the actual control or its derivative, and, correspondingly, also the uncertain drift term $\varphi(\cdot)$ may depend on two different sets of variables.

Indeed, we have shown in previous chapter that, if $r = 1$ (case A, sect. 2.2.2), $\varphi(\cdot) = \varphi(\mathbf{x}, u, t)$ and $v(t) = \dot{u}(t)$, while , if $r = 2$ (case B, sect. 2.2.2) $\varphi(\cdot) = \varphi(\mathbf{x}, t)$ and $v(t) = u(t)$.

In case A a 1-SMC-based relay control of the type

$$u(t) = -U(\mathbf{x}, t)\text{sign}(y_1(t)) \tag{63}$$

could be applied: the use of 2-SMC is only motivated by the chattering elimination aim.

On the contrary, in case B, the relative degree is two and the use of 2-SMC is not a choice but a necessity.

The contraction mechanism, on the basis of which the stabilization of system (62) is guaranteed, relies on the stable differential inequalities of order two discussed in previous chapter.

In particular, the second one is recalled

$$\ddot{y}_1 y_1 \leq -\xi(t)|y_1| \tag{64}$$

$$\begin{cases} \xi(t) \leq \xi^*(t) & \left(\sigma(t) - \frac{1}{2}\sigma(t_{M_i})\right) > 0 \\ \xi(t) \geq \alpha\xi^*(t) & otherwise \end{cases} \tag{65}$$

with $\xi^*(t) > \xi_1 > 0$ and $\alpha \geq 1$.

In order to find a control action that makes fulfilled the above SODI, the assumptions regarding the uncertain dynamics play a crucial role. Let us proceed step-by-step considering first the simple case of *constant known bounds* of the uncertain terms (subsect 3.2.1.). In the following subsect. 3.2.2 the more general (and realistic) case of *state-dependent uncertainty bounds* will be considered.

3.2.1 2-SMC for systems with constant bounds of the uncertainties

The historical development of SOSMC algorithms [Levant '93, Bartolini et al. '97] starts considering the global boundedness assumption for the uncertainties, i.e., that in some neighbour of the sliding manifold (not necessarily small) the uncertain terms are bounded by known positive constants according to

$$\begin{array}{l} |\varphi(\cdot)| \leq \Phi \\ 0 < G_1 \leq g\left[\mathbf{x}(t)\right] \leq G_2 \end{array} \tag{66}$$

A solution was proposed in [Bartolini et al. '97]

Proposition 1: *Consider system* (62) *with its uncertain dynamics satisfying (66) and* y_2 *not measurable but with known sign. Assume that the sequence of the singular values of* $y_1(t)$, $y_{1_{M_k}} = y_1(T_{M_k})$, T_{M_k} *s.t.* $y_2(T_{M_k}) = 0$, $k = 1, 2, \ldots$, *is available with ideal precision.*
The control strategy

$$v(t) = -\alpha(t)V_M \text{sign}\left[y_1(t) - \frac{1}{2}y_{1_{M_k}}\right] \tag{67}$$

where

$$\alpha(t) = \begin{cases} \alpha^* & if \;\; y_{1_{M_k}}[y_1(t) - \frac{1}{2}y_{1_{M_k}}] > 0 \\ 1 & otherwise \end{cases} \tag{68}$$

and V_M *and* α^* *are such that*

$$\begin{cases} V_M > max\left\{\frac{\Phi}{G_1}, \frac{4\Phi}{3\alpha^* G_1 - G_2}\right\} \\ \alpha^* > min\left\{1, \frac{G_2}{3G_1}\right\} \end{cases} \tag{69}$$

causes the finite time convergence of y_1 and y_2 to the origin of the state plane.

Proof: See [Bartolini et al. '97]

The associated stabilization problem is relevant to the fact that in the convergence process the state of the controlled system does not leave the boundary layer, which is the reason why the stability properties of this SOSMC algorithm are intrinsically local, in contrast to FOSMC strategies.

More precisely, the contractive mechanism is based on the generation of a sequence $\{y_1(T_{M_k})\}$ of singular values of $y_1(t)$, that is of points corresponding to the time instants T_{M_k} in which $y_2(T_{M_k}) = 0$, $k = 1, 2, \ldots$.

The control law is defined in order to ensure that:

1. the sequence $\{y_1(T_{M_k})\}$ is monotonically-decreasing,
2. the sequence $\{T_{M_k} - T_{M_{k-1}}\}$ is summable

Item 1 ensures that both y_1 and y_2 converge to zero, while Item 2 guarantees that such convergence process takes place in a finite time.

First, the reaching of a first singular value $y_1(T_{M_1})$ is proven. Then, the *worst-case analysis* of the system trajectories is performed, in which *the uncertainties are assumed to act against the contraction at their maximum effort.* On the basis of this analysis, sufficient conditions for the controller parameters are derived such that *all the possible system trajectories converges to the origin of the y_1Oy_2 plane after a finite transient.*

3.2.2 SOSMC for systems with state-dependent uncertainty bounds

In order to endow SOSMC algorithms with properties analogous to that shown by FOSMC ones it is necessary to proceed gradually. The natural step in this direction consists in considering more general upper bounds to the drift term $\varphi(\cdot)$, explicitly depending on the state and/or the control.

To this end, now we consider the class of uncertainties described by

$$\begin{array}{cc} Case A & Case B \\ \\ \begin{array}{c} |\varphi(\mathbf{x}, u, t)| \leq \Psi_0(\|\mathbf{x}\|) + \Psi_1(\|\mathbf{x}\|)|u| \\ 0 < G_1 \leq g(\mathbf{x}) < G_2 \end{array} & \begin{array}{c} |\varphi(\mathbf{x}, t)| \leq \Psi_0(\|\hat{\mathbf{x}}\|) + \Psi_1(\|\hat{\mathbf{x}}\|)|x_n| \\ 0 < G_1 \leq g(\mathbf{x}) < G_2 \end{array} \end{array} \tag{70}$$

where $\Psi_i(\cdot)$, $i = 0, 1$, are known non decreasing functions of the state norm (for any norm $\|\cdot\|_k$, $(k = 1, 2, \ldots, \infty)$) and $\hat{\mathbf{x}} = [x_1, x_2, \ldots, x_{n-1}]^T$.

It makes sense to consider, in the first part of this treatment, the sliding variable dynamics independent from the original system, assuming that the uncertainties upperbounds depend only on y_1 and y_2, that is

$$\begin{array}{l} |\varphi(\cdot)| \leq \overline{\Psi}_0(y_1(t)) + \overline{\Psi}_1(y_1(t))|y_2(t)| \\ 0 < G_1 \leq g(\cdot) \leq G_2 \end{array} \tag{71}$$

where $\overline{\Psi}_i(\cdot)$, $i = 0, 1$, are known positive non-decreasing functions.

It will be shown that in both cases A and B the mapping between the $\mathbf{x}-u$ and y_1-y_2 subspaces is such that *bounded domains in the state-control space correspond to bounded domains in the sliding variable phase space*, and vice–versa, and this allows to express both conditions (70) in the compact form

The problem is to find a feedback control law $v(t)$ capable of reducing y_1 and y_2 to zero. The control of system (62)-(71) is significantly more complex than that of system (62)-(66).

In the previous case, under the assumption of a global constant upper bound of $|\varphi(\cdot)|$, it was easy to identify a procedure guaranteeing a contractive behaviour of the trajectories in the $y_1 - y_2$ plane.

In the considered case, on the contrary, an upper bound of the uncertain drift term is found on-line, by relying on some forms of prediction of the system future behaviour.

More precisely, at each time instants $t = T_{M_k}$, it is necessary to identify a constant value Φ_k^*, which has the meaning of an expected upper bound of $|\varphi(\cdot)|$, such that a control law can be defined, depending on Φ_k^* and acting until $t = T_{M_{k+1}}$, which achieves the twofold task of forcing the contraction, that is $|y_1(T_{M_{k+1}})| < |y_1(T_{M_k})|$, and guaranteeing, at the same time, that $|\varphi(\cdot)| \leq \Phi_k^*$. This procedure gives rise to an algebraic loop in the controller design, which admits solution in strict dependence with the assumption made on the uncertain drift term.

As a result, the following Theorem can be proved

Theorem 1: *Consider system (62) with its uncertain dynamics satisfying (71) and y_2 not measurable but with known sign. Assume that the sequence of the singular values of $y_1(t)$, $y_{1_{M_k}} = y_1(T_{M_k})$, T_{M_k} s.t. $y_2(T_{M_k}) = 0$, $k = 1, 2, \ldots$, is available with ideal precision. Assume also that $|y_2(0)| \leq Y_{20M}$, where Y_{20M} is a known constant.*

The control strategy

$$v(t) = \begin{cases} -\frac{h}{G_1}\overline{\Phi}_0^*(t)\mathrm{sign}\{y_1(t) - y_1(0)\} & 0 \leq t \leq T_{M_1} \qquad h > 1 \\ -\alpha(t)V_{M_k}\mathrm{sign}\left[y_1(t) - \frac{1}{2}y_{1_{M_k}}\right] & T_{M_k} < t \leq T_{M_{k+1}} \qquad k = 1, 2, \ldots \end{cases} \tag{72}$$

$$\overline{\Phi}_0^*(t) = \overline{\Psi}_0(y_1(t)) + \overline{\Psi}_1(y_1(t))|Y_{20M}| \tag{73}$$

$$V_{M_k} = \eta\beta^*\overline{\Phi}_k^* \qquad \eta > 1 \qquad k = 1, 2, \ldots \tag{74}$$

$$\overline{\Phi}_k^* = \overline{\Psi}_0(y_{1_{M_k}}) + \frac{1}{2}a_k^2 + a_k\sqrt{4\overline{\Psi}_0(y_{1_{M_k}}) + a_k^2} \tag{75}$$

$$a_k = \overline{\Psi}_1(y_{1_{M_k}})|y_{1_{M_k}}|\sqrt{\alpha^* G_2\eta\beta^* + 1} \tag{76}$$

where

$$\begin{aligned} &\alpha(t) = \begin{cases} \alpha^* & if \;\; [y_1(t) - \frac{1}{2}y_{1_{M_k}}][y_{1_{M_k}} - y_1(t)] > 0 \\ 1 & if \;\; otherwise \end{cases} \\ &\alpha^* \in (0, \tfrac{3G_1}{G_2}) \cap (0, 1] \\ &\beta^* = max(\tfrac{1}{\alpha^* G_1}; \tfrac{4}{3G_1 - \alpha^* G_2}) \end{aligned} \tag{77}$$

causes the finite time convergence of the system trajectory to the origin of the state plane.

Proof: See the Appendix.

REMARK 1: Assumption (71) can be considered a particular case of more general conditions of the type

$$\begin{array}{l} |\varphi(\cdot)| \leq \sum_{i=0}^{N} \overline{\Psi}_i(y_1(t))|y_2(t)|^i \\ 0 < G_1 \leq g(\cdot) \leq G_2 \end{array} \tag{78}$$

with $N = 1$. A feasible solution could exist for $N = 2$ also, but at the price of the solution of very involved alebraic inequalities. For $N \geq 3$ no sufficient conditions for the convergence can be provided by existing methods. Such a generalization will be the object of future researches.

REMARK 2: The time-varying term $\overline{\Phi}_0^*(t)$ constitutes an upper bound of the drift term $\varphi(\cdot)$ for any $t \in [0, T_{M_1}]$, while the term $\overline{\Phi}_k^*$ has the meaning of a constant upper bound of the drift term $\varphi(\cdot)$, valid for any $t \in [T_{M_k}, T_{M_{k+1}})$, evaluated at $t = T_{M_k}$. The term Y_{20M} is an upper bound of the starting value of $|y_2|$.

REMARK 3: The on-line computation of $\overline{\Phi}_k^*$ could be not feasible as $T_{M_{k+1}} - T_{M_k}$ tends to zero. Due to the contraction of the sequence $|y_{1_{M_k}}|$, the sequence $\overline{\Phi}_k^*$ is monotone non increasing, and this means that $\overline{\Phi}_k^*$ is an upper bound of the drift term not only for $t \in [T_{M_k}, T_{M_{k+1}})$, but also for any $t \geq T_{M_k}$. Then, the adaptation of the control amplitude can be stopped, with no consequence on the contractive behaviour of $|y_{1_{M_k}}|$, at any time instant $t = T_{M_k}$. In any case, the adaptation of the gain reduces the control amplitude as the contractive process goes on, so that it is worth to continue it until the time interval $T_{M_{k+1}} - T_{M_k}$ is comparable with that needed to compute the new upper bound.

3.3 Sub-optimal SOSMC algorithm: the real accuracy

In real applications, the above *ideal* implementation of the sub-optimal algorithm is not feasible for two reasons: first, the control v will commute at very high (but non infinite) switching frequency, secondly, the sequence of the singular values of y_1, y_{1M_k}, will be available only approximately.

Let δ be the time delay between two successive switchings of v, and let the sequence y_{1M_k} be estimated by means of the following approximate peak-detector

APPROXIMATE PEAK DETECTOR

set $k = 0$, $y_{1M_0} = y_1(0)$ $y_1(t-\delta) = y_1(t-2\delta) = 0$ if $t < 2\delta$

set $\Delta(t)$=($y_1(t)$-$y_1(t-\delta)$)($y_1(t-\delta)$-$y_1(t-2\delta)$)

if $\Delta(t) < 0$ then { $k = k+1$

$y_{1M_k} = y_1(t-\delta)$ }

The consequence is that y_1 and y_2 converge to a residual set of the origin, whose size defines the real accuracy featured by the algorithm.

The FOSMC approach is well known to produce a sliding motion confined to a δ-vicinity of $y_1 = 0$.

SOSMC schemes have been proved to feature higher accuracy as compared with FOSMC ones [Levant '93, Bartolini et al. '97]. The size of the boundary layer in which the real sliding motion occurs is $O(\delta^2)$ and $O(\delta^2)$ as for y_1 and y_2, respectively.

More specifically, the following steady state accuracy is guaranteed by the use of 1-SMC and 2-SMC respectively

$$\begin{array}{cc} 1-SMC & 2-SMC \\ \\ |s| \approx O(\delta) & \left\{ \begin{array}{l} |s| \approx O(\delta^2) \\ |\dot{s}| \approx O(\delta) \end{array} \right. \end{array} \tag{79}$$

As it will be shown in the simulation results (sect 3.5, fig (15)) if the switching frequency is sufficiently high, then the difference of accuracy can be conspicuous.

3.4 Robust Stabilization of Nonlinear Uncertain Systems: the Second Order Sliding Mode Approach

Consider a single–input nonlinear uncertain system whose dynamics is defined by the differential system

$$\left\{ \begin{array}{ll} \dot{x}_i(t) = x_{i+1}(t) & i = 1, \dots, n-1 \\ \dot{x}_n(t) = f(\mathbf{x}(t)) + g(\mathbf{x}(t))u(t) & \end{array} \right. \tag{80}$$

where $\mathbf{x} = [x_1 \dots x_n]$ is the state variable. Assume that any solution of (80) is well defined for all t, provided $u(t)$ is bounded. The functions $f[\mathbf{x}(t)]$ and $g[\mathbf{x}(t)]$ are uncertain but satisfying proper boundedness inequalities which will be discussed later.

In this Section the problem of the asymptotic stabilization of system (80) is solved by means of the control strategy presented in the previous Section. The complete availability of the state is first assumed, and then the case in which the last component of the state vector, x_n, is not measurable is dealt with.

In the first case, the control problem falls within the case A, while in the latter the case B arises.

3.4.1 Case A: Full state availability (antichattering procedure)

Consider system (80), assume that the whole state vector is measurable, and choose as a sliding manifold

$$\sigma(\mathbf{x}(t)) = x_n(t) + \sum_{i=1}^{n-1} c_i x_i(t) = 0 \tag{81}$$

with c_i, $i = 1, \dots, n-1$, real positive constants such that $P(z) = z^{n-1} + \sum_{i=1}^{n-1} c_i z^{i-1}$ is a Hurwitz polynomial. Once on $s(\mathbf{x}(t)) = 0$, the system behaves like a reduced-order asymptotically stable linear system.

Consider now the first time derivative of $s[\mathbf{x}(t)]$, namely

$$\dot{\sigma}(\mathbf{x}(t)) = f\left(\mathbf{x}(t)\right) + g\left(\mathbf{x}(t)\right) u(t) + \sum_{i=1}^{n-1} c_i x_{i+1}(t) \tag{82}$$

consider the second derivative of σ

$$\ddot{\sigma}[\mathbf{x}(t)] = \frac{d}{dt} f\left[\mathbf{x}(t)\right] + \frac{d}{dt} g[\mathbf{x}(t)]u(t) + c_{n-1}\left[f\left[\mathbf{x}(t)\right] + g\left[\mathbf{x}(t)\right]u(t)\right] + \sum_{i=1}^{n-2} c_i x_{i+2}(t) \\ + g\left[\mathbf{x}(t)\right]\dot{u}(t) \tag{83}$$

Set $y_1(t) = \sigma$ and $y_2(t) = \dot{\sigma}$, then, the system dynamics (80) along with the second order sliding variable dynamics (82), (83), can be rewritten in the form

$$\begin{cases} \dot{\hat{\mathbf{x}}}(t) & = \hat{\mathbf{A}}\hat{\mathbf{x}}(t) + \hat{\mathbf{b}}y_1(t) \\ x_n(t) & = -\hat{\mathbf{c}}\hat{\mathbf{x}} + y_1(t) \\ \dot{y}_1(t) & = y_2(t) \\ \dot{y}_2(t) & = \mathcal{F}_1[\mathbf{x}(t)] + \mathcal{F}_2[\mathbf{x}(t)]u(t) + \frac{\partial g}{\partial x_n} g[\mathbf{x}(t)]u^2(t) + g[\mathbf{x}(t)]\dot{u}(t) \end{cases} \tag{84}$$

where $\hat{\mathbf{x}} = [x_1, x_2, \ldots, x_{n-1}]^T$, $\hat{\mathbf{c}} = [c_1, c_2, \ldots, c_{n-1}]$, $\hat{\mathbf{A}}$ is a $(n-1)\times(n-1)$–matrix in companion form with the last row coinciding with vector $-\hat{\mathbf{c}}$, $\hat{\mathbf{b}} = [0, \ldots, 0, 1]^T \in \Re^{n-1}$, and $\mathcal{F}_1[\mathbf{x}(t)]$, $\mathcal{F}_2[\mathbf{x}(t)]$ collect all the uncertainties not involving $u(t)$, $u^2(t)$ and $\dot{u}(t)$.

Note that the first two lines of (84) correspond to a stable linear system controlled by $y_1(t)$.

Setting $y_1 = 0$ yields the so-called *system's zero-dynamics* with respect to the "output" y_1. The global asymptotic stability (GAS) of the zero-dynamics implies that the control objective (robust stabilization of $\mathbf{x}$) is simply fulfilled by steering to zero the sliding output y_1.

The second two equations of (84), called the *input-output dynamics*, correspond to a non linear uncertain second-order system with control $\dot{u}(t)$ and with $y_2(t)$ not available for measurements, to be stabilized to attain the control task.

The input-output dynamics is coupled with the first two lines of (84) through the state-dependent uncertainty terms.

If the time derivative of the plant control, $\dot{u}(t)$, is considered as the control variable, the 2–sliding mode control approach allows to design a suitable discontinuous control signal $\dot{u}(t)$ steering both the sliding variable σ and its time derivative $\dot{\sigma}$ to zero, so that the actual plant control $u(t)$ is continuous and chattering is avoided [Levant '93, Bartolini et al. '98b].

As for the system uncertain dynamics, assume what follows

$$|f[\mathbf{x}(t)]| \leq F[\|\mathbf{x}(t)\|] \tag{85}$$

$$0 < G_1 \leq g[\mathbf{x}(t)] \leq G_2 \tag{86}$$

$$\left|\frac{\partial f[\mathbf{x}(t)]}{\partial x_i}\right| \leq F_{d_i}[\|\mathbf{x}(t)\|] \qquad i = 1, 2, \ldots, n \tag{87}$$

$$\left|\frac{\partial g[\mathbf{x}(t)]}{\partial x_i}^T\right| \leq G_{d_i}[\|\mathbf{x}(t)\|] \qquad i = 1, 2, \ldots, n-1 \tag{88}$$

$$\frac{\partial g[\mathbf{x}(t)]}{\partial x_n} = 0 \tag{89}$$

where $F[\|\mathbf{x}(t)\|]$, $F_{d_i}[\|\mathbf{x}(t)\|]$, $G_{d_i}[\|\mathbf{x}(t)]\|$ are known positive non-decreasing functions and G_1, G_2 are known positive constants.

The traditional sliding mode control approach (FOSMC) consists in using the relay control

$$u(t) = -U(\mathbf{x}(t))sign(\sigma) \tag{90}$$

where the control amplitude $U[\mathbf{x}(t)]$ is chosen as

$$U(\mathbf{x}(t)) = \frac{F\left(\mathbf{x}(t)\right) + \sum_{i=1}^{n-1} |c_i x_{i+1}(t)| + \eta}{G_1} \qquad \eta > 0 \tag{91}$$

so that the invariance condition $\sigma\dot{\sigma} < -k^2|\sigma|$ holds. FOSMC acts discontinuously on $\dot{\sigma}$, and, as a result, the chattering phenomenon arises.

This control strategy globally satisfies the control objective. As a result, the control is a signal with non null amplitude switching at theoretically infinite frequency. In many practical cases this regime cannot be implemented because of chattering. The idea is to attain the same objective (that is the finite-time reaching of the sliding manifold (81)) by means of a continuous control.

This can be done by enforcing a second order sliding mode on the same manifold, by using the derivative of the actual control, $\dot{u}(t)$, as the discontinuous control signal to which to attribute the task of robustly stabilizing the controlled plant.

Now refer to the results of Theorem 1, in which it is explicitly stressed the role played by the quantities $\overline{\Phi}_0^*(t)$, $\overline{\Phi}_k^*$ and Y_{20M} in ensuring the contractive behaviour featured by the proposed control algorithm (see REMARK 2). While in Theorem 1 the above quantities have been evaluated on the basis of uncertainty bounds expressed in terms of y_1 and y_2 only, in this section the same procedure is followed by considering the full-state dependent uncertainty bound. To this end, the following Theorem is proved

Theorem 2: *Consider system (*80), with its uncertain dynamics satisfying ((85)-(89)) and with be completely available state. The, the control law

$$\dot{u}(t) = \begin{cases} -\frac{h}{G_1}\overline{\Phi}_0^*(t)\text{sign}\left[y_1(0)\right] & 0 \le t \le T_{M_1} \qquad h > 1 \\ -\alpha(t)V_{M_k}\text{sign}\left[y_1(t) - \frac{1}{2}y_{1_{M_k}}\right] & T_{M_k} < t \le T_{M_{k+1}} \qquad k = 1, 2, \ldots \end{cases} \tag{92}$$

$$u(0) = \frac{1}{G_1}[F[\|\mathbf{x}(0)\|] + |\sum_{i=1}^{n-1} c_i x_{i+1}(0)| + k]sign\left[y_1(0)\right] \qquad k > 0 \tag{93}$$

where

$$\overline{\Phi}_0^*(t) = \overline{\mathcal{F}}_{1M}[\|\mathbf{x}(t)\|] + \overline{\mathcal{F}}_{2M}[\|\mathbf{x}(t)\|]Y_{20M} \tag{94}$$

$$\overline{\mathcal{F}}_{1M}[\|\mathbf{x}(t)\|] = (c_{n-1} + \frac{1}{G_1} + F_{d_n}[\|\mathbf{x}(t)\|])F[\|\mathbf{x}(t)\|] + (\sum_{i=1}^{n-1} F_{d_i}[\|\mathbf{x}(t)\|] + \sum_{i=1}^{n-2} c_i)\|\mathbf{x}(t)\| \tag{95}$$

$$\overline{\mathcal{F}}_{2M}[\|\mathbf{x}(t)\|] = \frac{G_2}{G_1}(F_{d_n}[\|\mathbf{x}(t)\|] + c_{n-1}) + \frac{1}{G_1}\sum_{i=1}^{n-1} G_{d_i}[\|\mathbf{x}(t)\|]\|\mathbf{x}(t)\| \tag{96}$$

$$Y_{20M} = F[\|\mathbf{x}(0)\|] + |\sum_{i=1}^{n-1} c_i x_{i+1}(0)| + G_2 u(0) \tag{97}$$

and

$$
\begin{aligned}
V_{M_k} &= \eta\beta^*\overline{\Phi}_k^* \qquad\qquad\qquad \eta > 1 \qquad k = 1, 2, \ldots && (98)\\
\overline{\Phi}_k^* &= \overline{\mathcal{F}}_{1M}[\|\mathbf{x}(t)\|_{M_k}] + \frac{1}{2}a_k^2 + a_k\sqrt{4\overline{\mathcal{F}}_{1M}[\|\mathbf{x}(t)\|_{M_k}] + a_k^2} && (99)\\
a_k &= \overline{\mathcal{F}}_{2M}[\|\mathbf{x}(t)\|_{M_k}]|y_{1_{M_k}}|\sqrt{\alpha^* G_2\eta\beta^* + 1} && (100)\\
\|\mathbf{x}(t)\|_{M_k} &= Q_x\|\mathbf{x}(T_{M_k})\| + Q_y y_{1_{M_k}} && (101)
\end{aligned}
$$

moreover, y_1 is defined as in (81), T_{M_k} are the time instants at which $y_2(t)$ is zero, $y_{1_{M_k}} = y_1(T_{M_k})$, Q_x, Q_y are properly defined constants (see [Bartolini et al. '98b]), and

$$
\begin{aligned}
\alpha(t) = &\begin{cases} \alpha^* & if\ \ [y_1(t) - \frac{1}{2}y_{1_{M_k}}][y_{1_{M_k}} - y_1(t)] > 0 \\ 1 & if\ \ otherwise \end{cases}\\
&\qquad\alpha^* \in (0, \tfrac{3G_1}{G_2}) \cap (0, 1]\\
&\qquad\beta^* = max(\tfrac{1}{\alpha^* G_1}; \tfrac{4}{3G_1 - \alpha^* G_2})
\end{aligned} \qquad (102)
$$

causes the state $\mathbf{x}$ to exponentially converge to zero for any initial condition $\mathbf{x}(0)$.

Proof. See the appendix.

3.4.2 Systems with relative degree two

Consider system (80), and assume that x_n is not measurable.

The robust state stabilization can be achieved by enforcing a 2-sliding mode on the reduced-order manifold

$$\sigma(\mathbf{x}(t)) = x_{n-1}(t) + \sum_{i=1}^{n-2} c_i x_i(t) = 0 \qquad (103)$$

Double differentiating σ, it yields

$$\dot{\sigma}(t) = x_n(t) + \sum_{i=1}^{n-2} c_i x_{i+1}(t) \qquad (104)$$

$$\ddot{\sigma}(t) = f[\mathbf{x}(t)] + \sum_{i=1}^{n-2} c_i x_{i+2}(t) + g[\mathbf{x}(t)]u(t) \qquad (105)$$

The overall dynamics can be written, in analogy with (84), as

$$
\begin{cases}
\dot{\tilde{\mathbf{x}}}(t) = \tilde{\mathbf{A}}\tilde{\mathbf{x}}(t) + \tilde{\mathbf{b}}y_1(t)\\
x_{n-1}(t) = -\tilde{\mathbf{c}}\tilde{\mathbf{x}} + y_1(t)\\
x_n(t) = c_{n-2}\tilde{\mathbf{c}}\tilde{\mathbf{x}} - \sum_{i=1}^{n-3} c_i x_{i+1}(t) - c_{n-2}y_1(t) + y_2(t)\\
\dot{y}_1(t) = y_2(t)\\
\dot{y}_2(t) = f[\mathbf{x}(t)] + \sum_{i=1}^{n-2} c_i x_{i+2}(t) + g[\mathbf{x}(t)]u(t)
\end{cases} \qquad (106)
$$

where $\tilde{\mathbf{x}} = [x_1, x_2, \ldots, x_{n-2}]^T$, $\tilde{\mathbf{c}} = [c_1, c_2, \ldots, c_{n-2}]$, $\tilde{\mathbf{A}}$ is a $(n-2)\times(n-2)$–matrix in companion form with the last row coinciding with vector $-\tilde{\mathbf{c}}$ and $\tilde{\mathbf{b}} = [0, \ldots, 0, 1]^T \in \Re^{n-2}$.

The first three lines of (106) correspond to a stable linear system controlled by y_1 and y_2.

Setting $y_1 = y_2 = 0$ yields the so-called *system's zero-dynamics* with respect to the "output" $[y_1 y_2]$. The global asymptotic stability (GAS) of the zero-dynamics implies that the control objective can be fulfilled by steering to zero the sliding output y_1 and its derivative y_2.

The last two equations of (106) are the *input-output dynamics*, a non linear uncertain second-order system with control $u(t)$ and with $y_2(t)$ not available for measurements.

Also in this case, the input-output dynamics is coupled with the first three lines of (84) through the state-dependent uncertainty terms.

Assume that the uncertainties satisfy the following conditions

$$|f[\mathbf{x}(t)]| \leq F(\|\hat{\mathbf{x}}\|) + Q_f|x_n| \tag{107}$$

$$0 < G_1 \leq g[\mathbf{x}(t)] \leq G_2 \tag{108}$$

where $\hat{\mathbf{x}} = [x_1, x_2, \ldots, x_{n-1}]^T$, $F(\|\hat{\mathbf{x}}\|)$ is a positive non-decreasing function, Q_f, G_1, G_2 are positive real constants.

Note that FOSMC in its standard formulation cannot be applied as the control does not affect $\dot{s}$. In this case, the SOSMC approach can be used to define a suitable discontinuous control $u(t)$ that causes the whole state vector components $x_i(t)$, $i = 1, 2, \ldots, n$, to converge to zero despite of the unavailability of $x_n(t)$.

Following the same guidelines as in the previous subsection, the following Theorem can be proved

Theorem 3: *Consider system* (80)*, with x_n not available and with its uncertain dynamics satisfying* (107)*,* (108)*. Let a positive constant $X_{n0_{MAX}}$ is known such that $|x_n(0)| \leq X_{n0_{MAX}}$.*

The control law

$$u(t) = \begin{cases} -\frac{h}{G_1}\overline{\Phi}_0^*(t)\text{sign}\left[y_1(t) - y_1(0)\right] & 0 \leq t \leq T_{M_1} \qquad h > 1 \\ -\alpha(t)V_{M_k}\text{sign}\left[y_1(t) - \frac{1}{2}y_{1_{M_k}}\right] & T_{M_k} < t \leq T_{M_{k+1}} \qquad k = 1, 2, \ldots \end{cases} \tag{109}$$

where

$$\overline{\Phi}_0^*(t) = \overline{\mathcal{F}}_{1M}[\|\hat{\mathbf{x}}(t)\|] + (c_{n-2} + Q_f)Y_{20M} \tag{110}$$

$$\overline{\mathcal{F}}_{1M}[\|\hat{\mathbf{x}}(t)\|] = F(\|\hat{\mathbf{x}}\|) + \left(\sum_{i=1}^{n-3} c_i + (c_{n-2} + Q_f)\sum_{i=1}^{n-2} c_i\right)\|\hat{\mathbf{x}}(t)\| \tag{111}$$

$$Y_{20M} = X_{n0_{MAX}} + \sum_{i=1}^{n-2} c_i x_{i+1}(0) \tag{112}$$

and

$$V_{M_k} = \eta\beta^*\overline{\Phi}_k^* \qquad \eta > 1 \qquad k = 1, 2, \ldots \tag{113}$$

$$\overline{\Phi}_k^* = \overline{\mathcal{F}}_{1M}[\|\hat{\mathbf{x}}(t)\|_{M_k}] + \frac{1}{2}a_k^2 + a_k\sqrt{4\overline{\mathcal{F}}_M[\|\mathbf{x}(t)\|_{M_k}] + a_k^2} \tag{114}$$

$$a_k = |y_{1_{M_k}}|(c_{n-2} + Q_f)\sqrt{\alpha^* G_2 \eta \beta^* + 1} \quad (115)$$

$$\|\hat{\mathbf{x}}(t)\|_{M_k} = Q_x \|\hat{\mathbf{x}}(T_{M_k})\| + Q_y y_{1_{M_k}} \quad (116)$$

moreover y_1 is chosen as in (103), T_{M_k} are the time instants at which $y_2(t)$ is zero, $y_{1_{M_k}} = y_1(T_{M_k})$, Q_x, Q_y are properly defined constants (see [Bartolini et al. '98b]), *and*

$$\alpha(t) = \begin{cases} \alpha^* & if \;\; [y_1(t) - \frac{1}{2} y_{1_{M_k}}][y_{1_{M_k}} - y_1(t)] > 0 \\ 1 & if \;\; otherwise \end{cases}$$
$$\alpha^* \in (0, \tfrac{3G_1}{G_2}) \cap (0, 1]$$
$$\beta^* = max(\tfrac{1}{\alpha^* G_1}; \tfrac{4}{3G_1 - \alpha^* G_2}) \quad (117)$$

causes the state $\mathbf{x}$ to exponentially converge to zero for any initial condition $\hat{\mathbf{x}}(0)$.

Proof. See the appendix.

3.5 Simulation Results

Consider system (80) with $n = 3$ and

$$\begin{cases} f[\mathbf{x}, t] = 3 \cdot e^{x_1} + 5x_2 \cdot sin(20 \cdot t + x_1) cos(x_2^2 + x_3^2) \\ g[\mathbf{x}, t] = 3 + sin(3 \cdot t + x_1 + x_2) \end{cases} \quad (118)$$

The state vector is assumed to be completely available for measurements. The initial conditions are $\mathbf{x}(0) = [2, 2, 2]$. The control objective is that of asymptotically reducing the state vector components to zero, and, to this end, the sliding manifold is defined as

$$s[\mathbf{x}(t)] = x_3(t) + 8 \cdot x_2(t) + 16 \cdot x_1(t) \quad (119)$$

The known informations about the controlled plant are the following

$$\begin{array}{ll} |f(\mathbf{x}, t)| \leq 3 \cdot e^{x_1} + 5|x_2| & 2 \leq |g(\mathbf{x}, t)| \leq 4 \\ |\frac{\partial f}{\partial x_1}| \leq 3 \cdot e^{x_1} + 5|x_2| & |\frac{\partial f}{\partial x_2}| \leq 5 + 10x_2^2 \\ |\frac{\partial f}{\partial x_3}| \leq 10|x_2 x_3| & |\frac{\partial f}{\partial t}| \leq 100|x_2| \\ |\frac{\partial g}{\partial x_1}| \leq 1 & |\frac{\partial g}{\partial x_2}| \leq 1 \\ \frac{\partial g}{\partial x_n} = 0 & |\frac{\partial g}{\partial t}| \leq 3 \end{array} \quad (120)$$

The FOSMC control strategy (90) is first applied, with

$$U[\mathbf{x}(t)] = 1.5 \cdot e^{x_1} + 4.5 \cdot |x_2(t)| + 2 \cdot |x_3(t)| + 5 \quad (121)$$

The average control $u_{av}(t)$ is detected by means of a first order low-pass filter [Utkin '92]

$$\tau \dot{u}_{av}(t) + u_{av}(t) = u(t) \tag{122}$$

with τ=0.02. To attain the same control objective by continuous control, the anti-chattering SOSMC procedure (92)-(102) is then implemented with the same sliding manifold.

The results are depicted in Figg. 15-20.

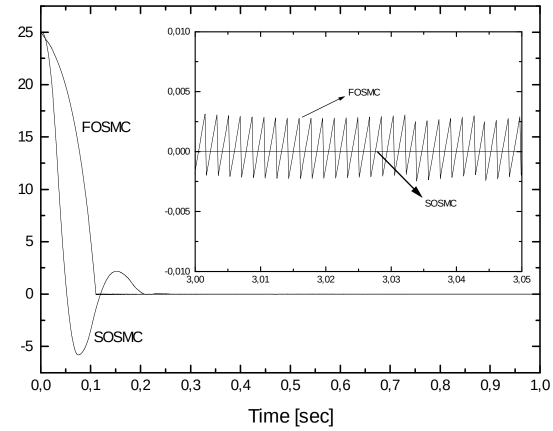

Figure 15: FOSMC and SOSMC (anti-chattering procedure). The sliding quantity.

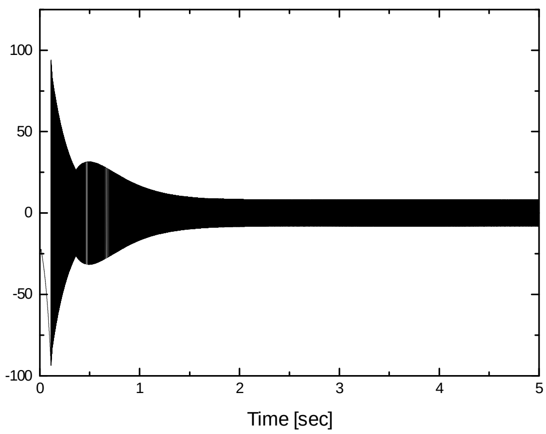

Figure 16: FOSMC. The Control input

In Fig. 15 the transient behaviour of the sliding variable is depicted, with a zoom highlighting the higher accuracy featured by the SOSMC scheme. In Fig. 16 the discontinuous FOSMC plant input is reported, and in Fig. 17 its average component is compared with the equivalent control. In Fig. 18 the actual SOSMC plant input is shown to track the equivalent control without any intermediate filtering. In Fig. 19 the convergence to zero of both the sliding variable and its derivative is put into evidence. Finally, in Fig. 20 the state behaviour is depicted.

Assuming x_3 not available, the SOSMC scheme (109)-(117) is applied using the manifold

$$s(\mathbf{x}) = x_2 + 4x_1 \tag{123}$$

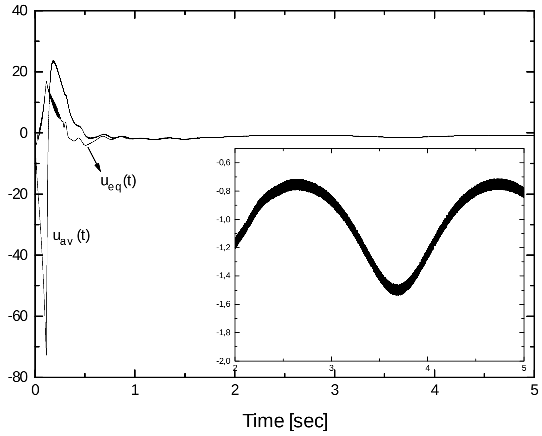

Figure 17: FOSMC. The equivalent control and the filtered discontinuos control

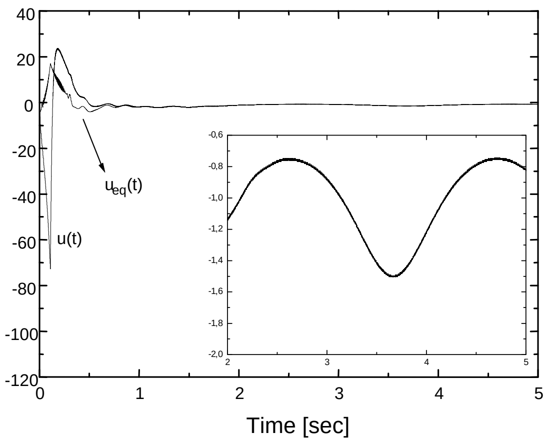

Figure 18: SOSMC (antichattering procedure). The actual control and the equivalent control.

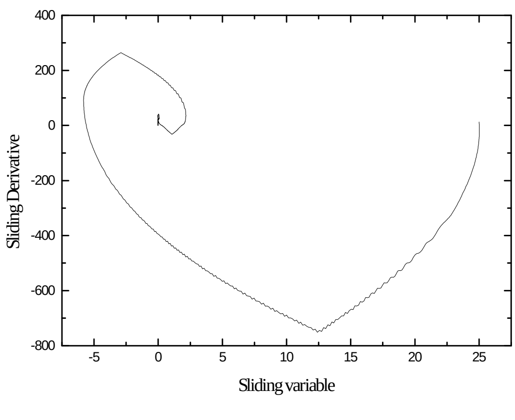

Figure 19: SOSMC (antichattering procedure). The sliding variable and its derivative.

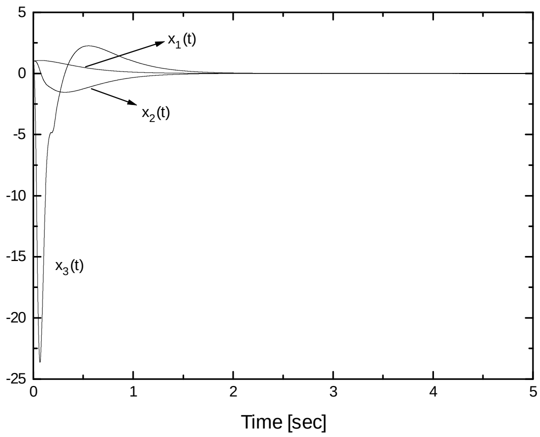

Figure 20: SOSMC (anti-chattering procedure). The state vector components.

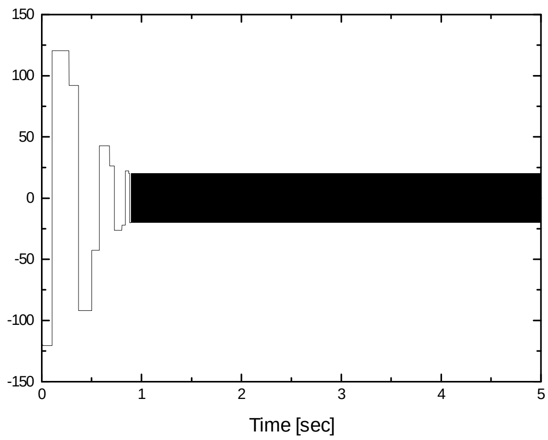

Figure 21: SOSMC (relative degree two systems). The actual control.

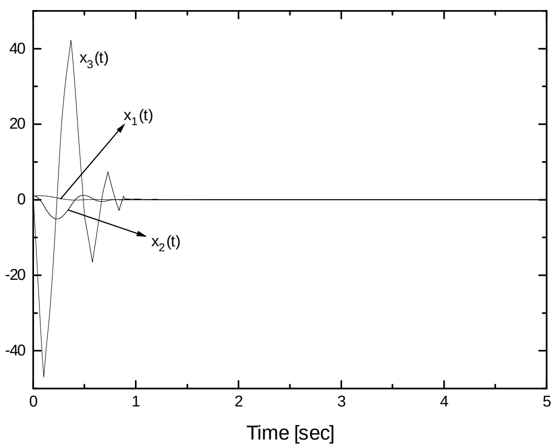

Figure 22: SOSMC (relative degree two systems) The state vector components.

Figg. 21 and 22 show the discontinuous plant input and the corresponding state behaviour respectively.

3.6 Summary

The new results presented in this chapter are based on [Bartolini et al. 2000] in which a generalization of the sub-optimal second order sliding mode control algorithm, relevant to the form of the allowed uncertainties with respect to which the global finite time reaching of the sliding mode behaviour is guaranteed, has been presented. Based on these results, an improved control law for the elimination of the chattering phenomenon has been introduced, and a feasible approach for stabilizing systems with incomplete state availability is proposed.

This research appears to be a promising prelude to further developments of the sliding mode control theory, e.g., multi–input systems and observers, and lend itself to immediate applications in advanced robotics and other important topics.

APPENDIX

Proof. of Theorem 1

Initialization - The idea is to prove that the initialization phase is such that the axis $y_2(t) = 0$ is reached in a finite time T_{M_1}.

By applying (72), until the first singular value of $y_1(t)$ is reached, one has

$$\dot{y}_2(t) = \varphi(\cdot) - h\frac{g(\cdot)}{G_1}\left(\overline{\Psi}_0(y_1(t)) + \overline{\Psi}_1(y_1(t))|Y_{20M}|\right)\text{sign}\{y_2(t_0)\} \tag{124}$$

It is easy to check that, for any $[y_1(0), y_2(0)]$, by considering (71) and (124), $\dot{y}_2(0)y_2(0) < 0$, then $|y_2|$ starts to decrease; as a consequence, the control dominance is always ensured. Thus, the sign of $\dot{y}_2$ is forced to be opposite to that of y_2, and $y_2(t) \to 0$ in finite time.

General case - It has been proved that a first singularity point $(y_{1_{M_1}}, 0)$ is reached in finite time at $t = t_{M_1}$. Let $y_{1_{M_k}}$ be the k–th singular value of $y_1(t)$, t_{M_k} the corresponding time instant and t_{c_k} the time instant, subsequent to t_{M_k}, at which a control switching occurs ($k = 1, 2, \ldots$).

Suppose, without lost of generality, that the actual value of the $k-th$ singular value is positive. Analogous consideration are still valid if $y_{1_{M_k}} < 0$.

The proof of the finite time convergence to the origin of the y_1Oy_2 plane can be split into the following steps. First it is proved that the control law causes a sequence of singular values featuring the contraction condition

$$|y_{1_{M_{k+1}}}| < \gamma^2|y_{1_{M_k}}| \qquad 0 \leq \gamma^2 < 1 \qquad k = 1, 2, \ldots \tag{125}$$

which implies that the system trajectory approaches the origin of the state plane. Then, such a contraction is proved to occur in a finite time.

Contraction property:

Let Φ_k be the maximum modulus of the drift term $\varphi(\cdot)$ in the time interval between two subsequent singular values, i.e. $|\varphi(\cdot)| \leq \Phi_k$, $t \in [T_{M_k}, T_{M_{k+1}}]$.

If the control amplitude is chosen such that

$$\alpha^* G_1 V_{M_k} > \Phi_k \tag{126}$$

then, taking into account (72), the system dynamics is such that

$$-(\Phi_k + G_2\alpha^* V_{M_k}) \leq \dot{y}_2(t) \leq -(G_1\alpha^* V_{M_k} - \Phi_k) \qquad t \in [T_{M_k}, T_{c_k}) \tag{127}$$

$$G_1 V_{M_k} - \Phi_k \leq \dot{y}_2(t) \leq \Phi_k + G_2 V_{M_k} \qquad t \in [T_{c_k}, T_{M_{k+1}}) \tag{128}$$

The above inequalities can be intended in terms of parabolic limiting curves, the actual system trajectory being confined between two limiting arcs (see fig. 23).

By considering the worst-case trajectory along the limiting curves, that is that to which corresponds the faster decrease of y_2 in the time interval $[T_{M_k}, T_{c_k})$ and the slower increase of y_2 in the time interval $[T_{c_k}, T_{M_{k+1}})$, the following relationships hold

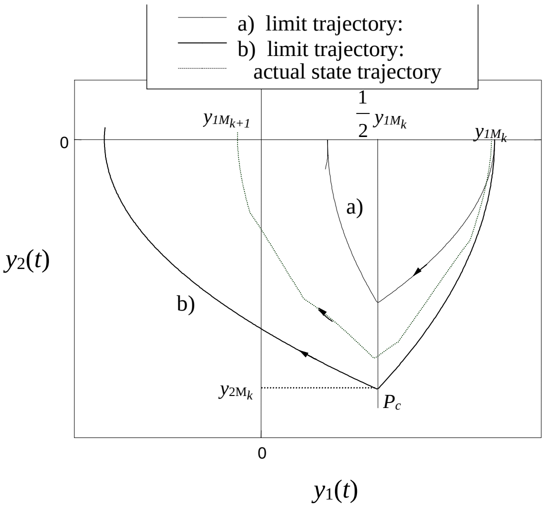

Figure 23: The 2-sliding trajectory

$$|y_2(T_{c_k})| = max_{t \in [T_{M_k}, T_{M_{k+1}}]} \{|y_2(t)|\} \leq y_{2_{M_k}} = \sqrt{|y_{1_{M_k}}|((\Phi_k + G_2 \alpha^* V_{M_k}))} \tag{129}$$

$$\frac{y_{1_{M_{k+1}}}}{y_{1_{M_k}}} \in [-\frac{(\alpha^* G_2 - G_1)V_{M_k} + 2\Phi_k}{2(G_1 V_{M_k} - \Phi_k)}; \frac{(G_2 - \alpha^* G_1)V_{M_k} + 2\Phi_k}{2(G_1 V_{M_k} + \Phi_k)}] \tag{130}$$

Taking into account the definition of the modulation parameter $\alpha(t)$, from (126) and (130) it follows that a sufficient condition for the contraction condition (125) to occur is that the following system of inequalities is satisfied

$$\begin{cases} \alpha^* > 0 \\ \alpha^* \leq 1 \\ \alpha^* G_1 V_{M_k} > \Phi_k \\ \frac{(\alpha^* G_2 - G_1)V_{M_k} + 2\Phi_k}{2(G_1 V_{M_k} - \Phi_k)} < 1 \end{cases} \tag{131}$$

The above relationships are based on the existence of the upper bound Φ_k of $|\varphi(\cdot)|$ in $[T_{M_k}$, $T_{M_{k+1}}]$. To prove that such a bound exists, and to evaluate an its overestimate, an algebraic loop has to be solved.

In fact, as mentioned in the paper, the control amplitude depends on the uncertainty bound, but, at the same time, the uncertainty bound depends on the control through the uncertain, state-dependent, term $\varphi(\cdot)$. The existence of a solution to this loop is strictly connected to the assumptions made on the uncertain dynamics.

Consider the following bounds on the uncertainties

$$\begin{array}{l} |\varphi(\cdot)| \leq \sum_{i=0}^{N} \overline{\Psi}_i(y_1(t))|y_2(t)|^i \\ 0 < G_1 \leq g(\cdot) \leq G_2 \end{array} \tag{132}$$

where N is an integer number and $\overline{\Psi}_i(\cdot)$ are non decreasing positive functions.

Let $\overline{\Phi}_k$ be an overestimate of the unknown bound Φ_k.

$$\begin{aligned}\Phi_k &\leq \sum_{i=0}^{N} \overline{\Psi}_i(y_{1_{M_k}})|y_{2_{M_k}}|^i = \sum_{i=0}^{N} \overline{\Psi}_i(y_{1_{M_k}}) \left(\sqrt{|y_{1_{M_k}}|(\Phi_k + G_2\alpha^* V_{M_k})}\right)^i = \\ &= \sum_{i=0}^{N} \overline{\Psi}_i(y_{1_{M_k}})|y_{1_{M_k}}|^{\frac{i}{2}}(\Phi_k + G_2\alpha^* V_{M_k})^{\frac{i}{2}} \leq \\ &\leq \sum_{i=0}^{N} \overline{\Psi}_i(y_{1_{M_k}})|y_{1_{M_k}}|^{\frac{i}{2}}(\overline{\Phi}_k + G_2\alpha^* V_{M_k})^{\frac{i}{2}} \leq \overline{\Phi}_k\end{aligned} \tag{133}$$

A sufficient condition for the inequality

$$\overline{\Phi}_k \geq \sum_{i=0}^{N} \overline{\Psi}_i(y_{1_{M_k}})|y_{1_{M_k}}|^{\frac{i}{2}}(\overline{\Phi}_k + G_2\alpha^* V_{M_k})^{\frac{i}{2}} \tag{134}$$

to admit solution is that the growth of the right-hand side with respect to $\overline{\Phi}_k$ is slower than that of the left-hand side. This implies that the N parameter has to be less than 2, and this condition is satisfied by choosing $N = 1$.

In that case, (134) reduces to

$$\overline{\Phi}_k \geq \overline{\Psi}_0(y_{1_{M_k}}) + \overline{\Psi}_1(y_{1_{M_k}})\sqrt{|y_{1_{M_k}}|(\alpha^* G_2 V_{M_k} + \overline{\Phi}_k^*)} \tag{135}$$

which admits solution on a semi-infinite interval, i.e. there exists a positive number $\overline{\Phi}_k^* = \overline{\Phi}_k^*(y_{1_{M_k}})$ such that condition (135) holds for any $\overline{\Phi}_k \geq \overline{\Phi}_k^*$. It is convenient to choose the lower bound of the interval ,$\overline{\Phi}_k^*$, as an overestimate of the unknown upper bound Φ_k to be used in the definition of the control law, i.e.

$$\overline{\Phi}_k^* = \overline{\Psi}_0(y_{1_{M_k}}) + \overline{\Psi}_1(y_{1_{M_k}})\sqrt{|y_{1_{M_k}}|(\alpha^* G_2 V_{M_k} + \overline{\Phi}_k^*)} \tag{136}$$

Since the left-hand side of the fourth of (131) is an increasing function of $\overline{\Phi}_k$, system (131) with $\Phi_k = \overline{\Phi}_k^*$ is still a sufficient condition for the contraction.

To explicitly find Φ_k^*, substitute (74) into (136) and solve the resulting second order algebraic equation. The positive root is given by (75)-(76).

For $N = 2$, both sides of (134) increase with the same degree with respect to $\overline{\Phi}_k$. However, if the slope of the right-hand side of (134) is less than one, that is

$$\overline{\Psi}_2(y_{1_{M_k}})|y_{1_{M_k}}|(G_2\alpha^*\eta\beta^* + 1) < 1 \tag{137}$$

then a solution exists. In this case, it cannot be ensured that the overall system (131)-(137) has a not empty solution set, and the existence of a solution must be investigated case by case. Moreover, the dependence on $|y_{1_{M_k}}|$ could make the attained result valid in a neighbourhood of the sliding manifold.

The contraction condition with respect to V_{M_k} and α^* turns out to be given by

$$V_{M_k} > \begin{cases} \frac{\overline{\Phi}_k^*}{\alpha^* G_1} & if \;\; \alpha^* \in (0, \frac{3G_1}{4G_1+G_2}] \\ \frac{4\overline{\Phi}_k^*}{3G_1 - \alpha^* G_2} & if \;\; \alpha^* \in (\frac{3G_1}{4G_1+G_2}, 1] \cap (\frac{3G_1}{4G_1+G_2}, \frac{3G_1}{G_2}) \end{cases} \tag{138}$$

which is true by assumption.

From (130) the following is true

$$|y_{1_{M_{k+1}}}| \leq \frac{1}{2} max \left\{ \frac{(|\alpha^* G_2 - G_1) V_{M_k} + 2\Phi_k|}{2(G_1 V_{M_k} - \Phi_k)}; \frac{(G_2 - \alpha^* G_1) V_{M_k} + 2\Phi_k}{2(G_1 V_{M_k} + \Phi_k)} \right\} |y_{1_{M_k}}| \tag{139}$$

Thus, it is possible to define

$$\gamma^2 = \frac{1}{2} max_k \left\{ max \left\{ \frac{(|\alpha^* G_2 - G_1) V_{M_k} + 2\Phi_k|}{2(G_1 V_{M_k} - \Phi_k)}; \frac{(G_2 - \alpha^* G_1) V_{M_k} + 2\Phi_k}{2(G_1 V_{M_k} + \Phi_k)} \right\} \right\} \tag{140}$$

so that (125) holds. Recursively, taking into account (130),

$$\begin{cases} |y_{1_{M_{k+1}}}| \leq \gamma^{2k} |y_{1_{M_1}}| \\ |y_{2_{M_k}}| \leq \gamma^{k-1} \sqrt{|y_{1_{M_1}}| (\Phi_k + G_2 \alpha^* V_{M_k})} \end{cases} \tag{141}$$

which implies that

$$\begin{cases} lim_{k \to \infty} |y_{1_{M_k}}| = 0 \\ lim_{k \to \infty} |y_{2_{M_k}}| = 0 \end{cases} \tag{142}$$

Finite time convergence:

Starting from $y_{1_{M_k}}$ at time instant $t = T_{M_k}$, and considering the slowest limit curve defined by

$$\begin{cases} \varphi(\cdot) = \Phi_k sign(y_2(t)) \\ g\left[\mathbf{x}(t)\right] = G_2 \quad if \;\; \alpha(t) = \alpha^* \\ g\left[\mathbf{x}(t)\right] = G_1 \quad if \;\; \alpha(t) = 1 \end{cases} \tag{143}$$

one obtains by means of simple algebraic computations

$$t_{M_{k+1}} = t_{M_k} + \frac{(G_1 + \alpha^* G_2) V_{M_k}}{(G_1 V_{M_k} - \Phi_k)} \sqrt{\frac{|y_{1_{M_k}}|}{\alpha^* G_2 V_{M_k} + \Phi_k}} \tag{144}$$

Taking into account (74), (144) can be rewritten as

$$t_{M_{k+1}} = t_{M_k} + \frac{(G_1 + \alpha^* G_2) \eta \beta^* \overline{\Phi}_k^*}{(G_1 \eta \beta^* \overline{\Phi}_k^* - \Phi_k)} \sqrt{\frac{|y_{1_{M_k}}|}{\alpha^* G_2 \eta \beta^* \overline{\Phi}_k^* + \Phi_k}} \tag{145}$$

Since the ratio

$$\frac{(G_1 + \alpha^* G_2) \eta \beta^* \overline{\Phi}_k^*}{(G_1 \eta \beta^* \overline{\Phi}_k^* - \Phi_k)} \tag{146}$$

is a monotone increasing function of Φ_k, an upper bound of (146) can be defined as that corresponding to $\Phi_k = \overline{\Phi}_k^*$, that is

$$\frac{(G_1 + \alpha^* G_2) \eta \beta^*}{(G_1 \eta \beta^* - 1)} \tag{147}$$

The square root argument in (145) can be maximized by minimizing its denominator.

$$t_{M_{k+1}} = t_{M_k} + \frac{(G_1 + \alpha^* G_2)\eta\beta^*}{(G_1\eta\beta^* - 1)}\sqrt{\frac{|y_{1_{M_k}}|}{\alpha^* G_2 \eta\beta^* \overline{\Psi}(0)}} \tag{148}$$

from which, recursively,

$$t_{M_{k+1}} = t_{M_1} + \frac{(G_1 + \alpha^* G_2)\eta\beta^*}{(G_1\eta\beta^* - 1)(\alpha^* G_2 \eta\beta^* \overline{\Psi}(0))}\sum_{j=1}^{k}\sqrt{|y_{1_{M_k}}|} \tag{149}$$

By considering (141) and (149), the finite time convergence can be proved as the following relationship holds

$$\lim_{k\to\infty} t_{M_k} \le t_{M_1} + \frac{(G_1 + \alpha^* G_2)\eta\beta^*}{(G_1\eta\beta^* - 1)(\alpha^* G_2 \eta\beta^* \overline{\Psi}(0))}\frac{\sqrt{|y_{1_{M_1}}|}}{1 - \bar{\gamma}} \tag{150}$$

As mentioned in the paper, a nice property of the proposed algorithm is that the control amplitude decreases as the origin of the state plane is approached. In fact, relying on the properties of the uncertainty bound,

$$\lim_{(y_1;y_2)\to(0;0)} \overline{\Phi}_k^* = \overline{\Psi}_0(0) \tag{151}$$

so that

$$V_{M_k} \to \eta\beta^* \overline{\Psi}_0(0) \tag{152}$$

Proof. of Theorem 2

By (84), taking into account (89), the drift term of the second order sliding dynamics for the considered case is given by

$$\varphi(\cdot) = \mathcal{F}_1[\mathbf{x}(t)] + \mathcal{F}_2[\mathbf{x}(t)]u(t) \tag{153}$$

where

$$\mathcal{F}_1[\mathbf{x}(t)] = \sum_{i=1}^{n-1}\frac{\partial f}{\partial x_i}x_{i+1}(t) + (c_{n-1} + \frac{\partial f}{\partial x_n})f[\mathbf{x}(t)] + \sum_{i=1}^{n-2} c_i x_{i+2}(t) \tag{154}$$

$$\mathcal{F}_2[\mathbf{x}(t)] = \sum_{i=1}^{n-1}\frac{\partial g}{\partial x_i}x_{i+1}(t) + (\frac{\partial f}{\partial x_n} + c_{n-1})g[\mathbf{x}(t)] \tag{155}$$

Rewrite (153) as

$$\varphi(\cdot) = \overline{\mathcal{F}}_1[\mathbf{x}(t)] + \overline{\mathcal{F}}_2[\mathbf{x}(t)]y_2(t) \tag{156}$$

where

$$\overline{\mathcal{F}}_1[\mathbf{x}(t)] = \mathcal{F}_1[\mathbf{x}(t)] - [\frac{f[\mathbf{x}(t)] + \sum_{i=1}^{n-1} c_i x_{i+1}(t)}{g[\mathbf{x}(t)]}] \tag{157}$$

and

$$\overline{\mathcal{F}}_2[\mathbf{x}(t)] = \frac{\mathcal{F}_2[\mathbf{x}(t)]}{g[\mathbf{x}(t)]} \tag{158}$$

State-dependent upper bounds of $\overline{\mathcal{F}}_1[\mathbf{x}(t)]$ and $\overline{\mathcal{F}}_2[\mathbf{x}(t)]$ can be found by (85)-(88), and can be given by

$$\begin{aligned} &|\overline{\mathcal{F}}_1[\mathbf{x}(t)]| \le \overline{\mathcal{F}}_{1M}[\|\mathbf{x}(t)\|] = \\ &= (c_{n-1} + \tfrac{1}{G_1} + F_{d_n}[\|\mathbf{x}(t)\|])F[\|\mathbf{x}(t)\|] + (\textstyle\sum_{i=1}^{n-1} F_{d_i}[\|\mathbf{x}(t)\|] + \sum_{i=1}^{n-2} c_i)\|\mathbf{x}(t)\| \end{aligned} \tag{159}$$

$$\begin{aligned} &|\overline{\mathcal{F}}_2[\mathbf{x}(t)]| \le \overline{\mathcal{F}}_{2M}[\|\mathbf{x}(t)\|] = \\ &= \tfrac{G_2}{G_1}(F_{d_n}[\|\mathbf{x}(t)\|] + c_{n-1}) + \tfrac{1}{G_1} \textstyle\sum_{i=1}^{n-1} G_{d_i}[\|\mathbf{x}(t)\|]\|\mathbf{x}(t)\| \end{aligned} \tag{160}$$

By virtue of (82), taking into account (85) and (86), the sign of $y_2(0)$ can be forced by suitable initial condition $u(0)$ of the control.

In particular choosing

$$u(0) = \frac{1}{G_1}[F[\|\mathbf{x}(0)\|] + |\sum_{i=1}^{n-1} c_i x_{i+1}(0)| + k] sign(y_1(0)) \qquad k > 0 \tag{161}$$

one has that $sign(y_2(0)) = sign(y_1(0))$ and also that

$$Y_{20M} = F[\|\mathbf{x}(0)\|] + |\sum_{i=1}^{n-1} c_i x_{i+1}(0)| + G_2 u(0) \tag{162}$$

The time-varying upper bound $\overline{\Phi}_0^*(t)$ of the drift term in the initialization phase can be expressed as

$$\overline{\Phi}_0^*(t) = \overline{\mathcal{F}}_{1M}[\|\mathbf{x}(t)\|] + \overline{\mathcal{F}}_{2M}[\|\mathbf{x}(t)\|] Y_{20M} \tag{163}$$

Relying on the BIBO nature of the linear subsystem in the first two lines of (84), the following relationship can be written

$$\|\mathbf{x}(t)\| \le Q_x \|\mathbf{x}(t_i)\| + Q_y sup_{t_i \le \tau \le t} |y_1(\tau)| \tag{164}$$

where Q_x and Q_y are properly defined constants [Bartolini et al. '98b].

Observe that, for all $t \ge T_{M_1}$

$$|y_1(t)| \le y_{1_{M_k}} \qquad T_{M_k} \le t \le T_{M_{k+1}} \qquad k = 1, 2, \dots \tag{165}$$

then, relying on (164)

$$\|\mathbf{x}(t)\| \le \|\mathbf{x}(t)\|_{M_k} = Q_x \|\mathbf{x}(T_{M_k})\| + Q_y y_{1_{M_k}} \qquad T_{M_k} \le t \le T_{M_{k+1}} \qquad k = 1, 2, \dots \tag{166}$$

and

$$\begin{matrix} \overline{\mathcal{F}}_1[\mathbf{x}(t)] \le \overline{\mathcal{F}}_{1M}[\|\mathbf{x}(t)\|_{M_k}] \\ \overline{\mathcal{F}}_2[\mathbf{x}(t)] \le \overline{\mathcal{F}}_{2M}[\|\mathbf{x}(t)\|_{M_k}] \end{matrix} \qquad T_{M_k} \le t \le T_{M_{k+1}} \tag{167}$$

A direct correspondence occurs with the uncertainty bounds dealt with in Theorem 1, with $\overline{\Psi}_0(y_{1_{M_k}}) = \overline{\mathcal{F}}_{1M}[\|\mathbf{x}(t)\|_{M_k}]$ and $\overline{\Psi}_1(y_{1_{M_k}}) = \overline{\mathcal{F}}_{2M}[\|\mathbf{x}(t)\|_{M_k}]$. On this basis, $\overline{\Phi}^*_k$ can be evaluated as in (99)-(101), and the effectiveness of control law (92)-(102) is ensured relying on the proof of Theorem 1.

Proof. of Theorem 3

The drift term of the second order sliding dynamics for the considered case is given by

$$\varphi(\cdot) = f[\mathbf{x}(t)] + \sum_{i=1}^{n-2} c_i x_{i+2}(t) \tag{168}$$

Rewrite (168) as

$$\varphi(\cdot) = f[\mathbf{x}(t)] + \sum_{i=1}^{n-3} c_i x_{i+2}(t) - c_{n-2} \sum_{i=1}^{n-2} c_i x_{i+1}(t) + c_{n-2} y_2(t) \tag{169}$$

By (107) and (108) one has

$$\begin{aligned} |\varphi(\cdot)| &\le F(\|\hat{\mathbf{x}}\|) + \textstyle\sum_{i=1}^{n-3} c_i x_{i+2}(t) + (c_{n-2} + Q_f) |\sum_{i=1}^{n-2} c_i x_{i+1}(t)| + (c_{n-2} + Q_f)|y_2(t)| = \\ &= \overline{\mathcal{F}}_1[\hat{\mathbf{x}}(t)] + (c_{n-2} + Q_f)|y_2(t)| \end{aligned} \tag{170}$$

$$\overline{\mathcal{F}}_1[\hat{\mathbf{x}}(t)] \le \overline{\mathcal{F}}_{1M}[\|\hat{\mathbf{x}}(t)\|] = F(\|\hat{\mathbf{x}}\|) + \left(\sum_{i=1}^{n-3} c_i + (c_{n-2} + Q_f) \sum_{i=1}^{n-2} c_i \right) \|\hat{\mathbf{x}}(t)\| \tag{171}$$

The sign of $y_2(0)$ is assumed to be known, and, by assumption

$$\mathrm{Y}_{20M} = X_{n0_{MAX}} + \sum_{i=1}^{n-2} c_i x_{i+1}(0) \tag{172}$$

The time varying upper bound $\overline{\Phi}_0^*(t)$ of the drift term in the initialization phase can be expressed as

$$\overline{\Phi}_0^*(t) = \overline{\mathcal{F}}_{1M}[\|\hat{\mathbf{x}}(t)\|] + (c_{n-2} + Q_f)Y_{20M} \tag{173}$$

Analogously to the previous Theorem, two constants Q_x and Q_y can be found such that

$$\|\hat{\mathbf{x}}(t)\| \leq \|\hat{\mathbf{x}}(t)\|_{M_k} = Q_x\|\hat{\mathbf{x}}(T_{M_k})\| + Q_y y_{1_{M_k}} \qquad T_{M_k} \leq t \leq T_{M_{k+1}} \qquad k = 1, 2, \ldots \tag{174}$$

and the term (171) can be upper bounded as

$$\overline{\mathcal{F}}_{1M}[\|\hat{\mathbf{x}}(t)\|] \leq \overline{\mathcal{F}}_{1M}[\|\hat{\mathbf{x}}(t)\|_{M_k}] \qquad T_{M_k} \leq t \leq T_{M_{k+1}} \tag{175}$$

From this point on, the proof proceeds as that of Theorem 2.

References

[Bartolini et al. '96] G. Bartolini and P. Pydynowski "An improved chattering free VSC scheme for uncertain dynamical systems", *IEEE Trans. on Automatic Control*, vol. 41, pp. 1220–1226, 1996.

[Bartolini et al. '97] G. Bartolini, A. Ferrara and E. Usai "Applications of a sub–optimal discontinuous control algorithm for uncertain second order systems", *Int. J. of Robust and Nonlinear Control*, vol. 7, no.4, pp. 299–319, 1997.

[Bartolini et al. '98a] G. Bartolini, A. Ferrara, A. Pisano and E. Usai "Adaptive reduction of the control effort in chattering-free sliding mode control of uncertain nonlinear plants", *J. Appl. Math. and Comp. Sc.*, vol. 8, no. 1, pp. 51–71, 1998.

[Bartolini et al. '98b] G. Bartolini, A. Ferrara and E. Usai "Chattering Avoidance by Second Order Sliding Mode Control", *IEEE Trans. on Automatic Control*, vol. 43, no. 2, pp. 241–246, 1998.

[Bartolini et al. 2000] G. Bartolini, A. Ferrara, A. Pisano, E. Usai "On the convergence properties of a 2-sliding control algorithm for nonlinear uncertain systems", *Int. J. of Control*, in press.

[Bartolini et al. '99] G. Bartolini, A. Ferrara, A. Levant, E. Usai "On Second Order Sliding Mode Controllers", in "Variable Structure Systems, Sliding Mode and Nonlinear Control", K.D. Young and U. Ozguner eds., Lecture Notes in Control and Information Sciences, Springer-Verlag, 1999, in press.

[Young and Ozguner (eds.)'99] K.D. Young and U. Ozguner (eds.) "Variable Structure Systems, Sliding Mode and Nonlinear Control", Lecture Notes in Control and Information Sciences, Springer-Verlag, 1999, in press.

[DeCarlo et al. '88] R.A. De Carlo, S.H. Zak, G.P. Matthews "Variable Structure Control of Nonlinear Multivariable Systems: A Tutorial", *Proceedings of the IEEE*, vol. 76, no. 3, pp. 212–232, 1988.

[Elmali and Olgac '92] H. Elmali H. and N. Olgac, "Robust Output Tracking Control of Nonlinear MIMO Systems via Sliding Mode Technique", *Automatica*, vol. 28, pp. 145–151, 1992.

[Isidori '89] A. Isidori *Non Linear Control Systems*, Springer Verlag, Berlin, 1989.

[Levant '93] A. Levant "Sliding order and sliding accuracy in sliding mode control", *International Journal of Control*, vol. 58, pp. 1247–1263, 1993.

[Levant and Fridman '96] A. Levant, L. Fridman "Higher order sliding modes as a natural phenomenon in control theory" in *Robust control via variable structure and Lyapunov techniques*, F. Garofalo and L. Glielmo Eds., Lecture Notes in Control and Information Sciences, vol. 217, pp. 107–133, Springer–Verlag, London, 1996.

[Sira-Ramirez '92] H. Sira–Ramirez "On the sliding mode control of nonlinear systems," *Syst. Contr. Lett.*, vol. 19, pp. 303–312, 1992.

[Slotine and Li '91] J.J.E.Slotine, W. Li *Applied Nonlinear Control*, Prentice–Hall International, Englewood Cliffs, New Jersey, 1991.

[Yu and Zihong '96] X. Yu and M. Zihong, "Model Reference Adaptive Control Systems with Terminal Sliding Modes" *Int. J. Contr.*, vol. 64, pp. 1165–1176, 1996.

[Venkataraman et al. '89] S.T. Venkataraman and S. Gulati, "Control of Nonlinear Systems using Terminal Sliding Modes", *ASME J. Dyn. Syst. Meas. Contr.*, vol. 115, pp. 554–560, 1989.

[Utkin '92] V.I. Utkin *Sliding Modes in Control and Optimization*, Springer Verlag, Berlin, 1992.

4 Second Order Sliding Mode Control for Sampled-Data Systems

4.1 Introduction

This chapter is devoted to analyze the discrete-time implementation of second order SMC schemes.

Due to the growing diffusion of computer–controlled systems, discrete time implementation of variable structure controllers is one of the emerging topics in modern VSS theory. The sample-and-hold effect makes not straightforward a direct extension of the structural properties showed by continuous time sliding modes to the discrete time context.

For this reason, a great research effort has been devoted at giving a consolidated theoretical basis to this particular kind of VSSs. In [Milosavljevic '85] Milosavljevic analyzed the effect of the discretization of measures in a proximity of the sliding surface, defining the so called "quasi-sliding" motion. Drakunov and Utkin developed a semigroup approach to the analysis of discrete time VSSs [Drakuno and Utkin '90], and they proposed a synthesis procedure which extends the well known equivalent control concept to discrete–time control systems. This procedure, which can be viewed as an extension of the "dead beat control", requires a mathematical characterization of the system to be controlled in terms of the delay operator, and it is theoretically able to constrain the system state on the sliding surface in one sampling period, even if at the cost of a very high control effort [Drakunov et al. '93, Utkin '93, Utkin and Drakunov '93]. Nevertheless, an important feature of this approach is that the control effort decreases while the sliding manifold is approached, and the discrete time equivalent control turns out to be smooth within the boundary layer. Then the ringing phenomenon, appearing as a discrete time counterpart of the chattering phenomenon when a direct discretization of continuous-time VSC is performed, is avoided. To achieve this task, the discrete time equivalent control is defined in a slightly different form than the continuous time one, since it provides both the reaching and the sliding phase [Utkin '93].

Furuta developed the sliding sector approach, a two stages control strategy which consists in a direct discretization of a continuous-time sliding mode control outside a properly chosen sector in the state space including the sliding manifold, and commutes to a smooth discrete time robust control within this sector [Furuta '90, Furuta and Pan '94].

In presence of disturbances and/or uncertainties some adaptation or estimation technique should be adopted to counteract them, in order to reduce the size of the boundary layer. In [Bartolini et al. '95] a discrete time MRAC approach is used to improve the performances of the VSC in presence of model uncertainties. By using a predictor of the uncertainties, in [Drakunovet al. '96] Drakunov *et al.* dealt with the sliding mode control of a large class of sampled data nonlinear uncertain systems, attaining a $\mathcal{O}(T^2)$ accuracy, being T the sampling period, and avoiding the ringing phenomenon. This result is an improvement respect to the $\mathcal{O}(T)$ accuracy provided by discretized first order SMC. By resorting to a second order sliding mode control technique, the accuracy can be further improved, and the effectiveness can be extended to a larger class of systems.

Let the "sliding variable" be the state-dependent quantity that vanishes when the manifold is reached. The relative degree q between the sliding variable and the control input, plays a fundamental role in solving the control problem.

The sliding order r is defined as the relative degree between the sliding variable and the discontinuous control signal. In classical SMC the sliding order is equal to one, so that the first derivative of the sliding quantity is discontinuous and its sign changes with theoretically infinite frequency. In second order sliding modes $r = 2$, and both the sliding variable and its first time derivative converge to zero in a finite time.

Obviously, the sliding order cannot be smaller than q, and, for this reason, first order SMC is not effective if $q = 2$, meaning that the control input does not affect the first time derivative of the sliding variable directly.

Moreover, when $q = 1$, second order SMC allows to obtain chattering elimination. The second derivative of the sliding quantity can be properly modified by using, as a discontinuous auxiliary control signal, the derivative of the actual control input. The control input, obtained by integrating the discontinuous derivative, results to be continuous, and chattering is avoided.

The digital realization of the control law is treated by using both the continuous model and a sufficiently accurate discrete model, which allow direct visibility on the intersampling system behavior and preserve bad phenomena such as nonminimum phase effects.

The aim of this Chapter is that of dealing with the sliding mode control of a class of uncertain nonlinear sampled data systems in which, due to the not complete availability of the state, a relative-degree-two sliding variable is chosen (case B).

The Chapter is organized as follows: the next Section is devoted to the problem statement. In Section 3 the discrete model is derived, while in Section 4 a digital VSC, based on a dead-beat like procedure involving the discrete time equivalent control concept, is proposed, providing ringing avoidance and $\mathcal{O}(T^3)$ accuracy. Section 6 deals with simulation results, while in the final Section some remarks regarding both the proposed algorithms and future researches are discussed.

4.2 The Control Problem

Consider the class of uncertain nonlinear feedback linearizable systems whose dynamics is defined by

$$\begin{cases} \dot{x}_i = x_{i+1} \qquad\qquad i = 1, 2, \ldots, n-1 \\ \dot{x}_n = f(\mathbf{x}) + [g_n(\mathbf{x}_m) + \Delta g(\mathbf{x}_m)]\, u(t) \\ \quad\;\; = f(\mathbf{x}) + g(\mathbf{x}_m) u(t) \end{cases} \tag{176}$$

where $\mathbf{x} = [x_1, x_2, \ldots, x_n] \in \mathbf{X} \subseteq \mathbf{R^n}$ is the state vector, $u(t) \in \mathbf{U} \subseteq \mathbf{R}$ is the system input and $\mathbf{X}$, $\mathbf{U}$ are proper compact domains of interest. $f(\mathbf{x})$ is uncertain, $g_n(\mathbf{x}_m)$ is the nominal control gain and $\Delta g(\mathbf{x}_m)$ represents the unknown deviation from the nominal gain. The last component of the state vector, x_n, is not measurable, so that $\mathbf{x}_m = [x_1, x_2, \ldots, x_{n-1}]$ represents the measurable part of the state.

The assumption of a control gain that does not depend on the last state variable is frequently met in practice, such as, for instance, in the Lagrangian systems.

The control objective is the stabilization of the whole state vector by using digital control devices.

To this end, it is customary to choose the sliding manifold as

$$s(t) = x_{n-1} + \sum_{i=1}^{n-2} c_i x_i(t) \tag{177}$$

where c_i are s.t. the polynomial $P(q) = q^{n-2} + \sum_{i=1}^{n-2} c_i q^{i-1}$ is a Hurwitz one.

The reduced-order linearized dynamics is given by

$$\begin{cases} \dot{\tilde{\mathbf{x}}}(t) &= \tilde{\mathbf{A}}\tilde{\mathbf{x}}(t) + \tilde{\mathbf{b}}s(t) \\ x_{n-1}(t) &= -\tilde{\mathbf{c}}\tilde{\mathbf{x}} + s(t) \\ x_n(t) &= c_{n-2}\tilde{\mathbf{c}}\tilde{\mathbf{x}} - \sum_{i=1}^{n-3} c_i x_{i+1}(t) - c_{n-2}s(t) + \dot{s}(t) \end{cases} \tag{178}$$

where $\tilde{\mathbf{x}}=[x_1, x_2, \ldots, x_{n-2}]^T$, $\tilde{\mathbf{c}} = [c_1, c_2, \ldots, c_{n-2}]$, $\tilde{\mathbf{A}}$ is a $(n-2) \times (n-2)$–matrix in companion form with the last row coinciding with vector $-\tilde{\mathbf{c}}$ and $\tilde{\mathbf{b}} = [0, \ldots, 0, 1]^T \in R^{n-2}$.

It is straightforward to show that the finite-time convergence to zero of the s and $\dot{s}$ variables guarantees the asymptotic stabilization of the whole state vector $\mathbf{x}$. However, it is not easy to accomplish this task, as the relative degree between the sliding variable s and the control input u is two, and $\dot{s}$ is not available for measurements.

In fact, the sliding variable dynamics can be defined as

$$\ddot{s}(t) = \varphi(\mathbf{x}(t)) + g(\mathbf{x}_m(t))u(t) \tag{179}$$

where

$$\varphi(\mathbf{x}(t)) = f(\mathbf{x}(t)) + \sum_{i=1}^{n-2} c_i x_{i+2}(t) \tag{180}$$

Assume what follows:

- There exist positive known constants Φ, G_1, G_2 such that, for all $\mathbf{x} \in \mathbf{X}$

$$|\varphi(\mathbf{x}(t))| \leq \Phi \tag{181}$$

$$0 < G_1 \leq g(\mathbf{x}_m(t)) \leq G_2 \tag{182}$$

This problem has been solved, in the continuous time context, by means of a set of algorithms, namely "second-order sliding mode controllers" [Bartolini et al. '98a, Bartolini et al. '99a, Levant '93]. They are characterized by a discontinuous control that acts on $\ddot{s}$ using informations on s and on the sign of $\dot{s}$ only. See [Bartolini et al. '99a] for a survey on existing 2-SMC algorithms.

Here the same control problem is addressed with the further constraints that the control is piecewise-constant within the sampling period of length T, and that the available part of the system's state is measured only at the sampling instants $t = kT$, $k = 0, 1, 2, \ldots$

4.3 Direct discretization of 2-SMC

The first step of this treatment consists in analyzing the behaviour of the controlled system when a direct discretization of the continuous time suboptimal 2-sliding control scheme is performed.

Consider system (176), and let $s[k]$ be the sequence of sampled values of the sliding variable (177)

$$s[k] = s(kT) \qquad k = 0, 1, \ldots$$

T being the sampling period.

The plant input is piecewise-constant within the intersampling period (zero-horder-hold D/A device), i.e.

$$u(t) = u[k] \qquad t \in [kT, (k+1)T) \tag{183}$$

The discrete-time version of the sub-optimal 2-SMC algorithm (see [Bartolini et al. '98a, Bartolini et al. '99a] for the continuous-time version) is resumed as follows:

Apply the control

$$\begin{aligned} u[k] &= -\alpha[k] U_M \text{sign}\left[s[k] - \frac{1}{2}\hat{s}_{M_i}\right] \qquad (184) \\ U_M &\in \left(\frac{\Phi}{\alpha^* G_1}, \infty\right) \cap \left(\frac{4\Phi}{3G_1 - \alpha^* G_2} + \theta_1 T, \theta_2 T^{-2}\right) \qquad (185) \end{aligned}$$

where θ_1, θ_2 are proper constants, $\hat{s}_{M_i}$ is evaluated by means of the following algorithm

Approximate digital peak-detector

$$\begin{array}{l} set\ \ s[-1] == s(0)\ \ ;\ \ s[-2] = 0 \quad i = -1 \\ set\ \ \Lambda[k] = (s[k] - s[k-1])(s[k-1] - s[k-2]) \\ If\ \ (\Lambda[k] \le 0) \qquad then \left\{ \begin{array}{l} i = i + 1 \\ \hat{s}_{\mathrm{Mi}} = s[k-1] \end{array} \right. \end{array} \tag{186}$$

and $\alpha[k]$ is adjusted according to

$$\alpha[k] = \left\{ \begin{array}{ll} 1 & if\ \{s[k] - \frac{1}{2}\hat{s}_{M_i}\}\ \{s[k] - \hat{s}_{M_i}\} \le 0 \\ \alpha^* & otherwise \end{array} \right. \tag{187}$$

where the constant α^* is set in accordance with

$$\alpha^* \in (0, 1) \cap \left(0, \frac{3G_1}{G_2}\right) \tag{188}$$

The attained performances are summarized in the following Theorem.

Theorem 1. *Consider system* (176)*, which verifies assumptions* (181)–(182) *and with x_n not available. Let the sliding quantity $s(t)$ be defined as in* (177)*. Then, the digital control strategy* (184)–(188) *guarantees that, after a finite transient T_R, the following conditions are satisfied at any $t \ge T_R$*

$$\begin{array}{l} |s(t)| \le O(T^2) \\ |\dot{s}(t)| \le O(T) \end{array} \tag{189}$$

Proof. See the Appendix.

A similar result was attained by Drakunov *et al.* for systems with $q = 1$ and known control gain [Drakunov et al. '2000], and then generalized to systems with unknown control gain in [Young et al. '99] and [Drakunov et al. '2000]. The use of a predictor of the uncertain dynamics was the main point of the above approach, increasing by one the order of the accuracy provided by first order sliding mode control and reducing the control effort.

The aim of the present Chapter is that of showing that the application of second order sliding mode control strategies allows to achieve a system motion confined within a $\mathcal{O}(T^3)$ boundary layer of the sliding manifold, that is the same accuracy featured by real third order sliding mode control. Note that, in any case, the attained motion cannot be defined as a third order sliding mode, since $\ddot{s}$ has discontinuous dynamics [Levant '93].

In next section we derive a sufficiently accurate discrete model of the controlled plant which will be used for the synthesis of two control strategies providing the desired accuracy.

4.4 A discrete time uncertain model with $\mathcal{O}(T^3)$ accuracy

Our first purpose is to provide a discrete model of the continuous system (179) with an approximation, at any time instant, not worse than the accuracy of the sliding motion that it is wanted to be assured by the proposed digital control, that is $\mathcal{O}(T^3)$. To this end, let us indicate with $a[k] = a(kT)$ the k–th sample of a generic variable a. Assume that the control is applied by means of a ZOH.

Consider system (179), (181)-(182), and assume that the uncertainties are globally Lipschitz, i.e.

$$
\begin{aligned}
|\dot{\varphi}[\mathbf{x}(t)]| &\leq \Phi_\mathrm{d} && (190)\\
|\dot{g}[\mathbf{x}(t)]| &\leq \Gamma_\mathrm{d} && (191)
\end{aligned}
$$

Two subsequent samples of the sliding variable s satisfy the following relationship

$$
s[k+1] = s[k] + \int_{kT}^{(k+1)T} \dot{s}(\tau)d\tau \tag{192}
$$

The argument of the integral function, $\dot{s}(\tau)$, can be reduced in Taylor series as follows:

$$
\begin{gathered}
\dot{s}(\tau) = \dot{s}[k] + \varphi[k](\tau - kT) + g[k]u[k](\tau - kT) + \\
+\tfrac{1}{2}\left(\dot{\varphi}[\mathbf{x}(\xi), \dot{\mathbf{x}}(\xi), \xi] + \tfrac{1}{2}\dot{g}[\mathbf{x}(\xi), \xi]u[k]\right)(\tau - kT)^2 \\
\tau \in [kT\ ;\ (k+1)T] \\
\xi \in (kT\ ;\ (k+1)T)
\end{gathered} \tag{193}
$$

Considering (193) into (192) yields

$$
s[k+1] = s[k] + \dot{s}[k]T + \frac{1}{2}\left[\varphi[k] + g[k]u[k]\right]T^2 + \eta_1(T) \tag{194}
$$

where $\eta_1(T)$ is the discretization error due to the Taylor approximation in (193), satisfying, in accordance with (190)-(191), the following constraint

$$
|\eta_1(T)| \leq \frac{1}{6}\left(\Phi_\mathrm{d} + \Gamma_\mathrm{d} u[k]\right)T^3 \tag{195}
$$

In order to obtain a discrete model effective for the synthesis procedure, the unavailable sample $\dot{s}[k]$ in (194) must be eliminated. To this end, consider (194) in two subsequent sampling and subtract one each other, then it follows

$$\begin{array}{l} s[k+1] = 2s[k] - s[k-1] + (\dot{s}[k] - \dot{s}[k-1])T + \\ \quad + \frac{1}{2}\left(\varphi[k] - \varphi[k-1] + g[k]u[k] - g[k-1]u[k-1]\right)T^2 + \eta_2(T) \end{array} \tag{196}$$

being, by (190)-(191),

$$|\eta_2(T)| \leq \left[\frac{1}{3}\Phi_{\mathrm{d}} + \frac{1}{6}\Gamma_{\mathrm{d}}(u[k] + u[k-1])\right] T^3 \tag{197}$$

By (193) it results

$$\begin{array}{c} \dot{s}[k] - \dot{s}[k-1] = \varphi[k-1]T + g[k-1]u[k-1]T + \\ \quad + \frac{1}{2}\left(\dot{\varphi}[\mathbf{x}(\xi'), \dot{\mathbf{x}}(\xi'), \xi'] + \dot{g}[\mathbf{x}(\xi'), \xi']u[k-1]\right)T^2 \\ \\ \xi' \in ((k-1)T\ ;\ kT) \end{array} \tag{198}$$

and, consequently,

$$\dot{s}[k] - \dot{s}[k-1] = \left(\varphi[k-1] + g[k-1]u[k-1]\right)T + \eta_3(T) \tag{199}$$

with, by (190)-(191)

$$|\eta_3(T)| \leq \frac{1}{2}\left(\Phi_{\mathrm{d}} + \Gamma_{\mathrm{d}}u[k-1]\right)T^2 \tag{200}$$

Taking into account (196) and (199), the discrete time model of the sliding variable dynamics is

$$\begin{array}{rl} s[k+1] & = 2s[k] - s[k-1] + \varphi[k-1]T^2 \\ & \quad + \frac{1}{2}\left(g[k]u[k] + g[k-1]u[k-1]\right)T^2 + \varepsilon[k] \\ & \qquad k = 0, 1, 2\ldots \end{array} \tag{201}$$

At any sampling time, by (197) and (200), the discretization error $\varepsilon[k]$ is such that

$$|\varepsilon[k]| \leq \left(\frac{4}{3}\Phi_{\mathrm{d}} + \frac{1}{6}\Gamma_{\mathrm{d}}u[k] + \frac{2}{3}\Gamma_{\mathrm{d}}u[k-1]\right)T^3 \tag{202}$$

The discrete time sliding mode control problem can be therefore re–defined as that of finding, by means of the above approximate model, a control sequence $u[k]$ $(k = 0, 1, \ldots)$ such that the sliding variable s is constrained within a $\mathcal{O}(T^3)$ boundary layer of the origin from a finite time instant on.

4.5 Discrete-Time Equivalent Control Based 2-SMC

The discrete model (201)-(202) may be used to define a digital control law ensuring that system (179), (181)-(182), (190)-(191) is confined within a small vicinity of the sliding set (30).

In [Utkin and Drakunov '93] the discrete–time equivalent control has been defined as the control sequence $u[k]$ such that $s[k+1] = 0$ $(k = 1, 2, \ldots)$. The discrete equivalent control $u^{\mathrm{d}}_{\mathrm{eq}}[k]$

$(k = 1, 2, \ldots)$ is able to drive the system into the sliding surface in one sampling period, and to constrain on the system state in all the subsequent sampling time instants.

For the actual model, the discrete time equivalent control can be defined as

$$u_{\mathrm{eq}}^{\mathrm{d}}[k] \quad = \quad -\tfrac{1}{g_n[k]}\left(g_n[k-1]u[k-1] + d[k] + 2\tfrac{2s[k]-s[k-1]}{T^2}\right) \tag{203}$$

where

$$d[k] \quad = \quad 2\left[\dot{\varphi}[k-1] + \tfrac{1}{2}\left(\Delta g[k]u[k] + \Delta g[k-1]u[k-1]\right)\right] \tag{204}$$

While it is conceptually very simple, the main problem in using the DTEC method is that the amplitude of the DTEC is inversely proportional to the sampling period T, unless some small neighbor of the sliding manifold is reached. The size of this boundary layer is $\mathcal{O}(T)$ as far as systems with relative degree one are dealt with [Drakunov et al. '93, Young et al. '99], while contracts to $\mathcal{O}(T^2)$ in the considered case [Bartolini et al. '99b]. In both cases, an initialization procedure must be implemented in order to reach the admissible boundary layer in which the boundedness of the control signal is ensured.

In the case under investigation, the admissible $\mathcal{O}(T^2)$-vicinity of the sliding manifold can be reached by means of the discrete-time 2-SMC scheme presented in the previous section. From this point on the sliding variable can be steered to $\mathcal{O}(T^3)$ by means of the DTEC.

Unfortunately, the equivalent control is not directly measurable, due to the uncertain dynamics of the controlled system, and some form of prediction must be implemented to estimate it.

The one-step-delay estimate of the uncertain term $d[k]$ can be performed on the basis of the above discrete model, delaying it by one sampling period, leading to

$$\hat{d}[k] = \tfrac{s[k]-2s[k-1]+s[k-2]}{T^2} - \tfrac{1}{2}\left(g_n[k-1]u[k-1] + g_n[k-2]u[k-2]\right) \tag{205}$$

If one put $\hat{d}[k]$ in place of $d[k]$ in (203), and define $\hat{u}_{\mathrm{eq}}^{\mathrm{d}}[k]$ accordingly, it yields

$$\hat{u}_{\mathrm{eq}}^{\mathrm{d}}[k] = \tfrac{1}{g_n[k]}\left(g_n[k-2]u[k-2] - 2\tfrac{3s[k]-3s[k-1]+s[k-2]}{T^2}\right) \tag{206}$$

After the initialization phase, the control $\hat{u}_{\mathrm{eq}}^{\mathrm{d}}[k]$, which is available at the beginning of any control interval, is used, and its effect on the reduction of the size of the boundary layer is stated in the following Theorem. The stability of the sliding motion is nontrivial to demonstrate, and suitable assumptions regarding the uncertainties are needed to ensure that the system trajectory reaches, and does not leave, the $\mathcal{O}(T^3)$ boundary layer of $s = 0$.

Theorem 2: *Consider system* (176),(177) *with its uncertain dynamics satisfying* (181), (182), (190)-(191). *Then the digital feedback controller*

$$u[k] = \begin{cases} u_1[k] & if \;\; kT < T_{\mathrm{R}} \\ \hat{u}_{\mathrm{eq}}^{\mathrm{d}}[k] & if \;\; kT \geq T_{\mathrm{R}} \end{cases} \tag{207}$$

where $u_1[k]$ is the control strategy in Theorem 1, T_{R} is the finite reaching time of a $O(T^2)$ boundary layer and $\hat{u}_{\mathrm{eq}}^{\mathrm{d}}[k]$ is defined as in (206), *guarantees the finite-time reaching of a $\mathcal{O}(T^3)$ vicinity of the sliding manifold $s = 0$ characterized by*

$$\begin{aligned} |s(t)| &\leq \mathcal{O}(T^3) \\ |\dot{s}(t)| &\leq \mathcal{O}(T^2) \end{aligned} \tag{208}$$

Proof:

Once the $O(T^2)$ boundary layer of $s = 0$ is reached in a finite time T_R (Theorem 1) the control commutes from the discrete-time 2-SMC to the estimated DTEC (206). We must prove that, as a result, the boundary layer size contracts to $O(T^3)$, and that the corresponding motion is stable.

To prove the assert, we start from the fact that, at any sampling time, the discretization error introduced by the discrete model (201) is $O(T^3)$ [Bartolini et al. '99a].

It is not difficult to show that the behaviour of $s[k]$ under the action of the proposed controller is described by

$$s[k+1] = \frac{1}{2}\left(d[k] - d[k-1]\right) + O(T^3) \tag{209}$$

which can be rewritten, by virtue of the smoothness assumptions (190)-(191), in the form

$$s[k+1] = \frac{1}{4}\Delta g[k]\left(u[k] - u[k-2]\right) + O(T^3) \tag{210}$$

The *coupling* between $s[k]$ and $u[k]$ makes necessary the analysis of the closed loop behaviour of the system in a neighbor of the sliding manifold.

By the above considerations, as the control effort does not depend on the sampling time T, substituting the expression for the DTEC into (210), it results

$$s[k+1] \quad = \quad \tfrac{1}{2}\tfrac{\Delta g[k]}{g_n[k]}\left(3s[k] - 3s[k-1] + s[k-2]\right) + O(T^3) \tag{211}$$

i.e, a third order difference equation. Considering the frozen discrete models obtained for all possible values of $\Delta g[k]$ and $g_n[k]$, the discrete system (211) has all poles inside the unit circle for sufficiently small $\Delta g[k]$. The admissible uncertainties in the control gain are dictated by the above stability condition, together with the "small" variation of $\Delta g[k]/g_n[k]$ (i.e., G_d is sufficiently small) that ensures that the stability of the whole set of the above frozen models implies the stability of the overall time varying discrete system. It is easy to derive conditions (208) from the analysis of (211), which is a stable difference equation with a $O(T^3)$ disturbing term.

4.6 Simulation results

Consider system (176), with $n = 3$ and

$$\begin{cases} f(\mathbf{x}, t) = 3 + sin(10t + x_1) * cos(x_2^2 + x_3^2) \\ g(\mathbf{x}, t) = 1 + 0.5sin(3 + x_1 + x_2) \end{cases} \tag{212}$$

x_3 is not available for measurements, and the initial conditions are set to $\mathbf{x}(0) = [1, 1, 1]$. The control task is to reduce the state vector components to zero, and the sliding manifold is $s = x_2 + 2x_1 = 0$ is defined. A sampling period of $T = 10^{-4}s$ is used.

The nominal control gain on the basis of which it is computed the control law is

$$g_n(\mathbf{x}) = 2 + sin(3 + x_1 + x_2) \tag{213}$$

i.e. the actual control gain parameters are assumed to differ by the 50% with respect to the nominal ones.

The control strategy in Theorem 2 is implemented with $\alpha^* = 1$, $U_M = 20$ and $T_R = 2s$. The modification of the controller at $t = T_R$ is apparent from Fig. 24.

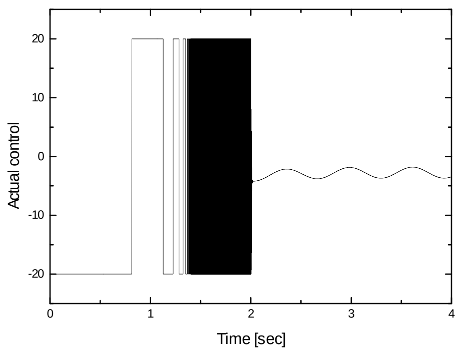

Figure 24: The actual control.

In the steady state, the actual control turns out to track the equivalent control, as it is evidenced in Fig. 25.

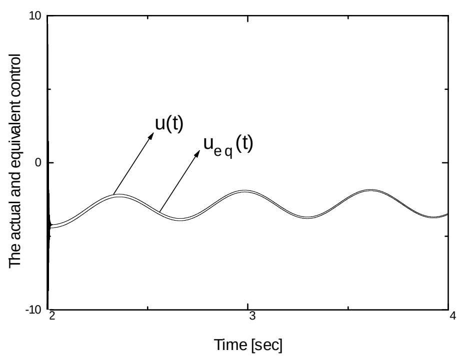

Figure 25: The actual control and the equivalent control.

The improvement in the accuracy is evidenced in Fig. 26, while the asymptotic convergence of the state to the origin is shown in the last Fig. 27.

4.7 Conclusions

In this chapter the discrete time control of uncertain nonlinear systems with incomplete state availability has been dealt with. The adopted philosophy was that of resorting to the equivalent control principle, in both its discrete-time and continuous-time versions.

The proposed approach involves a controller synthesis completely developed in the discrete-time domain. It leads to very good performances of the controlled system, due to the $\mathcal{O}(T^3)$ size of the attained boundary layer and to the smoothness of the resulting control law. As a result, output chattering is eliminated in the steady state, since there is no switching component in the control input. Moreover, the above procedure is feasible only after a $\mathcal{O}(T^2)$ vicinity of the manifold is reached. Moreover, by taking into account in the synthesis procedure the errors due to the discretization, the choice of the sampling period is not subjected to possible non minimum phase behaviors of the controlled system, and the resulting controllers show, theoretically, better robustness properties.

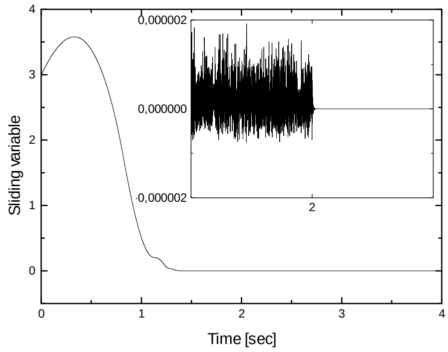

Figure 26: The sliding variable.

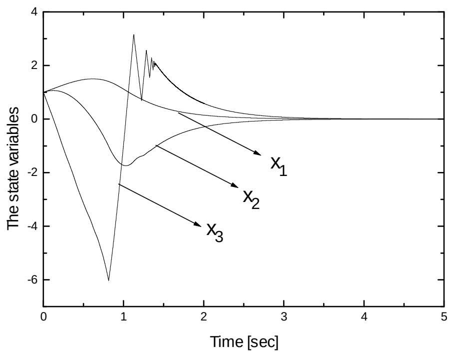

Figure 27: The system state.

APPENDIX

Proof. of Theorem 1

The proposed algorithm requires the approximate real-time evaluation of the singular points of the available state variable $y_1(t)$, (that is of the values corresponding to the time instants at which its derivative $y_2(t)$ is zero). The approximate peak holder (186) is implemented with this aim.

The *modus operandi* of the Algorithm consists in constraining the state trajectories on the y_1Oy_2 plane between two limiting lines, defined taking into account the extreme constant bounds, $\pm\Phi$, G_1 and G_2, of the uncertain dynamics, both converging to a neighbourhood of the origin (fig. 28).

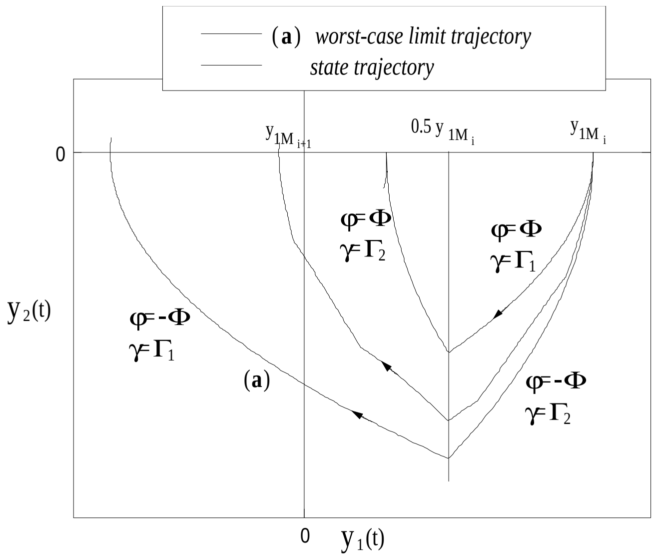

Figure 28: The limit trajectories.

The proposed feedback law causes subsequent crossings of the state trajectory with the abscissa axis, and the control aim is attained by choosing the controller parameters in order to assure that these subsequent crossings are nearer and nearer to the origin of the state plane, so assuring the convergence property.

Let $y_{1\mathrm{M}_j}$ be the actual $j-th$ singular value of $y_1(t)$, $\hat{y}_{1\mathrm{M}_j}$ its estimate, t_{M_j} the corresponding time instant and t_{c_j} the time instant subsequent t_{M_j} at which a commutation occurs ($j = 1, 2, \ldots$).

The proof can be splitted into three different parts:

1. Reaching of the first singular value

It is trivial to verify that, if the control amplitude satisfies the dominance condition $U_\mathrm{M} \geq \frac{\Phi}{\alpha^* G_1}$ (such that the sign of $\dot{y}_2(t)$ is directly affected by that of the input $u(t)$), for any initial condition $(y_1(0), y_2(0))$ a point of the abscissa axis is reached in a finite time, and it is the first singular value $y_{1\mathrm{M}_1}$ of the trajectory $y_1(t)$.

2. Contraction property

U_M and α^* are chosen such that the contractive behavior defined by condition

$$|y_{1\mathrm{M}_{j+1}}| < |y_{1\mathrm{M}_j}| \qquad j = 1, 2, \ldots \tag{214}$$

takes place.

Suppose, without loss of generality, that the actual value of the $j-th$ singular value is such that $y_{1\mathrm{M}_j} > 0$, i.e. it lies on the right side of the abscissa axis. Due to the symmetry of the problem with respect to the origin of the state plane, analogous consideration are also valid if $y_{1\mathrm{M}_j} < 0$.

Due to the sampled nature of the measures, the updating of the gain coefficient $\alpha[k]$ and the switching of the control can occur with a delay at most equal to T with respect to the ideal ones in $t = t_{\mathrm{M}_j}$ and in $y_1[k] = \frac{1}{2}\hat{y}_{1\mathrm{M}}[k]$ respectively.

Consequently, at the actual switching time instant $t = t_{\mathrm{c}_j}$, the states satisfy the following conditions

$$\begin{aligned} y_1(t_{\mathrm{c}_j}) \in [&\tfrac{1}{2}y_{1\mathrm{M}_j} - \tfrac{1}{16}(\Phi + G_2U_{\mathrm{M}})T^2 - \tfrac{1}{2}(\Phi + \alpha^* G_2 U_{\mathrm{M}})T^2 \\ &-T\sqrt{y_{1\mathrm{M}_j}(\Phi + \alpha^* G_2 U_{\mathrm{M}}) + aT^2}\ ,\ \tfrac{1}{2}y_{1\mathrm{M}_j}] \\ y_2(t_{\mathrm{c}_j}) \in [&-(\Phi + \alpha^* G_2 U_{\mathrm{M}})T - \sqrt{y_{1\mathrm{M}_j}(\Phi + \alpha^* G_2 U_{\mathrm{M}}) + aT^2}\ , \\ &-\sqrt{y_{1\mathrm{M}_j}(\Phi - \alpha^* G_1 U_{\mathrm{M}})}] \end{aligned} \tag{215}$$

$$a = \frac{1}{8}(\Phi + G_2U_{\mathrm{M}})[(\Phi + \alpha^* G_2 U_{\mathrm{M}}) + 18 G_2 U_{\mathrm{M}}(1-\alpha^*)] \tag{216}$$

As the system trajectory is constrained between the limit lines in fig. 28, the subsequent crossing of the abscissa axis belongs to the interval

$$\begin{aligned} y_{1\mathrm{M}_{j+1}} \in [&-\tfrac{1}{2}\tfrac{(\alpha^* G_2 - G_1)U_{\mathrm{M}} + 2\Phi}{G_1 U_{\mathrm{M}} - \Phi} y_{1\mathrm{M}_j} - bT^2 \\ &-\tfrac{G_1 + \alpha^* G_2}{G_1 U_{\mathrm{M}} - \Phi} U_{\mathrm{M}} T \sqrt{y_{1\mathrm{M}_j}(\Phi + \alpha^* G_2 U_{\mathrm{M}}) + aT^2}\ , \\ &\tfrac{1}{2}\tfrac{(G_2 - \alpha^* G_1)U_{\mathrm{M}} + 2\Phi}{G_2 U_{\mathrm{M}} + \Phi} y_{1\mathrm{M}_j}] \end{aligned} \tag{217}$$

$$\begin{aligned} b = \tfrac{1}{16}(\Phi + G_2U_{\mathrm{M}})\left[\tfrac{(G_1+\alpha^* G_2)}{G_1U_{\mathrm{M}} - \Phi}U_{\mathrm{M}}\right] + \tfrac{9}{8}(\Phi + G_2U_{\mathrm{M}})(1-\alpha^*)G_2U_{\mathrm{M}} + \\ +\tfrac{1}{2}(\Phi + \alpha^* G_2 U_{\mathrm{M}})\left[\tfrac{(G_1+\alpha^* G_2)}{G_1U_{\mathrm{M}} - \Phi}U_{\mathrm{M}}\right] \end{aligned} \tag{218}$$

Define the following normalized non negative variables

$$z = \frac{U_{\mathrm{M}}}{\Phi} \tag{219}$$

$$\rho = \frac{|y_{1\mathrm{M}_j}|}{\Phi T^2} \tag{220}$$

Sufficient condition for the fulfillment of the contraction condition (214) is represented by the following system of inequalities

$$\begin{cases} \rho \geq 0 \\ z \geq \frac{1}{\alpha^* G_1} \\ (3G_1 - \alpha^* G_2)z - 4 > (G_1 + \alpha^* G_2)(1 + \alpha^* G_2 z)\frac{z}{\rho} + \\ \quad +\frac{1}{8}[G_1 + (18 - 17\alpha^*)G_2](1 + G_2 z)\frac{z}{\rho} + \\ \quad\quad +2(G_1 + \alpha^* G_2)\frac{z}{\rho}\sqrt{(1 + \alpha^* G_2 z)\rho + \frac{1}{8}(1 + G_2 z)[1 + (18 - 17\alpha^*)G_2 z]} \end{cases} \tag{221}$$

The second inequality represents the control's dominance condition, ensuring that the sign of the control $u(t)$ sets the sign of $\dot{y}_2(t)$. The third inequality in (221) defines the set $\mathcal{Z} \subseteq \mathcal{R}$ such that, $\forall z \in \mathcal{Z}$, the points of the straight line defined by the left-hand side term $w_1(z) = (3G_1 - \alpha^* G_2)z - 4$ lie above the points of the parametric function

$$\begin{aligned} w_2(z) = (G_1 + \alpha^* G_2)(1 + \alpha^* G_2 z)\tfrac{z}{\rho} + \tfrac{1}{8}[G_1 + (18 - 17\alpha^*)G_2](1 + G_2 z)\tfrac{z}{\rho} + \\ +2(G_1 + \alpha^* G_2)\tfrac{z}{\rho}\sqrt{(1 + \alpha^* G_2 z)\rho + \tfrac{1}{8}(1 + G_2 z)[1 + (18 - 17\alpha^*)G_2 z]} \end{aligned} \qquad (222)$$

The function $w_2(z;\rho)$ crosses the origin of the cartesian plane zOw_2, and it has a negative local minimum for $z < 0$ and positive first and second derivatives with respect to z if $z > 0$. Moreover, the value of the local minimum is an increasing function of the parameter ρ, and the parametric function $w_2(z;\rho)$ degenerates into the abscissa axis as the parameter ρ goes to infinity. By means of the above considerations it is possible to claim that the two lines defined by the functions $w_1(z)$ and $w_2(z;\rho)$ have at most two cross points, which degenerate into a double contact point for a specific lower value of the parameter ρ called ρ^*. For values of $\rho < \rho^*$ there is no intersection between the two lines and system (221) has not solutions.

This fact imply that the convergence of the sliding variable and of its time derivative to zero is assured only if the the control amplitude is chosen within a proper open set.

The limits of the admissible set depend on ρ, nevertheless the control amplitude could be chosen such that the non negative normalized variable ρ, defining the size of the boundary layer, can reach its minimum at ρ^*. In this case, the admissible set collapses into a single point, which represent a sort of *optimal value* of the control amplitude, which minimizes the theoretical size of the corresponding boundary layer.

The ρ^* value, and the corresponding point $z = z^*$, have been calculated in [Bartolini et al. '98c] under the assumption that no gain affects the control input, that is $G_1 = G_2 = \alpha^* = 1$, leading to the following approximate solution

$$\begin{cases} \rho^* = 85 \\ z^* = 6 \end{cases} \qquad (223)$$

This means that, if $G_1 = G_2 = \alpha^* = 1$, then $U_M = 6F$ is the control effort that minimizes the size of the boundary layer.

By re–considering the general case, it can be noted that, as ρ^* does not depend on T, then, by (215), (216) and (220),Theorem's statement (189) is directly derived.

The dependence of the bounds of the admissible set $\mathcal{Z}$ by the sampling period T can be investigated by analyzing the limit behaviour of system (221) for $T \to 0$.

Since $\rho = \mathcal{O}(T^{-2})$, an intersection between $w_1(z,\rho)$ and $w_2(z)$ can occur iff $z = \frac{4}{3G_1 - \alpha^* G_2} + \mathcal{O}(T)$ or $z = \mathcal{O}(T^{-2})$.

By these considerations, (185) is directly justified. So the Theorem is proved.

3. Finite time reaching of the boundary layer

As the time interval between two subsequent singular values of $y_1(t)$ is finite, the finite time convergence of the system to the residual set is a straightforward consequence of the contraction condition.

References

[Bartolini et al. '95] G. Bartolini, A. Ferrara, V.I. Utkin, "Adaptive sliding mode control in discrete time systems", *Automatica*, vol. 31, no. 6, pp. 769–773, 1995

[Bartolini et al. '97] G. Bartolini, A. Ferrara, E. Usai, "Output Tracking Control of Uncertain Nonlinear Second-Order Systems", *Automatica*, vol. 33, no. 12, pp. 2203–2212, 1997

[Bartolini et al. '98a] G. Bartolini, A. Ferrara and E. Usai, "Chattering Avoidance by Second Order Sliding Mode Control", *IEEE Trans. on Aut. Control*, **43**, 241–246 (1998)..

[Bartolini et al. '98b] G. Bartolini, A. Ferrara, A. Pisano, E. Usai, "Adaptive reduction of the control effort in chattering free sliding mode control of uncertain nonlinear systems", *App. Math. and Computer Science*, vol. 8, no. 1, pp. 51–71, 1998

[Bartolini et al. '98c] G. Bartolini, A. Pisano, E. Usai, "Digital Second Order Sliding Mode Control of SISO Uncertain Nonlinear Systems", *Proc. of the 1998 American Control Conference ACC'98*, vol. 1, pp. 119–124, Philadelfia, Pensylvania, June 1998

[Bartolini et al. '99a] G. Bartolini, A. Ferrara, A. Levant, E. Usai "On Second Order Sliding Mode Controllers", in "Variable Structure Systems, Sliding Mode and Nonlinear Control", K.D. Young and U. Ozguner eds., Lecture Notes in Control and Information Sciences, Springer-Verlag, **247**, 329-350, (1999).

[Bartolini et al. '99b] G. Bartolini, A. Pisano, E. Usai "Variable Structure Control of Nonlinear Sampled Data Systems by Second Order Sliding Modes", in " Variable Structure Systems, Sliding Mode and Nonlinear Control", K.D. Young and U. Ozguner eds., Lecture Notes in Control and Information Sciences, Springer-Verlag, vol. 247, 43-68, (1999).

[Drakuno and Utkin '90] S.V. Drakunov, V.I. Utkin, "Sliding mode in dynamic systems", *Int. Journal of Control*, vol. 55, pp. 1029–1037, 1990

[Drakunov et al. '93] S.V. Drakunov, U. Ozguner, W.C. Su, K.D. Young, "Sliding Mode with Chattering Reduction in Sampled Data Systems", *Proc. of the 32th Conf. on Decision and Control - CDC'93*, pp. 2452–2457,

[Drakunovet al. '96] S.V. Drakunov, U. Ozguner, W.C. Su, "Implementation of Variable Structure Control for Sampled–Data Systems", in *Robust Control via variable structure and Lyapunov techniques.* F.Garofalo and L.Glielmo eds., Lecture Notes in Control and Information Science no. 217, pp. 87–106, Springer-Verlag, London, 1996

[Drakunov et al. '2000] S.V. Drakunov, U. Ozguner, W.C. Su "An O(T^2) Boundary Layer in Sliding Modefor Sampled Data Systems", *IEEE Trans. on Aut. Control*, **45**, 482–485 (2000)..

[Furuta '90] K. Furuta, "Sliding mode control of a discrete system", *System and Control Letters*, vol. 14, no. 2, pp. 145–152, 1990

[Furuta and Pan '94] K. Furuta, Y. Pan, "VSS controller design for discrete time systems", *Control Theory and Advanced Technology*, vol. 10, no. 4/1, pp. 669–687, 1994

[Levant '93] A. Levant, "Sliding order and sliding accuracy in sliding mode control", *Int. Journal of Control*, vol. 58, pp. 1247–1263, 1993.

[Milosavljevic ‘85] C. Milosavljevic, “General conditions for the existence of a quasisliding mode on the switching hyperplane in discrete variable systems”, *Automation Remote Control*, vol. 43, no. 1, pp. 307–314, 1985

[Young et al. ‘99] D. Young, U. Ozguner and V. Utkin “A control engineers guide to sliding mode control”, *IEEE T-CST*, vol. 7, pp. 328–342, 1999.

[Utkin and Drakunov ‘93] V.I. Utkin, S.V. Drakunov, “On Discrete–Time Sliding Mode Control”, *Proc. of the IFAC Symposium on Nonlinear Control Systems - NOLCOS*, pp. 484–489, Capri, Italy, 1989, San Antonio, Texas, December 1993

[Utkin ‘93] V.I. Utkin, “Sliding Mode Control in Discrete–Time and Difference Systems”, in *Variable Structure and Lyapunov Control.* A.S.I. Zinober ed., pp. 83–102, Springer-Verlag, London, 1993

5 2-SMC with global convergence properties

5.1 Preliminaries

All the results presented in previous chapters were based on some assumptions regarding the existence of suitable upperbounds to the drift term and control gain of the second-order sliding dynamics. In particular, it has to be pointed out that all 2-SMC schemes up to now published in the literature are based on the standing assumption that the drift term has a linear growth with respect to the sliding variable derivative. In many cases, especially when a nonlinear dynamic actuator is present at the input of the plant, this assumption prevents the effectiveness of 2-SMC strategies.

In this chapter it is proposed a new algorithm that overcomes such limitations by means of an adaptive switching rule

The affine dependence on the control was a further important standing assumptions of previous treatments, and it will be relaxed at the same time in this chapter.

It will be also shown that the proposed algorithm is able to have a direct control on the peaking behaviour that often affects the transient of nonlinear uncertain systems. So, the proposed approach reveals to be an effective alternative to the use of saturating filters at the inputs.

5.2 Problem Formulation

Consider a nonlinear single–input system that can be modeled by a differential equation in normal form with non-affine dependence on the control input, that is,

$$x^{(n)} = f(\mathbf{x}, u) \tag{224}$$

and assume that the actuator has a first-order dynamics of the type

$$\dot{u} = h(u) + v \tag{225}$$

where $\mathbf{x} = [x, \dot{x}, \ldots, x^{(n-1)}] \in R^n$ is the measurable state vector, $u \in R$ is the plant input, $v \in R$ is the actuator input, and $f(\mathbf{x}, u)$, $h(u)$ are sufficiently smooth uncertain functions. Let any solutions of (224),(225) be well defined for all $t > 0$, provided that v is bounded and continuous.

The problem of generalizing the globality features of the 2-SMC approach to wider class of systems, that can be obtained by combining existing techniques (backstepping and so on) with 2-SMC (see, for instance, [2]) is postponed to further works.

It is well known that if the system output is defined by a proper linear combination of the state variables

$$s(\mathbf{x}) = \mathbf{c}\mathbf{x} \tag{226}$$

where $\mathbf{c} = [c_1, c_2, \ldots c_{n-1}, 1]$ and c_i $(i = 1, 2, \ldots, n-1)$ are real positive constants such that the polynomial $P(z) = z^{n-1} + \sum_{i=1}^{n-1} c_i z^{i-1}$ is a Hurwitz one, then the origin of the state space is a globally asymptotically stable (GAS) equilibrium point for the corresponding zero dynamics.

From (224)-(226), it follows

$$
\begin{cases}
\dot{\hat{\mathbf{x}}}(t) & = \hat{\mathbf{A}}\hat{\mathbf{x}}(t) + \hat{\mathbf{b}}s(t) \\
x_n(t) & = -\hat{\mathbf{c}}\hat{\mathbf{x}} + s(t) \\
\dot{s}(t) & = f(\mathbf{x}, u) + \sum_{i=1}^{n-1} c_i x_{i+1} = k(\mathbf{x}, u) \\
\ddot{s}(t) & = \varphi(\mathbf{x}, u) + \gamma(\mathbf{x}, u)v
\end{cases} \tag{227}
$$

where $\hat{\mathbf{x}} = [x_1, x_2, \dots, x_{n-1}]^T$, $\hat{\mathbf{c}} = [c_1, c_2, \dots, c_{n-1}]$, $\hat{\mathbf{A}}$ is an $(n-1)\times(n-1)$–matrix in companion form with the last row coinciding with the vector $-\hat{\mathbf{c}}$, $\hat{\mathbf{b}} = [0, \dots, 0, 1]^T \in R^{n-1}$, and

$$
\begin{array}{l}
\varphi(\mathbf{x}, u) = \sum_{i=1}^{n-1} \frac{\partial f(\mathbf{x},u)}{\partial x_i} x_{i+1} + \left(\frac{\partial f(\mathbf{x},u)}{\partial x_n} + c_{n-1}\right) f(\mathbf{x}, u) + \sum_{i=1}^{n-2} c_i x_{i+2} + \frac{\partial f(\mathbf{x},u)}{\partial u} h(u) \\
\gamma(\mathbf{x}, u) = \frac{\partial f(\mathbf{x},u)}{\partial u}
\end{array} \tag{228}
$$

Assume that the map $k(\mathbf{x}, \cdot)$ is one to one on any subset $u \in \mathcal{U} \subseteq R$. We refer the reader to [6], and references therein, for a survey of many explicit sufficient conditions on the global injectivity of $\varphi(\mathbf{x}, \cdot)$. Our attention is focused on smooth maps falling into the classes therein considered.

The unique solution (if any) $u \in \mathcal{U}$ of the equation

$$
k(\mathbf{x}, u) = w \tag{229}
$$

for any given $w \in R$, will be denoted by $u^*(\mathbf{x}, \dot{s})$.

On the basis of the above considerations, assume the following

$$
\begin{aligned}
|\varphi(\mathbf{x}, u)| &\leq \Phi\left[\|\mathbf{x}(t)\|, |u|\right] \leq \Phi(\|\mathbf{x}(t)\|, |u^*(\mathbf{x}, \dot{s})|) \leq \overline{\Phi}(\|\mathbf{x}(t)\|, |\dot{s}|) && (230) \\
|h(u)| &\leq H(u) && (231) \\
0 < \Gamma_1 &\leq \gamma(\mathbf{x}, u) \leq \Gamma_2 && (232)
\end{aligned}
$$

where Γ_1, Γ_2 are known positive constants and $\Phi(\cdot)$, $\overline{\Phi}(\cdot)$, $H(u)$ are known positive radially-non-decreasing functions without any particular assumption about their growth.

According to the above assumptions and considerations, the stabilization problem for system (224),(225) can be reduced to the finite-time stabilization of the second-order uncertain system described by the last two equations in (227). As the uncertain system is of relative degree two, a 2-SMC approach appears reasonable.

In previous chapter a class of systems with affine dependence on the control was considered. In that case, if the actual control u were directly modifiable, the relay control the control would act directly on $\dot{s}$).

If a first-order unmodeled actuator dynamics of the type

$$
\dot{u}(t) = h(u) + v(t) \tag{233}
$$

is taken into account, where $v(t)$ is the actuator input and $h(u)$ is unknown, the relative degree is under-estimated, so the above procedure might fail.

By singular perturbation analysis, it has been proven that 1-SMC is robust to the sufficiently fast unmodeled dynamics of the actuators [17]. A discontinuous control $v(t)$ can lead to either a stable or an unstable second-order sliding mode (i.e., a sliding motion on the manifold $s = \dot{s} = 0$), depending on the actual actuator dynamics [13].

Here the presence of the actuator dynamics is considered explicitly, and a suitable control strategy is developed.

It is worth noting that a control

$$v(t) = -(\Phi(\|\mathbf{x}\|, |u|) + k^2) sign(s(t) - s(t_0)) \tag{234}$$

globally forces $\dot{s}$ in a finite time t_{M_1} to zero, t_0 being the initial control time. Therefore, the starting point of the proposed procedure can be regarded as a singular point of the s variable, $s(t_{M_1})$, t_{M_1} s.t. $\dot{s}(t_{M_1}) = 0$.

At $t = t_{M_1}$, it would be necessary to evaluate constant upper bounds to the uncertainties. As a result, the control strategy in chapter 3 could be applied, but the following problem would arise: how can one choose the control effort at the time instant t_{M_1} such that, at least until the subsequent singular point is reached, the uncertain drift term $|\varphi(\mathbf{x}, u)|$ increases without exceeding the constant bound on the basis of which the control amplitude has been evaluated?

The sign and modulus of v remain constant until a commutation condition of the type $s(t_{c1}) = \beta s_{M_1}$ ($\beta = 0$ for the twisting algorithm, $\beta = \frac{1}{2}$ for the suboptimal algorithm) is encountered, and then the sign of v changes. If, before this event occurs, the uncertainty exceeds the constant limit on the basis of which the control amplitude V_M has been computed, the method might fail, in that the existence of both the commutation instant and the subsequent singular point cannot be guaranteed.

With a constant β, the solutions to the problems of predicting a constant upper bound to $|\varphi(\cdot)|$ and of choosing, accordingly, the controller parameters V_M and α such that, over the entire control time interval, the uncertainty does not exceed the predicted upperbound exist only for systems with an affine dependence of the drift term $\varphi(\mathbf{x}, u, t)$ on the plant control u [4].

When this assumption is not verified, the controller structure has to be modified. The solution proposed in this paper, called "solution with variable β", exploits the idea of selecting the commutation instants on line, as soon as a current overestimate of the uncertain drift term modulus is equal to a pre-specified value. After the commutation, it can be proved that a new singular point, closer to the origin than the previous one, is reached at $t = t_{M_2}$, whereas the uncertainties are kept below the pre-specified threshold. The repetition of the same procedure over any successive interval $\left[t_{M_i}, t_{M_{i+1}}\right]$ $(i = 2, 3, \ldots)$ ensures that the convergence to the sliding manifold will take place in a finite time.

In the next section this approach is described and its global convergence properties are proven. Section 3 deals with simulation results, and, in Section 4, some final conclusions are drawn.

5.3 Main result

Our proposed approach can be summarized as follows.

First, we define a compact region $\mathcal{R}$ in the state space containing the 2-sliding set $s = \dot{s} = 0$; within this region, constant bounds to the uncertainties can be found. Then, the control must be able to accomplish the following tasks:

1. globally driving the system trajectories into the region $\mathcal{R}$ in a finite time;

2. constraining the system motion within this region over the entire control time interval;

3. guaranteeing the finite-time reaching of the 2-sliding manifold $s = \dot{s} = 0$

To this end, consider the rectangular region on the $sO\dot{s}$ plane

$$\mathcal{R}_k \equiv \left\{ (s, \dot{s}) \in R^2 : |s| \leq |s_{M_k}|, |\dot{s}| \leq \eta \sqrt{|s_{M_k}|} \right\} \tag{235}$$

where s_{M_k} is the generic k–th singular value of s, ($s_{M_k} = s(t_{M_k})$, $t_{M_k} : \dot{s}(t_{M_k}) = 0$), and η is a positive design parameter to be specified on the basis of the control requirements. In the region $\mathcal{R}_k$, a constant upper bound to the uncertain drift term modulus $|\varphi(\mathbf{x}, u)|$ is given by (230) as

$$\overline{\Phi}_k = \overline{\Phi} \left(\|\mathbf{x}_{M_k}\|, \eta \sqrt{|s_{M_k}|} \right) \tag{236}$$

where $\|\mathbf{x}_{M_k}\|$ is an upper bound to $\|\mathbf{x}\|$, whenever the output phase trajectory is within the region $\mathcal{R}_k$. Due to the bounded-input-bounded-state (BIBS) property of the linear subsystem in (227), the following relationship holds [4]

$$\|\mathbf{x}(t)\| \leq \|\mathbf{x}_{M_k}\| = Q_x \|\mathbf{x}(t_{M_k})\| + Q_y |s_{M_k}| \qquad t \geq t_{M_k} \tag{237}$$

where Q_x and Q_y are properly defined constants.

The control strategy is designed such that the controlled plant may reach, and then never leave, any region $\mathcal{R}_k$.

During the *initialization phase*, the system is globally driven in a finite time toward the $\dot{s} = 0$ axis, that is, a first singular point s_{M_1} is attained after a finite transient process. Then the control signal v is defined such that a sequence of singular values $s_{M_k} = s(t_{M_k})$, $k = 2, 3, \ldots$, satisfying the contraction condition (47) is generated. This implies that $\mathcal{R}_{k+1} \subset \mathcal{R}_k$ and that $\mathcal{R}_k \to O$ in a finite time, O being the origin of the $sO\dot{s}$ plane.

The possibility of accomplishing this twofold task strictly depends on the assumptions made on the uncertain plant dynamics. In previous works, the problem has been solved by assuming that the the modulus of the uncertain drift term $\varphi(\mathbf{x}, u)$ in (228) increases linearly with the control magnitude $|u|$ [3, 4]. This assumption ensures that the inequality representing the algebraic loop between the control amplitude and the uncertainty bounds (the amplitude depends on the bounds and vice versa) will be solved. In case $|\varphi(\mathbf{x}, u)|$ were nonlinear with respect to $|u|$, a solution could not exist.

In this note, it is shown that, if the *anticipating factor* β in the switching logic is properly adjusted, two main results are obtained. First, the modulus of the output derivative can be maintained smaller than a pre-specified value, thus counteracting the peaking phenomenon; secondly, the controlled class of plants is enlarged, now encompassing a class of systems nonlinear in the control law and/or with nonlinear dynamic actuators.

The control algorithm based on the above considerations is formally defined by the following Theorem:

Theorem 1: *Consider system* (224)-(225) *with a completely available state. Let the sliding output* s *be defined according to* (226), *and let it be such that the corresponding zero-dynamics* *is asymptotically stable. Assume that the uncertain input-output dynamics* (227)-(228) *satisfies* (230)-(232)*.*

The control law

$$v(t) = \begin{cases} -\frac{1}{\Gamma_1}\left[\Phi\left[\|\mathbf{x}(0)\|, |u(0)|\right] + \chi\right] \mathrm{sign}\left(s(0)\right) & t = 0 \\ -\frac{1}{\Gamma_1}\left[\Phi\left[\|\mathbf{x}(t)\|, |u(t)|\right] + \chi\right] \mathrm{sign}\left(s(t) - s(0)\right) & 0 < t \leq t_{M_1} \end{cases} \quad \chi > 0 \tag{238}$$

ensures the reaching of a first singular point s_{M_1} at the time instant $t = t_{M_1} \leq \frac{\dot{s}(0)}{\chi}$. From this point on, the control law

$$v(t) \quad = \quad -V_{M_k}\mathrm{sign}\left[s(t) - \beta_k s_{M_k}\right] \qquad t_{M_k} < t \leq t_{M_{k+1}} \qquad k = 1, 2, \ldots \tag{239}$$

guarantees the finite-time vanishing of the system output s and of its derivative, provided that the controller parameters are chosen according to

$$V_{M_k} \quad = \quad \frac{\alpha}{\Gamma_1}\left[\overline{\Phi}_k + \frac{1}{3}\eta^2\right] \qquad \alpha > 1 \tag{240}$$

$$\beta_k \quad = \quad max\left\{\frac{1}{2}, 1 - \frac{\eta^2}{2[\overline{\Phi}_k + \Gamma_2 V_{M_k}]}\right\} \tag{241}$$

where η is a positive constant, $\overline{\Phi}_k$ is defined in (236),(237)*, t_{M_k} are the time instants at which $\dot{s}$ is zero, and $s_{M_k} = s(t_{M_k})$. As a consequence, the state $\mathbf{x}(t)$ globally exponentially converges to zero.*

Proof.

Initialization phase: $\quad 0 \leq t \leq t_{M_1}$

The initialization phase is designed such that the axis $\dot{s}(t) = 0$ is reached in a finite time t_{M_1}.

According to (238), and taking into account (230)-(232), the sign of $\dot{s}$ is forced to be opposite to that of $\ddot{s}$. The behavior of the system is different in the two cases $s(0)\dot{s}(0) > 0$ and $s(0)\dot{s}(0) < 0$. In the former case, $|\dot{s}|$ monotonically converges to zero with no switchings of the control sign. In the latter case, the same behavior is attained with an instantaneous switching of the control at $t = 0^+$. In both cases, at $t = t_{M_1} < (\dot{s}(0)/\chi)$, a first singular value of $s(t)$, s_{M_1}, is reached, and this value is available for control purposes.

Reaching phase $\quad t_{M_k} < t \leq t_{M_{k+1}} \qquad (k = 1, 2, \ldots)$

Let s_{M_k} be the k–th singular value of $s(t)$, t_{M_k} the corresponding time instant, and t_{c_k} the time instant (following t_{M_k}) at which a control switching occurs.

Suppose, without loss of generality, that s_{M_k} is positive. Due to the symmetry of the limit trajectories, analogous considerations still apply in the case $s_{M_k} < 0$.

The proof of the finite-time convergence to the origin of the state plane can be split into the following steps.

Contraction property:

According to (240), the control magnitude is such that the dominance condition

$$\Gamma_1 V_{M_k} > \overline{\Phi}_k \tag{242}$$

is always ensured in the $\mathcal{R}_k$ region, and the sign of v sets the sign of $\ddot{s}$. Then, over the $(t_{M_k}, t_{c_k}]$ and $(t_{c_k}, t_{M_{k+1}}]$ intervals, the control is given by $-V_{M_k}$ and V_{M_k}, respectively. The limit trajectories on the $sO\dot{s}$ plane are obtained by considering the uncertain terms always acting with their maximum effort, and are defined by parabolic arcs. In particular, Fig. 29 shows that the actual system trajectory between two successive singular points, s_{M_i} and $s_{M_{i+1}}$, is confined between the $c-d$ and $a-b$ limit curves.

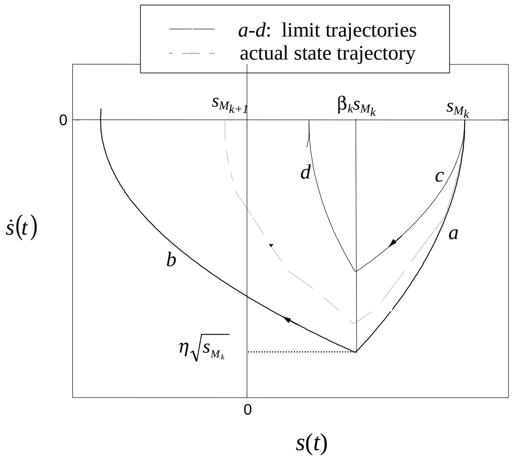

Figure 29: The actual and limit state trajectories.

A control switching occurs when the lower boundary of $\mathcal{R}_k$ is reached in the worst case, and this defines the value of β_k. Considering the limit line a in Fig. 29 , a predictor of the worst case evolution of $\dot{s}$ can be derived as

$$|\dot{s}|_M(t) = \sqrt{\frac{2(s(t) - s_{M_k})}{\Gamma_2 V_{M_k} + \overline{\Phi}_k}} \tag{243}$$

where $|\dot{s}|_M(t)$ overestimates the modulus of $\dot{s}$ at any time instant.

β_k is set to ensure that $|\dot{s}|$ will remain upperbounded by $\eta\sqrt{s_{M_k}}$, and considering the switching condition $s(t) = \beta_k s_{M_k}$, it yields, according to (243),

$$\beta_k = 1 - \frac{\eta^2}{2[\overline{\Phi}_k + \Gamma_2 V_{M_k}]} \tag{244}$$

In order to avoid that, for large negative values of β, the left margin of $\mathcal{R}_k$ may be exceeded, a lower threshold greater than -1 must be introduced. To take advantage of the time-optimal derivation of the suboptimal 2-SMC, it is reasonable to use the lower bound $\frac{1}{2}$.

The parabolic arc b in Fig. 29 is described by

$$s(t) = \beta_k s_{M_k} + \frac{1}{2}\frac{\dot{s}^2 - \eta^2 s_{M_k}}{\Gamma_1 V_{M_k} - \overline{\Phi}_k} \tag{245}$$

then $s_{M_{k+1}}$ can be easily evaluated by substituting $\dot{s} = 0$ into (245), and the contraction condition (47) is equivalent to

$$0 < \frac{1}{2}\frac{\eta^2}{\Gamma_1 V_{M_k} - \overline{\Phi}_k} < 1 + \beta_k \tag{246}$$

Taking into account that $\beta_k \in [\frac{1}{2}, 1)$, condition (246) is satisfied, whatever β_k may be, provided that V_{M_k} is chosen according to (240); then the region $\mathcal{R}_k$ is never left during the considered time interval $t \in (t_{M_k}, t_{M_{k+1}}]$.

If condition (246) is satisfied at any k, then a real positive constant $\nu^2 < 1$ such that $|s_{M_{k+1}}| < \nu^2 |s_{M_k}|$ $(k+1, 2, \ldots)$ can always be defined; therefore, if one sets

$$\dot{s}_{M_k} = \sup_{t \in [t_{M_k}, t_{M_{k+1}}]} |\dot{s}(t)| \tag{247}$$

one obtains

$$\begin{cases} |s_{M_{k+1}}| \leq \nu^{2k} |s_{M_1}| \\ \dot{s}_{M_k} \leq \eta \nu^{k-1} \sqrt{\dot{s}_{M_1}} \end{cases} \tag{248}$$

which implies $|s_{M_k}| \to 0$ and $|\dot{s}_{M_k}| \to 0$ as $k \to \infty$.

Finite time convergence:

Starting from $(s_{M_k}, 0)$ at the time instant $t = t_{M_k}$ and considering the limit trajectories $a - b$ and $c - d$ in Fig. 29 , it can be proved that the $a - b$ trajectory is slower than the $c - d$ one. Algebraic computations lead to

$$t^{ab}_{M_{k+1}} = t_{M_k} + \sqrt{2(1-\beta_k)} \left[\frac{(\Gamma_1 + \Gamma_2) V_{M_k} + 2\overline{\Phi}_k}{(\Gamma_2 V_{M_k} + \overline{\Phi}_k)\sqrt{\Gamma_1 V_{M_k} - \overline{\Phi}_k}} \right] \sqrt{|s_{M_k}|} \tag{249}$$

Relying on the contraction property, the terms $\overline{\Phi}_k$ and V_{M_k} are bounded; then it is possible to define the constant

$$\Psi = \max_k \left\{ \sqrt{2(1-\beta_k)} \left[\frac{(\Gamma_1 + \Gamma_2) V_{M_k} + 2\Phi^*_k}{(\Gamma_2 V_{M_k} + \Phi^*_k)\sqrt{\Gamma_1 V_{M_k} - \Phi^*_k}} \right] \right\} \tag{250}$$

and hence

$$t^{ab}_{M_{k+1}} \leq t_{M_k} + \Psi \sqrt{|s_{M_k}|} \tag{251}$$

from which one recursively derives

$$t^{ab}_{M_{k+1}} \leq t_{M_1} + \Psi \sum_{j=1}^{k} \sqrt{|s_{M_j}|} \tag{252}$$

Taking into account (248), the finite-time convergence is proved as the following relationship holds

$$T_r = \lim_{k\to\infty} t^{ab}_{M_{k+1}} \leq t_{M_1} + \Psi \frac{\sqrt{|s_{M_1}|}}{1-\nu} \tag{253}$$

Remark: Because of the lack of information assumed in the statement of the problem, the sufficient conditions stated in Theorem 1 are derived on the basis of a worst-case analysis, thus they are very conservative. Computer simulations show that the control effort may be set to smaller values than those in (240), thus one can obtain a higher smoothness of the resulting control law and a higher accuracy in the practical realization of the control scheme; the control effort may be set even to a-priori established constant values, thus one can reduce the on-line computational effort.

5.4 Some simulation examples

In this section, the proposed procedure is illustrated and compared with other methodologies by means of a simple, yet challenging, example.

Consider the dynamic system

$$\dot{x} = ax^2 + u \qquad |a| \leq 4 \tag{254}$$

with the actuator dynamics

$$\tau\dot{u} = -u + v \tag{255}$$

Assume that the control objective is to stabilize it in a finite time; then, $x = 0$ can be defined as the sliding manifold, and the 1-SMC scheme

$$v = -(k^2 + 4x^2)\text{sign}(x) \tag{256}$$

guarantees the global convergence of x to zero if $\tau = 0$ (i.e. if $u = v$).

Transient peaking and instability occur for increasing values of τ (as pointed out in Fig. 30) if one sets $a = 2$, $k^2 = 1$.

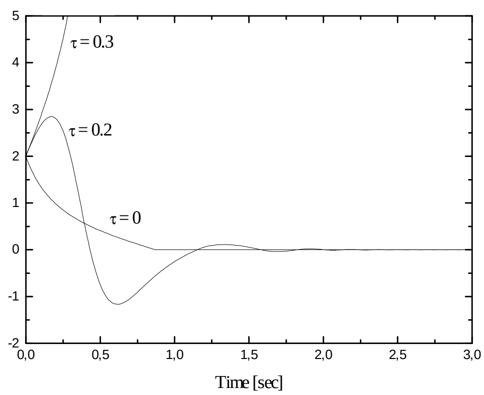

Figure 30: 1-SMC. The x behaviour for different values of τ.

A sensible way to recover stability is to use sliding-mode control algorithms for systems of relative degree two (2-SMC algorithms). Differentiating twice the sliding output locally leads to a second-order sliding dynamics such that it is possible to use one of the 2-SMC algorithms presented in chapter 3.

Fig. 31 shows the state evolution when the suboptimal 2-SMC algorithm is implemented; the peaking effect is pointed out.

Moreover, it may happen that the uncertain drift term $\varphi(\mathbf{x}, u)$ in (227) does not satisfy the boundedness conditions relevant to the linear growth with respect to u. As an example, consider system (254), and assume that the actuator dynamics is represented by

$$\dot{u} = -u^2 + v \tag{257}$$

Then the second-order sliding dynamics is given by

$$\ddot{x} = 2x^3 + 2xu + u^2 + v = \varphi(x, u) + v \tag{258}$$

In this case, the nonlinear growth of $|\varphi(x, u)|$ is not affine any more in the variable u; as a consequence the "conventional" suboptimal 2-SMC scheme cannot be applied.

If one considers system (254),(257), for $x(0) = 2$ and $u(0) = -4$, the performance of the new control scheme, which has been presented and discussed in the previous section, is displayed in Fig. 32 , showing the x evolution. If one introduce the time-varying anticipating factor to improve the convergence properties, outlined in the Introduction, the stability of the system can be recovered and the peaking phenomenon is avoided as well.

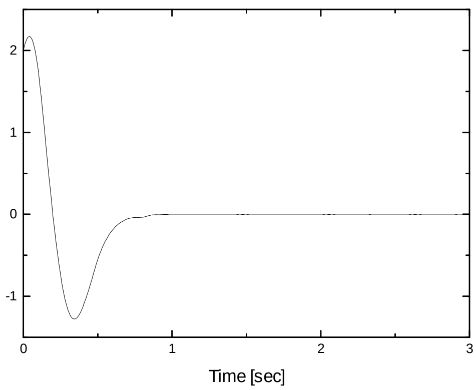

Figure 31: 2-SMC (suboptimal algorithm). The x behaviour for $\tau = 0.3$.

In Fig. 33 , the trajectories of the system on the phase plane are compared in the cases of suboptimal 2-SMC and 2-SMC with variable β, showing that the former solution fails to cope with the fast nonlinear growth of the uncertain actuator dynamics (257).

As mentioned in the previous section, a different way to deal with relative-degree-two systems, widely used in output-feedback control, is to implement an observer of the output derivative. Due to the uncertainties it is reasonable to use high-gain observers (HGO) [1], and the 1-SMC strategy could be applied by exploiting the new sliding output

$$s_1 = \hat{\dot{x}} + cx \qquad c > 0 \tag{259}$$

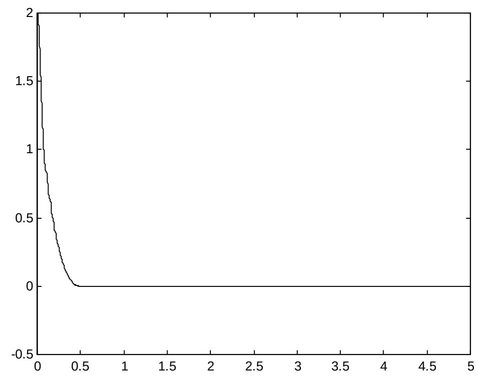

Figure 32: The x behavior under the action of the new 2-SMC scheme.

in which $\hat{\dot{x}}$ is an estimate of $\dot{x}$, that can be defined as

$$\hat{\dot{x}} = -k(\hat{x} - x) \tag{260}$$

Figure 34 depicts the attained behavior for $k = 400$ and $c = 2$.

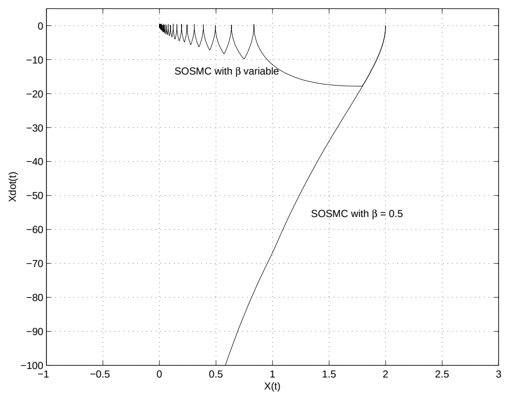

Figure 33: The system trajectories on the $xO\dot{x}$ plane.

The resulting transient peaking, which was counteracted by the SOSMC scheme proposed in this note (see Fig. 32) is pointed out. The advantages of our procedure seem to be the absence of an observer and a direct control of the peaking phenomenon.

In the authors' opinion, considerable improvements could be obtained in output feedback control systems by proper combinations of the proposed scheme with other observer-based approaches, deserving further analysis.

5.5 Conclusions

The sliding-mode control of nonlinear uncertain systems with unmodeled first-order actuator dynamics has been considered. A second-order sliding-mode control scheme with adaptive switching rule has been proposed, and its effectiveness has been shown for systems encompassing some classes of non zero-input-stable (ZIS) systems and non bounded-input-bounded-state (BIBS) stable plants. The proposed algorithm is easy to implement and therefore suited to being used

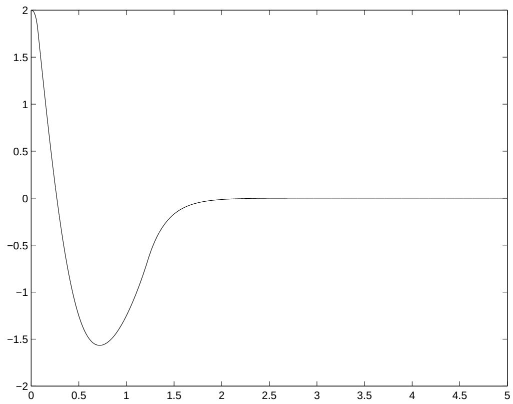

Figure 34: HGO-based 1-SMC. The x behavior.

in practice; it is also effective in counteracting the transient peaking phenomenon.

References

[1] N. Atassi and H. Khalil, "A Separation Principle for the Stabilization of a Class of Nonlinear Systems", *IEEE Trans. on Automatic Control*, vol. 44, no. 9, pp. 1672–1687, 1999.

[2] G. Bartolini, A. Ferrara, L. Giacomini and E. Usai, "Properties of a combined backstepping/second order sliding mode control algorithm for some classes of uncertain nonlinear systems", *IEEE Trans. Aut. Contr.*, to appear in 2000.

[3] G. Bartolini, A. Ferrara and E. Usai, "Applications of a suboptimal discontinuous control algorithm for uncertain second-order systems", *Int. J. of Robust and Nonlinear Control*, vol. 7, no.4, pp. 299–319, 1997.

[4] G. Bartolini, A. Ferrara and E. Usai, "Chattering Avoidance by Second Order Sliding Mode Control", *IEEE Trans. on Automatic Control*, vol. 43, no. 2, pp. 241–246, 1998.

[5] G. Bartolini, A. Ferrara, A. Levant and E. Usai, "On Second Order Sliding Mode Controllers", in *Variable Structure Systems, Sliding Mode and Nonlinear Control*, K.D. Young and U. Ozguner (Eds.), Lecture Notes in Control and Information Sciences, Springer-Verlag, vol. 247, pp. 329-350 , 1999.

[6] G. Bartolini and T. Zolezzi, "Control of Nonlinear Variable Structure Systems", *J. Math. Analysis Appl.*, vol.118, pp. 42–62, 1986.

[7] K.D. Young and U. Ozguner (Eds.), *Variable Structure Systems, Sliding Mode and Nonlinear Control*, Lecture Notes in Control and Information Sciences, vol. 247, Springer-Verlag, 1999.

[8] Furuta K. and Pan Y., "Variable structure control with sliding sector", *Automatica*, vol. 36, pp. 211–228, 2000.

[9] D. Young, U. Ozguner and V. Utkin, "A control engineers guide to sliding mode control", *IEEE Trans. Contr. Syst. Tech.*, vol 7, pp. 328–342, 1999.

[10] H. Elmali H. and N. Olgac, "Robust Output Tracking Control of Nonlinear MIMO Systems via Sliding Mode Technique", *Automatica*, vol. 28, pp. 145–151, 1992.

[11] A. Isidori, *Nonlinear Control Systems*, Springer Verlag, Berlin, 1989.

[12] A. Levant, "Sliding order and sliding accuracy in sliding mode control", *Int. J. Contr.*, vol. 58, pp. 1247–1263, 1993.

[13] A. Levant and L. Fridman, "Higher order sliding modes as a natural phenomenon in control theory", in *Robust control via variable structure and Lyapunov techniques*, F. Garofalo and L. Glielmo Eds., Lecture Notes in Control and Information Sciences, vol. 217, pp. 107–133, Springer–Verlag, London, 1996.

[14] H. Sira–Ramirez, "On the sliding mode control of nonlinear systems", *Syst. Contr. Lett.*, vol. 19, pp. 303–312, 1992.

[15] H.J. Sussmann and P.V. Kokotovic, "The Peaking Phenomenon and the Global Stabilization of Nonlinear Systems", *IEEE Trans. on Automatic Control*, vol. 36, no. 4, pp. 424–439, 1991.

[16] X. Yu and M. Zihong, "Model Reference Adaptive Control Systems with Terminal Sliding Modes" *Int. J. Contr.*, vol. 64, pp. 1165–1176, 1996.

[17] V.I. Utkin, *Sliding Modes in Control and Optimization*, Springer Verlag, Berlin, 1992.

[18] S.T. Venkataraman and S. Gulati, "Control of Nonlinear Systems using Terminal Sliding Modes", *ASME J. Dyn. Syst. Meas. Contr.*, vol. 115, pp. 554–560, 1989.

Part II

Applications

6 Control of Robotic Manipulators

The application of sliding mode control theory to mechanical systems, in principle, appears to be quite appropriate, compared with other methodologies. Indeed, by exploiting the positive definiteness of the inertia matrix, and on the basis of a rough description of the physical model, it is possible to perform high-precision tracking with very simple relay control devices, even for kinematic chains with a large number of degrees of freedom. Adaptive control approaches, for example, require regressors whose complexity increases with the number of degrees of freedom [Slotine and Li '91, Slotine *et al.* '85].

Even if, in theory, sliding mode controllers are simpler and more efficient of most of the traditional as well as advanced devices (PID, computed torque, adaptive, Lyapunov-based, high gain etc., see [Spong and Vidyasagar'89, Slotine *et al.* '85, Berghuis et al.'93]), they suffer from the so called chattering phenomenon, which is due to the discontinuous nature of the control laws.

If the control signal is a force or a torque , as in the standard modelization of robot control problem, the discontinuity of the control action would correspond to an unacceptable hammering of the wheels in the gear-boxes with disruptive effects. Some proposals to avoid the chattering behaviour appeared in the literature are based on the smoothing of the discontinuous control law by means of approximating continuous functions [Slotine and Li '91, Tang '98]). Under such approximations, the motion of the controlled system is proved to be confined within a boundary layer of suitable dimension. But the resulting motion, even if with bounded amplitude, is characterized by oscillatory behaviours with umpredictable frequency. This fact could excite medium frequency hidden modes of the unmodelled elastic dynamics usually neglected due to the rigid body assumption.

In contrast, the very spirit of sliding mode control is that of generating high (ideally infinite) frequency control signals, that is signal with frequency far beyond the bandwith of the actual mechanical system. This is the reason why it is advisory to preserve the discontinuous nature of the control law while trying to reduce the chattering effect.

The problem faced in this paper is that of the control of mechanical systems by using as discontinuous control signal the control torque derivative, that directly corresponds to the voltage at the input of the actuators. This philosophy is analogous to the practical solution with pulse-width modulators usually adopted in servo-mechanism in which the electric control signal switches at very high frequency (dozen of KHz), while the mechanical input (torque) is continuous, in average, with a residual oscillating at a frequency far beyond the system bandwidth.

The solution to the problem in question, naturally leads to second order sliding mode [Levant '93, Bartolini et al.'99]. In contrast to higher order sliding modes, second order sliding modes have achieved a sufficient degree of formalization to be used in applications. With the term "second order sliding mode", those behaviours are indicated for which the condition $s = \dot{s} = 0$ is attained in a finite time with a control affecting only $\ddot{s}$, and with unavailable $\dot{s}$, $s = 0$ being the sliding manifold. Second order sliding mode control algorithms recently developed, separately, by A. Levant and the authors have produced satisfactory results for single-input systems. The extension of second order sliding mode to multi-input systems, as in general, robotic manipulators are, is not trivial. The aim of this paper is just that of developing a special instance of multi-input second order sliding mode control for robotic systems by exploiting some structural properties of the inertia matrix. As a result, a chattering-free control acting on the mechanical dynamics is obtained, since the discontinuities are confined to the torque derivative (i.e. the actuators inputs). Moreover, the overall performances are extremely high in spite of large uncertainties on the system dynamics (the on-line computation of a complex regressor or a precise evaluation of the load-depending gravitational term is not required).

The control problem is formulated in the following subsection 6.1, while in the subsequent subsection 6.2 a suitable solution, based on a proper combination of first and second order SMC methodology, is proposed, and its effectiveness is demonstrated by simulations in subsect. 6.3.

6.1 Problem Formulation

In this work we shall consider the following model of a rigid n-link robot [Spong and Vidyasagar'89]

$$M(q)\ddot{q} + C(q,\dot{q})\dot{q} + g(q) = \tau \tag{261}$$

where $q \in R^n$ represents the arm coordinates, $M(q)$ is the n-by-n inertia matrix, $C(q,\dot{q})\dot{q}$ represents the Coriolis and centrifugal torques, $g(q)$ represents the gravity terms and τ is the vector of the applied torques.

The complex nonlinear dynamics (261) has some important properties of boundedness, positivity and simmetry, that facilitate both analysis and design. Among these properties, the following will be used in the present work

(1) Boundedness and positivity of the inertia matrix.

There are two constants k_1, k_2 s.t.

$$k_1 I \leq M(q) = M^T(q) \leq k_2 I \tag{262}$$

(2) Boundedness and smothness of the system matrixes and dynamics

There are some constants $k_3, k_4, \ldots, k_{15}$ s.t.

$$\begin{aligned} &\|\ddot{q}\| \leq k_3 + k_4\|\dot{q}\| + k_5\|\tau\| && \|\dot{M}(q)\| \leq k_6 + k_7\|\dot{q}\| \\ &\|C(q,\dot{q})\| \leq k_8 + k_9\|\dot{q}\| && \|\dot{C}(q,\dot{q})\| \leq k_{10} + k_{11}\|\dot{q}\| + k_{12}\|\tau\| \\ &\|g(q)\| \leq k_{13} && \|\dot{g}(q)\| \leq k_{14} + k_{15}\|\dot{q}\| \end{aligned} \tag{263}$$

(3) Skew-simmetry of the matrix

$$\dot{M}(q) - 2C(q,\dot{q}) \tag{264}$$

The tracking problem consists in finding a control action guaranteeing that

$$\lim_{t\to\infty} q(t) = q_d(t) \tag{265}$$

where $q_d(t)$ represents the desired profile for the robot coordinates.

The motor parameters are often not exactly known, therefore the use of robust control techniques appears sensible.

Let us define the sliding variable as follows

$$s = \dot{q} - \dot{q}_r \tag{266}$$

where $\dot{q}_r$ is given by

$$\dot{q}_r = \dot{q}_d - \Lambda(q - q_d) \tag{267}$$

in which Λ is an arbitrary diagonal positive-definite matrix of appropriate dimensions. It is worth noting that the system motion constrained on the sliding manifold $s = 0$ exhibits the desired asymptotic tracking performance.

The peculiarity of the second-order sliding mode control approach is that *the control action is applied to the second derivative of the sliding variable.*

Consider the second derivative of s

$$\ddot{s} = \psi(q, \dot{q}, \tau) + M^{-1}(q)\dot{\tau} \tag{268}$$

where

$$\psi(q, \dot{q}, \tau) = M^{-1}(q)[-\dot{M}(q)\ddot{q} - \dot{C}(q, \dot{q})\dot{q} - C(q, \dot{q})\ddot{q} - \dot{g}(q)] - \dddot{q}_r \tag{269}$$

It can be used, as a discontinuous control signal that drives the system in finite time onto the sliding manifold, the time derivative of the torque vector. The actual control torque vector τ, obtained by integrating the discontinuous derivative $\dot{\tau}$, results in being continuous.

Our proposal consists of the following steps

1. Consider an auxiliary dynamic system constituted by a double vector integrator with output z_1 and input w to be defined

$$\begin{cases} \dot{z}_1 = z_2 \\ \dot{z}_2 = w \end{cases} \qquad z_1, z_2, w \in \Re^n \tag{270}$$

2. Put

$$\varepsilon_1 = s - z_1 \qquad \varepsilon_1 \in \Re^n \tag{271}$$

and consider the associated second-order dynamics

$$\begin{cases} \dot{\varepsilon}_1 = \varepsilon_2 \\ \dot{\varepsilon}_2 = \ddot{s} - w \end{cases} \tag{272}$$

which consists of n non-interacting single input systems that can be separately controlled by means of the $i - th$ entry of the vector w.

3. Steer ε_1 and ε_2 to zero by means of a discontinuous control w.

The sliding motion on $\varepsilon_1 = \varepsilon_2 = 0$ is referred as second order sliding mode (2-SM). The theoretical properties of this special class of sliding modes have been thoroughly investigated in [Levant '93], while in [Bartolini et al.'98b] it has been evidenced that the equivalent control for 2-SM can be defined as the continuous control that solves the equation

$$\ddot{\varepsilon}_1 = 0 \tag{273}$$

According to the above definition, the equivalent control for system (272) is given by

$$w_{eq} = \ddot{s} = \psi(q, \dot{q}, \tau) + M^{-1}(q)\dot{\tau} \tag{274}$$

Once the 2-SM has been established on the manifold $\varepsilon_1 = \varepsilon_2 = 0$, the "equivalent representation" of system (270) can be obtained by substituting w_{eq} for w [Utkin '92], yielding to

$$\begin{cases} \dot{z}_1 = z_2 \\ \dot{z}_2 = w_{eq} = \psi(q, \dot{q}, \tau) + M^{-1}(q)\dot{\tau} \end{cases} \tag{275}$$

The equivalent system (275) can be stabilized by first order sliding mode control technique. The fourth step of the proposed procedure is

4. Define the sliding quantity

$$s_z = z_2 + \Lambda_z z_1 \tag{276}$$

where Λ_z is a positive definite diagonal matrix and steer the system (275) onto the manifold $s_z = 0$ by discontinuous control $\dot{\tau}$.

It is noteworthy that the simultaneous satisfaction of conditions

$$\begin{aligned} \varepsilon_1 &= 0 \\ \varepsilon_2 &= 0 \\ s_z &= 0 \end{aligned} \tag{277}$$

ensures the exponential tracking of the robot reference trajectory.

Unlike adaptive control schemes, the proposed controller is very simple to implement, even for manipulators with a large number of dof. Moreover, it is not strictly required for the inertia matrix to be PD, but it has only to satisfy the classical conditions for the existence of a solution to the multi-input first-order SMC problem [Utkin '92, Slotine and Li '91]. This property can be useful when the robot is described in terms of cartesian coordinates.

6.2 The control Algorithm

Summarizing the procedure described in previous section, the following Theorem is proved.

Theorem 1: *Consider system* (261) *satisfying* (262)-(263) *and with available state vector* $\mathcal{Q} = [q \;\; \dot{q}]$. *Let the sliding quantities* s *and* s_z *be defined according to* (266), (267), (270), (276). *If the control torque vector derivative* $\dot{\tau}$ *and the auxiliary control signal* w *are defined as*

$$\dot{\tau}_i = -\left[\Psi_{M_i}(\cdot) + \eta^2\right] sign(s_{z_i}) \tag{278}$$

$$w_i = \left[2\Upsilon^*_{Mi} + \eta^2\right] sign(\varepsilon_{1i} - \frac{1}{2}\varepsilon_{1i_M}) \tag{279}$$

where $\Psi_{M_i}(\cdot)$ *and* Υ^*_{Mi} *are defined in* (291) *and* (282), η *is a non-null arbitrary constant,* z_1 *and* z_2 *are the states of the auxiliary system* (270) *and* ε_1 *is defined according to* (271), *then the asymptotic tracking of any* C^3 *reference trajectory* q_d *is guaranteed.*

Proof.

Part I: Stabilization of system (272)

By (268), (269), the drift term $\ddot{s}$ of the system (272) can be expressed as

$$\ddot{s} = M^{-1}(q)[-\dot{M}(q)\ddot{q} - \dot{C}(q, \dot{q})\dot{q} - C(q, \dot{q})\ddot{q} - \dot{g}(q) + \dot{\tau}] - \dddot{q}_r \tag{280}$$

By (262)-(263), its entries $\ddot{s}_i$, $i = 1, 2, \ldots n$ can be upper bounded by known functions, so that

$$|\ddot{s}_i| \leq \Upsilon_{Mi}(\cdot) = \alpha_{1i} + \alpha_{2i}\mathcal{F}_i(\|\mathcal{Q}\|) + \alpha_{3i}\|\tau\| \tag{281}$$

The n non-interacting subsystems in which can be decomposed system (272), each one with drift term $\ddot{s}_i$ and control w_i, fall belong to the class of plants for which can be applied the sub-optimal 2-SMC algorithm [Bartolini et al.'98a, Bartolini et al.'99], and the finite-time stabilization of all entries of vectors s and $\dot{s}$ can be attained by suitable discontinuous control w.

In order to simplify the treatment it is assumed that a constant value Υ^*_{Mi} can be found such that

$$|\Upsilon_{Mi}(\cdot)| \leq \Upsilon^*_{Mi} \tag{282}$$

This latter assumption gives local validity to the attained result.

Part II: Stabilization of the equivalent system (275)

This part assumes that the finite-time attainment of the condition $\varepsilon_1 = \varepsilon_2 = 0$ (see Part I) has been already achieved. This implies that the following relationships hold

$$\begin{cases} z_1 = s = \dot{q} - \dot{q}_r \\ z_2 = \dot{s} = \ddot{q} - \ddot{q}_r \\ \ddot{q} = s_z - \Lambda_z s + \ddot{q}_r \end{cases} \tag{283}$$

The third one will be used during the proof. To prove that a suitably defined control $\dot{\tau}$ is able to force s_z to converge to zero in finite time, consider the following Lyapunov function candidate

$$V_z = \frac{1}{2} s_z^T M(q) s_z \tag{284}$$

with time derivative given by

$$\dot{V}_z = s_z^T M(q)\dot{s}_z + \frac{1}{2} s_z^T \dot{M}(q) s_z \tag{285}$$

Differentiating the sliding variable s_z yields

$$\dot{s}_z = \dot{z}_2 + \Lambda z_2 = \ddot{s} + \Lambda z_2 = \dddot{q} - \dddot{q}_r + \Lambda z_2 \tag{286}$$

while differentiating (261) leads to

$$M(q)\dddot{q} = -\dot{M}(q)\ddot{q} - \dot{C}(q,\dot{q})\dot{q} - C(q,\dot{q})\ddot{q} - \dot{g}(q) + \dot{\tau} \tag{287}$$

Substituting (286) and (287) into (285) one obtains

$$\begin{aligned} \dot{V}_z &= s_z^T \left[M(q)\dddot{q} - M(q)\dddot{q}_r + M(q)\Lambda_z z_2\right] + \tfrac{1}{2} s_z^T \dot{M}(q) s_z = \\ &= s_z^T \left[-\dot{M}(q)\ddot{q} - \dot{C}(q,\dot{q})\dot{q} - C(q,\dot{q})\ddot{q} - \dot{g}(q) - M(q)\dddot{q}_r + M(q)\Lambda_z z_2 + \dot{\tau}\right] + \tfrac{1}{2} s_z^T \dot{M}(q) s_z \end{aligned} \tag{288}$$

Considering the third of (283) into (288), and reordering,

$$\begin{aligned} \dot{V}_z &= s_z^T[M(q)\dddot{q} - M(q)\dddot{q}_r + M(q)\Lambda_z z_2 + \tfrac{1}{2}s_z^T\dot{M}(q)]s_z = \\ &= s_z^T[-\dot{M}(q)(s_z - \Lambda_z s + \ddot{q}_r) - \dot{C}(q,\dot{q})\dot{q} - C(q,\dot{q})(-\Lambda_z s + \ddot{q}_r) \\ &\quad -\dot{g}(q) - M(q)\dddot{q}_r + M(q)\Lambda_z z_2 + \dot{\tau}] + \tfrac{1}{2}s_z^T[\dot{M}(q) - 2C(q,\dot{q})]s_z \end{aligned} \tag{289}$$

The matrix $[\dot{M}(q) - 2C(q,\dot{q})]$ is skew-simmetric (see (264)), so that the latter addend of (289) is null.

Collecting all terms that do not contain the control signal $\dot{\tau}$, the time derivative of V_z can be finally rewritten as

$$\dot{V}_z = s_z^T[\Psi(\cdot) + \dot{\tau}] \tag{290}$$

where the term $\Psi(\cdot)$ depends on measurable quantities and on uncertain terms which can be upperbounded by known functions according to (262)-(263)

As a result, for each entry of the vector Ψ, the following inequality can be written

$$|\Psi_i(\cdot)| \leq \Psi_{M_i}(q, \dot{q}, \tau, q_r, \dot{q}_r, \ddot{q}_r, \dddot{q}_r) \tag{291}$$

where $\Psi_{M_i}(\cdot)$ is a known positive function of available quantities.

Substituting the expression (278) for the control law into (290), and taking into account (291), it can be derived that

$$\dot{V}_z \leq -\eta^2 s_z^T s_z \tag{292}$$

which implies that the surface $s_z = 0$ is globally reached in finite time.

6.3 Simulation Results

The feasibility of the proposed scheme is demonstrated considering the 2-dof rigid manipulator used by [Berghuis et al.'93], whose matrixes are given by

$$M(q) = \begin{bmatrix} 9.77 + 2.02cos(q_2) & 1.26 + 1.01cos(q_2) \\ 1.26 + 1.01cos(q_2) & 1.12 \end{bmatrix} \tag{293}$$

$$C(q,\dot{q}) = \begin{bmatrix} -1.01\dot{q}_2 sin(q_2) & 1.01(\dot{q}_1 + \dot{q}_2)sin(q_2) \\ 1.01\dot{q}_1 sin(q_2) & 0 \end{bmatrix} \tag{294}$$

$$g(q) = \begin{bmatrix} 8.1sin(q_1) + 1.13sin(q_1 + q_2) \\ 1.13sin(q_1 + q_2) \end{bmatrix} \tag{295}$$

The control scheme (266), (267), (270), (271), (276), (278), (279) has been implemented using the following parameters (the controllers for t_1 and t_2 are identical).

$$\begin{aligned} \Psi_{M_i}(\cdot) &= 100 \\ \Upsilon_{Mi}^* &= 350 \\ \eta &= 10 \end{aligned} \tag{296}$$

$$\Lambda = \Lambda_z = \begin{bmatrix} 2 & 0 \\ 0 & 2 \end{bmatrix} \tag{297}$$

In Fig. 1 the actual and reference position for the joint 1 are depicted, highlighting the good tracking performance, while in Fig. 2 the continuous control torques t_1 and t_2 are displayed.

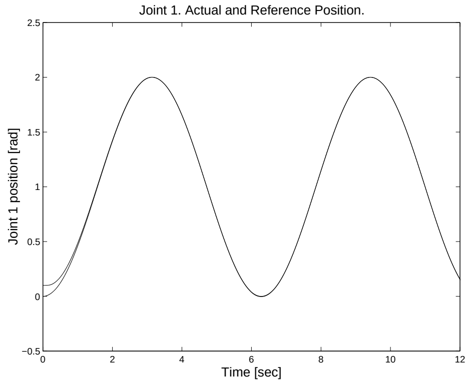

Figure 35: Joint 1. Actual and reference position.

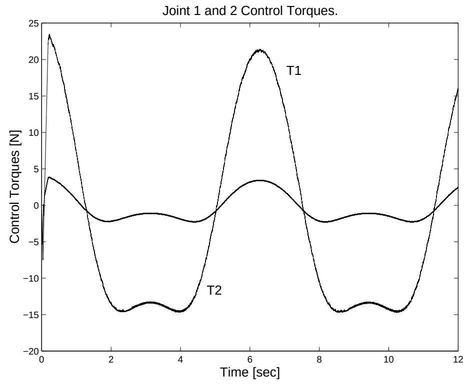

Figure 36: the control torques

References

[Bartolini et al.'98a] G. Bartolini, A. Ferrara, E. Usai "Chattering Avoidance by Second Order Sliding Mode Control", *IEEE Trans. on Automatic Control*, vol. 43, no. 2, pp. 241–246, 1998.

[Bartolini et al.'98b] G. Bartolini, A. Ferrara, A. Pisano, E. Usai "Adaptive reduction of the control effort in chattering-free sliding mode control of uncertain nonlinear systems Sliding Mode Control", *J. Appl. Math and Computer Sci.*, vol. 8, no. 1, pp. 51–71, 1998.

[Bartolini et al.'99] G. Bartolini, A. Ferrara, A. Levant, E. Usai "On Second Order Sliding Mode Controllers", in "Variable Structure Systems, Sliding Mode and Nonlinear Control", K.D. Young and U. Ozguner eds., Lecture Notes in Control and Information Sciences, Springer-Verlag, vol. 247, pp. 329-350 , 1999.

[Berghuis et al.'93] H. Berghuis and H. Nijmeijer "A passivity approach to controller-observer design for robots", *IEEE Trans. Rob. Aut.*, vol. 9, pp. 740–753, 1993.

[Young et al.(eds.)'98] K.D. Young and U. Ozguner (eds.) "Variable Structure Systems, Sliding Mode and Nonlinear Control", Lecture Notes in Control and Information Sciences, Springer-Verlag, 1999.

[Isidori '92] A. Isidori *Non Linear Control Systems*, Springer Verlag, Berlin, 1989.

[Levant '93] A. Levant "Sliding order and sliding accuracy in sliding mode control", *International Journal of Control*, vol. 58, pp. 1247–1263, 1993.

[Slotine and Li '91] J.J.E.Slotine, W. Li *Applied Nonlinear Control*, Prentice–Hall International, Englewood Cliffs, New Jersey, 1991.

[Slotine *et al.* '85] J.J.E.Slotine "The robust Control of Robotic Manipulators", *Int. J. Rob. Res.*, vol. 4, N. 2, 1985.

[Spong and Vidyasagar'89] M.W. Spong and M. Vidyasagar *Robot Dynamics and Control*, Wiley, New York.

[Tang '98] Yu Tang "Terminal Sliding Mode Control for Rigid Robots", *Automatica*, vol. 34, 1, 51-56, 1998.

[Utkin '92] V.I. Utkin *Sliding Modes in Control and Optimization*, Springer Verlag, Berlin, 1992.

[Zasadnisky *et al.* '98] M. Zasadnisky, E. Richard, F. Khelfi and M. Darouach "Disturbance Attenuation and Trajectory Tracking via a Reduced-order Output Feedback Controller for Robot Manipulators", *Automatica*, vol. 34, 12, pp.1539–1546, 1998.

7 Control of IM Motor drives

The induction motor (IM) is widely used in the industry, due to its reliability, maintenance-free operation and relatively low cost. However, precise and fast control of the flux and of the speed (or torque) is not simple to obtain, due to the complex multivariable nonlinear dynamics, to the unavailability of the rotor electrical quantities and to the parameter variations that occur during working conditions. Moreover, state and control constraints are to be taken into account for technical and/or economical reasons relevant to the sizing of the control hardware.

Over the years, field-oriented control has been recognized as the algorithm that gives the best dynamic performance to the IM drive . It is based on the de-coupling between the flux and torque control, which may be obtained in a suitable rotating reference frame (d-q transformation) [Bose '86, Vas '92], but it assumes the perfect knowledge of both rotor flux and motor parameters. As far as the rotor resistance is concerned, it is known that it may vary up to the 150% of its nominal value, due to rotor heating. This causes a de-tuning of the torque and flux controllers, which can decrease the drive performance [Bose '86, Vas '92].

A number of approaches which exploit passivity properties to ensure ultimate boundedness and asymptotic convergence [Espinoza-Perez and Ortega '95] or resort to adaptive techniques to on-line estimate the unknown rotor resistance [Marino et al. '99] have been presented in the literature to cope with such phenomena.

Variable structure systems exploit the most obvious and heuristic way to withstand the uncertainty. In such systems the control immediately reacts to any deviation of the system from the desired behavior, represented by a motion constrained on a proper manifold in the state space, steering it back onto the manifold by means of a sufficiently energetic control effort. This idea traduces in high-frequency switching control, which is a drawback in mechanical systems, due to the chattering phenomenon [Utkin '93, Utkin et al. '99], but it does not cause any difficulty when electric drives are controlled, since the on-off operation mode is the only admissible one for power converters. Therefore, it seems reasonable to use variable structure control algorithms that produces PWM-type control signals directly.

In this framework, variable structure systems can exploit their powerful features in terms of high efficiency, simplicity and robustness, and the sliding mode control methodology has been widely used for control and/or observation purposes [Utkin '93, Utkin et al. '99] [Sabanovic and Izosimov '81] [Benchaib et al. '99, Sangwongwanish et al. '90].

In this paper we propose a combined first-second order sliding mode control scheme that, by using the measured speed and currents only, guarantees that all the systems trajectories remain close to the desired profile, assuming weak informations about the motor parameters and thus resulting robust to their variations. In particular, some implementation issues are discussed, and, finally, the behaviour of the control scheme in presence of rotor resistance variation has been investigated by simulations, showing the good properties of robustness and efficiency of the proposed controller.

The proposed approach results to be conceptually similar to that used for the control of manipulators; it is reported mainly to made self-contained the argument of this chapter, while the main aim of the following treatment is to put into evidence the *implementation issues* relevant to the use of 2-sliding control for the control of IM drives.

7.1 Problem formulation

Assuming linear magnetic behaviour, the idealized two-axis IM vector equation in the stator reference frame [Vas '92] can be expressed as

$$\left\{\begin{array}{lcl} \frac{d\theta}{dt} & = & \omega \\ \frac{d\omega}{dt} & = & \frac{1}{J}(T_e - T_L) \\ \frac{d\mathbf{\Phi}_r}{dt} & = & \mathbf{M}(\omega)\mathbf{\Phi}_r + \alpha_r L_m \mathbf{i}_s \\ \frac{d\mathbf{i}_s}{dt} & = & -A[L_m^2\alpha_r + L_r r_s]\mathbf{i}_s - AL_m\mathbf{M}(\omega)\mathbf{\Phi}_r \\ & & +AL_r\mathbf{R}\mathbf{v}_s \end{array}\right. \tag{298}$$

where $\mathbf{i}_s = [i_{sa}, i_{sb}]^T$, $\mathbf{\Phi}_r = [\phi_{ra}, \phi_{rb}]^T$ are the stator current and rotor flux space vector respectively, $\mathbf{v}_s = [v_{s1}, v_{s2}, v_{s3}]^T$ is the three-phase stator voltage vector, θ and ω are the rotor position and speed. T_L is the unknown load torque, while the electromagnetic torque T_e is given by

$$T_e = \frac{3}{2}\frac{L_m}{L_r}p(i_{sb}\phi_{ra} - i_{sa}\phi_{rb}) \tag{299}$$

J is the rotor inertia, r_r and r_s are the rotor and stator resistances, $\alpha_r = r_r/L_r$ is the inverse rotor time constant, L_m, L_r, L_s are the linkage, rotor and stator inductances respectively, p is the pole pair number, $A = 1/(L_sL_r - L_m^2)$ and

$$\mathbf{M}(\omega) = \left[\begin{array}{cc} -\alpha_r & -p\omega \\ p\omega & -\alpha_r \end{array}\right] \qquad \mathbf{R} = \left[\begin{array}{ccc} \frac{2}{3} & -\frac{1}{3} & -\frac{1}{3} \\ 0 & \frac{1}{\sqrt{3}} & -\frac{1}{\sqrt{3}} \end{array}\right] \tag{300}$$

The main control objectives are:

1. To make one of the mechanical coordinates (position or speed) equal to a smooth reference input;
2. To keep the rotor flux vector modulus within the region of linear magnetic behaviour and good torque response.

These objectives are attained by constraining the system motion onto the intersection of suitable manifolds in the state space.

The three independent control variables v_{s1}, v_{s2}, v_{s3} allow to reach a three-dimensional manifold, and the additional degree of freedom can be used to satisfy some optimization criteria, such as the minimization of the inverter switching frequency, the reduction of losses and so on. The criterion we use is the requirement that the supply voltages form a three-phase balanced system [Utkin '93, Utkin et al. '99, Sabanovic and Izosimov '81].

7.1.1 Sliding Manifold Design

Let θ^* and ω^* be the position and speed reference signals to track, respectively. Choose the corresponding manifold as

$$s_1 = (\omega - \omega^*) + c(\theta - \theta^*) \qquad c \geq 0 \tag{301}$$

where $c = 0$ for the speed control and $c > 0$, $\omega^* = \dot{\theta}^*$, for the position control.

For the flux control, the sliding variable is chosen as the difference between the flux modulus and the nominal reference value, while a mean integral deviation criterion is used to control the voltage balancement.

$$s_2 = \mathbf{\Phi}_{rM} - \mathbf{\Phi}^*_{rM} \tag{302}$$

$$s_3 = \int_0^t \int_0^t (v_{s1} + v_{s2} + v_{s3}) \tag{303}$$

where $\mathbf{\Phi}_{rM} = \sqrt{\phi^2_{ra} + \phi^2_{rb}}$ is the rotor flux modulus.

Define the sliding vector $\mathbf{s}$ as

$$\mathbf{s} = \begin{bmatrix} s_1 \\ s_2 \\ s_3 \end{bmatrix} \tag{304}$$

The attainment of the sliding behaviour on the manifold $\mathbf{s} = 0$ guarantees the satisfaction of the control objectives.

7.1.2 Controller Design

The relative degree between the sliding vector and the stator voltage vector is two, and the relevant second order dynamics can be expressed as

$$\begin{cases} \mathbf{y}_1 = \mathbf{s} \\ \dot{\mathbf{y}}_1 = \mathbf{y}_2 \\ \dot{\mathbf{y}}_2 = \mathbf{F}_{\mathbf{y}}(\cdot) + \mathbf{D}(\mathbf{\Phi}_r)\mathbf{v}_{\mathbf{s}} \end{cases} \tag{305}$$

where

$$\mathbf{F}_{\mathbf{y}} = \begin{bmatrix} f_{1y}(\cdot) \\ f_{2y}(\cdot) \\ 0 \end{bmatrix} \qquad \mathbf{D} = \begin{bmatrix} & \mathbf{D}_1 & \\ 1 & 1 & 1 \end{bmatrix} \tag{306}$$

$$\begin{aligned} f_{1y}(\cdot) &= -\frac{A}{J}(r_r L_s + r_s L_r)T_e - \frac{3A}{2J}L_m p^2 \omega(\Phi_{ra}\Phi_{sa} + \Phi_{rb}\Phi_{sb}) \\ &\quad + \frac{1}{J}(c - \frac{b}{J})(T_e - T_r - b\omega)\frac{1}{J}\dot{T}_r - (\ddot{\omega}^* + c\dot{\omega}^*) \\ f_{2y}(\cdot) &= -\alpha_r(1 + AL_m^2)\dot{\mathbf{\Phi}}_{rM} + \frac{1}{\mathbf{\Phi}_{rM}}\left[p\omega(\dot{\Phi}_{ra}\Phi_{rb} - \dot{\Phi}_{rb}\Phi_{ra}) \right. \\ &\quad \left. -r_r r_s L_m A(\Phi_{ra} i_{sa} + \Phi_{rb} i_{sb})\right] - \ddot{\mathbf{\Phi}}^*_{rM} + \frac{1}{\mathbf{\Phi}_{rM}}(\dot{\Phi}^2_{ra} + \dot{\Phi}^2_{rb} - \dot{\mathbf{\Phi}}^2_{rM}) \end{aligned} \tag{307}$$

$$\mathbf{D}_1 = \begin{bmatrix} -k_1\Phi_{rb} & d_{12} & d_{13} \\ k_2\Phi_{ra} & d_{22} & d_{23} \end{bmatrix} \tag{308}$$

$$\begin{aligned} d_{12} &= k_1(\tfrac{1}{2}\Phi_{rb} + \tfrac{\sqrt{3}}{2}\Phi_{ra}) \\ d_{13} &= k_1(\tfrac{1}{2}\Phi_{rb} - \tfrac{\sqrt{3}}{2}\Phi_{ra}) \\ d_{22} &= k_2(-\tfrac{1}{2}\Phi_{ra} + \tfrac{\sqrt{3}}{2}\Phi_{rb}) \\ d_{23} &= k_2(-\tfrac{1}{2}\Phi_{ra} - \tfrac{\sqrt{3}}{2}\Phi_{rb}) \end{aligned} \tag{309}$$

$$k_1 = \frac{A}{J} L_m p \qquad\qquad k_2 = \frac{2}{3} \frac{r_r}{\|\mathbf{\Phi}_r\|} L_m A \tag{310}$$

The expression for the stator flux $\mathbf{\Phi}_s = \Phi_{sa} + j\Phi_{sb}$ is directly derived by combining the well known formulas

$$\begin{aligned} \mathbf{\Phi}_r &= L_r \mathbf{i_r} + L_m \mathbf{i_s} \\ \mathbf{\Phi}_s &= L_r \mathbf{i_s} + L_m \mathbf{i_r} \end{aligned} \tag{311}$$

Make the following assumptions:

H1. The electromechanical parameters of the motor belong to a known compact set.

H2. The state variables of the motor evolve within a compact subset in the state space.

If the motor parameters belong to some proper compact set, and the reference speed profile is sufficiently smooth, then the entries of the vector $\mathbf{F_y}$ are bounded during normal operating conditions, in which all the state variables are bounded. These assumptions are commonly verified in practice. Moreover, matrix $\mathbf{D}$ can be proved to be nonsingular [Utkin '92, Utkin '93, Utkin et al. '99].

The proposed strategy can be summarized as follows:

1. Consider an auxiliary dynamic system constituted by a double vector integrator with output $\mathbf{z}_1$ and input $\mathbf{w}$ to be defined

$$\begin{cases} \dot{\mathbf{z}}_1 = \mathbf{z}_2 \\ \dot{\mathbf{z}}_2 = \mathbf{w} \end{cases} \tag{312}$$

2. Put

$$\varepsilon_1 = \mathbf{s} - \mathbf{z}_1 \tag{313}$$

and consider the associated second order dynamics

$$\begin{cases} \dot{\varepsilon}_1 = \varepsilon_2 \\ \dot{\varepsilon}_2 = \ddot{\mathbf{s}} - \mathbf{w} \end{cases} \tag{314}$$

which consists of 3 non-interacting single-input systems controlled by means of the $i - th$ entry of the vector $\mathbf{w}$.

3. Steer ε_1 and the unmeasurable ε_2 to zero by means of a suitable discontinuous control $\mathbf{w}$. This task can be accomplished by using the sub-optimal second order sliding mode control algorithm.

Once step 3 is performed, system (314) is said to evolve in accordance with a "second order sliding mode" (2-SM) behaviour. The main theoretical properties of this special class of sliding modes have been thoroughly investigated in [Levant '93, Bartolini et al. '99], while in [Bartolini et al. '98b] it has been evidenced that the equivalent control for a 2-SM on the manifold $\sigma = \dot{\sigma} = 0$ (namely, the "second order sliding set") can be defined as the continuous control that solves the equation

$$\ddot{\sigma} = 0 \tag{315}$$

As for the behaviour of the dynamical system (312), after the 2-SM on $\varepsilon_1 = \varepsilon_2 = 0$ has been established, it can be analyzed by replacing the discontinuous control $\mathbf{w}$ with the corresponding equivalent control, which, according to the above definition, by (305) and (315), is given by

$$\mathbf{w}_{eq} = \mathbf{F_y}(\cdot) + \mathbf{D}(\mathbf{\Phi}_r)\mathbf{v_s} \tag{316}$$

The Filippov equivalent solution of the auxiliary system (312) can be therefore represented as

$$\begin{cases} \dot{\mathbf{z}}_1 = \mathbf{z}_2 \\ \dot{\mathbf{z}}_2 = \mathbf{w}_{eq} = \mathbf{F}_{\mathbf{y}}(\cdot) + \mathbf{D}(\boldsymbol{\Phi}_r)\mathbf{v}_{\mathbf{s}} \end{cases} \tag{317}$$

The equivalent system (317), with measurable state variables $\mathbf{z}_1$ and $\mathbf{z}_2$, can be stabilized by first order sliding mode control technique. Therefore, the fourth step of the proposed procedure is

4. Define the sliding quantity

$$\mathbf{s}_z = \mathbf{z}_2 + \Lambda_z \mathbf{z}_1 \tag{318}$$

where Λ_z is a positive definite diagonal matrix and steer the system (317) onto the manifold $\mathbf{s}_z = 0$ by discontinuous control $\mathbf{v}_{\mathbf{s}}$.

It is noteworthy that the simultaneous satisfaction of conditions

$$\begin{array}{l} \varepsilon_1 = \varepsilon_2 = 0 \\ s_z = 0 \end{array} \tag{319}$$

ensures the exponential convergence of vector $\mathbf{s}$ to zero

7.1.3 The Flux Observer

The reduced-oder observer proposed in [Damiano et al. '99], which is derived from a specific Luenberger-type one [Verghese and Sanders '88] by suitably modifying the prediction error term in order to obtain a semi-infinite stability range for the gain matrix entries, has been used for the implementation of the control law.

The observer dynamics is given by

$$\begin{array}{l} \dot{\mathbf{h}} = \left[\mathbf{I} + \frac{L_m}{L_r}\mathbf{K}\right]\left[-\alpha_r \mathbf{I} + \omega \mathbf{J}\right]\hat{\boldsymbol{\Phi}}_r \\ \quad +\alpha_r L_m \mathbf{i}_{\mathbf{s}} + \mathbf{K}\left[(r_s + \alpha_r \frac{L_m^2}{L_r}\mathbf{i}_{\mathbf{s}} - \mathbf{v}_{\mathbf{s}})\right] \\ \hat{\boldsymbol{\Phi}}_r = \mathbf{h} + \mathbf{K}\sigma L_s \mathbf{i}_{\mathbf{s}} \end{array} \tag{320}$$

where $\mathbf{I}$ and $\mathbf{J}$ are the 2-by-2 identity and unit rotation matrixes respectively, i.e.

$$\mathbf{I} = \begin{bmatrix} 1 & 0 \\ 0 & 1 \end{bmatrix} \qquad \mathbf{J} = \begin{bmatrix} 0 & -1 \\ 1 & 0 \end{bmatrix} \tag{321}$$

$\sigma = 1 - L_m^2 / L_s L_r$ is the leakage coefficient and the matrix $\mathbf{K}$ is the gain matrix to be defined in order to ensure stability and fast decay of the tracking error. Taking the $\mathbf{K}$ matrix as $\mathbf{K} = k\mathbf{I}$, it can be proved, by using as a Lyapunov candidate function the square norm of the tracking error, that the stability range for the k parameter is the semi-infinite set $\left(-\frac{L_r}{L_m}, \infty\right)$, and that the error rate decay arbitrarily increases as k tends to infinity. In [Damiano et al. '99] the robustness analysis of the proposed observer against the rotor resistance variation has been briefly performed, showing the ultimate boundedness of the error in case of a bounded variation of resistance, and its inverse proportionality with respect to the gain k.

7.2 The control Algorithm

The overall proposed controller is summarized in the following

Proposition 1:

Consider system (298),(300)*, satisfying assumptions H1-H2, and let the quantities* $\mathbf{s}$ *and* $\mathbf{s}_z$ *be defined according to* (301)-(304),(312),(318)*.*

The control strategy

$$\begin{aligned} v_{si} &= -V_M sign(s^*_{zi}) & (322)\\ w_i &= W_{M_i} sign(\varepsilon_{1i} - \frac{1}{2}\varepsilon_{1i_M}) & (323) \end{aligned}$$

where $i = 1, 2, 3$*,* $s^*_z = \mathbf{D}^T \mathbf{s}_z$*,* ε_1 *and* ε_{1i_M} *are defined according to* (313) *and* (327)*, the bus voltage* V_M *and the constants* W_{M_i}*, (i=1,2,3), are defined according to (333) and (326) respectively, ensures the local asymptotic convergence to zero of the components of the vector* $\mathbf{s}$*.*

Proof.

Part I: Stabilization of system (314)

The drift term $\ddot{\mathbf{s}}$ of system (314) takes the form

$$\ddot{s} = \mathbf{F_y}(\cdot) + \mathbf{D}(\mathbf{\Phi}_r)\mathbf{v_s} \tag{324}$$

Under assumptions H1-H2, the entries $\ddot{s}_i$, $i = 1, 2, 3$, of the vector $\ddot{s}$ can be upper bounded by known constants, in accordance with

$$|\ddot{s}_i| \leq \Upsilon_{Mi} \tag{325}$$

The three non-interacting subsystems in which can be decomposed system (314), each one with drift term $\ddot{s}_i$ and control w_i, fall in the class of plants that can be stabilized in finite time by using the sub-optimal 2-SMC algorithm [Bartolini et al. '98a, Bartolini et al. '99], and the finite-time stabilization of all entries of vectors $\mathbf{s}$ and $\dot{\mathbf{s}}$ can be attained by suitable discontinuous control $\mathbf{w}$, provided that the control amplitudes are chosen according to

$$W_{M_i} > 2\Upsilon_{Mi} \tag{326}$$

A precise evaluation of the constants Υ_{Mi} can be found exploting assumptions H1 and H2. It must be underlined that the exact knowledge of such bounds is not useful, as it is, in general, highly conservative. Simulation show that effectiveness of the control scheme is obtained even by using control values much smaller than the sufficient theoretical ones.

The switching logic of the sub-optimal algorithm is clarified for the reader's convenience. The term ε_{1Mi} ($i = 1, 2, 3$) in (323) represents the last singular value of ε_{i1}, according to

$$\begin{gathered} \varepsilon_{Mi}(t) = \begin{cases} \varepsilon_i(0) & 0 \leq t < t_{M_1} \\ \varepsilon_i(t_{M_k}) & t_{M_k} \leq t < t_{M_{k+1}} \end{cases} \\ t_{M_k} \;\; s.t. \;\; \dot{\varepsilon}_i(t_{M_k}) = 0 \qquad k = 1, 2, \ldots \end{gathered} \tag{327}$$

An algorithm for the approximate detection of the singular points has been presented in [Bartolini et al. '98a].

Part II: Stabilization of the equivalent system (317)

To prove that the control $\mathbf{v_s}$ forces s_z to converge to zero in finite time, following the same guidelines in [Utkin '93, Utkin et al. '99], consider the following Lyapunov function candidate

$$V_z = \frac{1}{2} s_z^T s_z \tag{328}$$

Taking into account that $\varepsilon_1 = \varepsilon_2 = 0$, its time derivative can be expressed as

$$\dot{V}_z = s_z^T (\mathbf{F_y}(\cdot) + \mathbf{D}(\mathbf{\Phi}_r)\mathbf{v_s} + \Lambda \mathbf{z}_2) \tag{329}$$

Substituting control (322) into (329) yields

$$\dot{V}_z = s_z^{*T} \mathbf{F_y}^* - V_M |s_z^*| \tag{330}$$

where

$$\mathbf{F_y}^* = (D^{-1}\mathbf{F_y})^T \tag{331}$$

As a consequence of assumptions H1 and H2, relying on the fact that the matrix $\mathbf{D}$ is nonsingular, the entries of the vector $\mathbf{F_y}^*$ can be upper bounded by proper constants according to

$$|F_{y_i}^*| \leq F_{yi}^* \qquad i = 1, 2, 3 \tag{332}$$

The condition

$$V_M \quad > \max_i F_{yi}^* \tag{333}$$

provide negativeness of $\dot{V}_z$, hence the origin of the s_z^* space is asymptotically stable. By virtue of $\det(\mathbf{D}) \neq \mathbf{0}$, the sliding mode arises on the manifold $s = 0$ as well.

7.3 Implementation Issues

The proposed control law is discontinuos, hence it is well suited to be implemented by means of power converters. No PWM seems to be necessary, as the control signal is already a pulse-width-modulated signal. The bus voltage V_M has to satisfy the inequality (333), and the state of the switches of the inverter legs can be directly set by the VSC according to the switching logic in (322). The problem of maintaining sufficiently high the switching frequency of the control is crucial in this context. Due to the inertias of the measurement devices and/or to the mechanical nature of some sliding quantities, the switching frequency of the control may be significantly smaller than typical PWM frequencies. This problem can be counteracted by using state observers, which "inject" high frequencies in the feedback loop by means of the measured electrical quantities used for the observer implementation [Utkin '92, Utkin '93, Utkin et al. '99]. In the proposed technique the high frequency dynamics of $\mathbf{z}$ (due to the discontinuos signal $\mathbf{w}$) gives to the sliding vector s_z the harmonic content (something similar to the persistent excitance condition in adaptive control) sufficient to establish a sliding regime characterized by a sufficiently high switching frequency of the PWM input voltage. Moreover, computer simulations show that, during the reaching phase and at every time instant at which the sliding mode is not established, an unacceptable current peaking occurs, as a direct consequence of the fact the no control switchings occur, and the motor is supplied with the bus voltage for a long period of about some ms. To solve this problem, in the practical implementation of the control law, **an accurate planning of the reference trajectories is mandatory**, in order to establish the sliding mode from the initial time instant on. As a result, the supply voltage immediately commutes at very high frequency, and the transient peaking of the stator currents is avoided.

7.4 Simulation Results

The proposed control algorithm has been simulated considering a commercial induction motor drive. All parameters and ratings are given in Table I. The bus voltage is set to $500V$. A speed regulation test has been first performed, in which the reference speed is first the nominal speed of the motor and then it is is reduced of the 50% . The flux exhibits a small oscillation around the nominal value during the transient phases but it promptly comes to the desired value. In Fig. 37 are reported the actual and desired speed profile, while in Fig. 38 is depicted the flux modulus, which is wanted to be kept at the nominal value $\mathbf{\Phi}^*_{rM} = 0.7$ Wb. The same test has been repeated by varying the actual motor resistance to test the robustness of the observer-controller structure. The actual resistance has been smoothly increased from the nominal value in Table I up to the 150% (see fig. 39). The control system is quite insensitive to the resistance variation, as it is evidenced in Figg. 40 and 41.

Secondly, the response of the system to a sinusoidal reference speed has been investigated. Unlike the previous test, a perfect speed tracking is achieved, due to the smooth profile of the reference speed (see Fig. 42). After the first reaching transient, the sliding mode is never lost, and the slight transient oscillation of the flux modulus, highlighted in Fig. 38 for the regulation test, disappears, as it can be seen in Fig. 43.

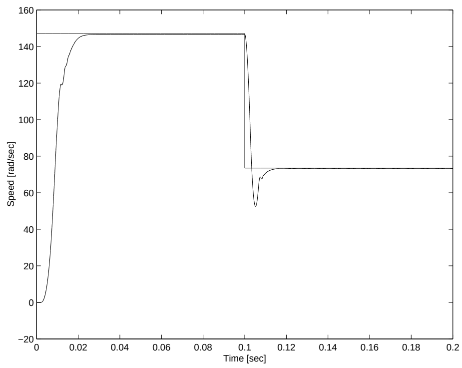

Figure 37: Speed regulation. Actual and reference speed.

Now we want put into evidence the basic issues relevant to the planning of the reference trajectories for the sake of reducing the current peaking. Making refrence to the problem of regulating the speed along some constant value, instead of step references for speed and flux we use we use smooth interpolations between the zero speed and the final desired value. In Fig. 44 can be noted the perfect matching between the reference and actual speed if a smooth profile is used, and also the capability of directly controlling the amplitude and the slew rate of the stator current during the transient must be pointed out.

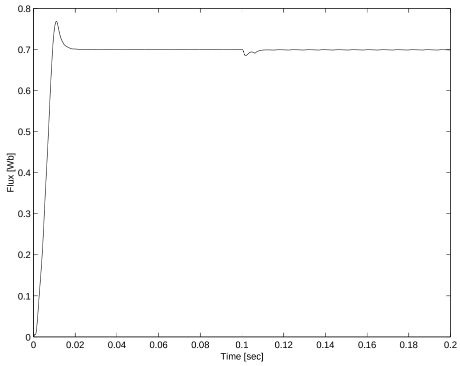

Figure 38: Speed regulation. The actual flux modulus.

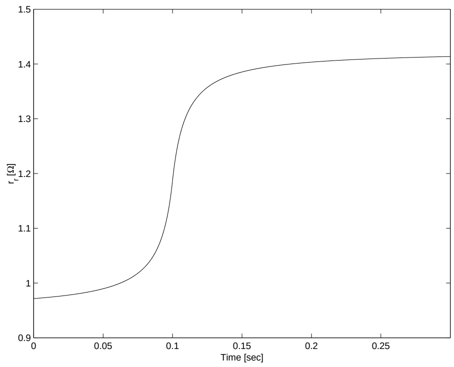

Figure 39: Speed regulation with rotor resistance variation. The rotor resistance.

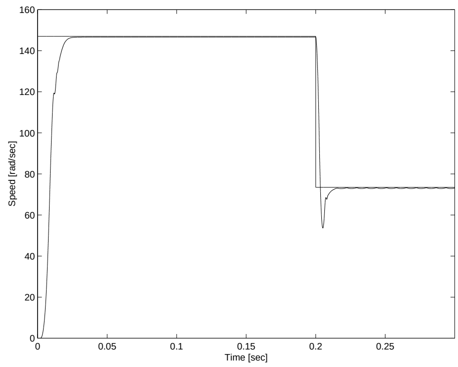

Figure 40: Speed regulation with rotor resistance variation. Actual and reference speed.

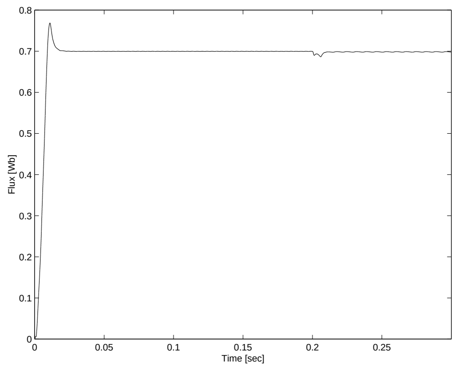

Figure 41: Speed regulation with rotor resistance variation. The actual flux modulus

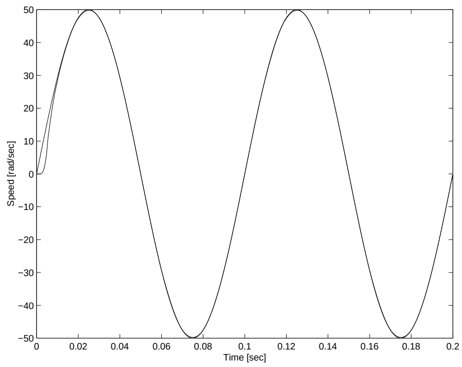

Figure 42: Speed Tracking. Actual and reference speed.

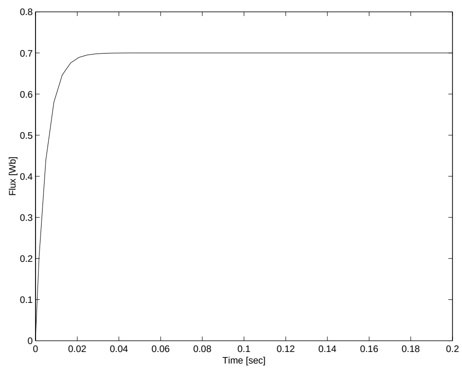

Figure 43: Speed Tracking. The actual flux modulus.

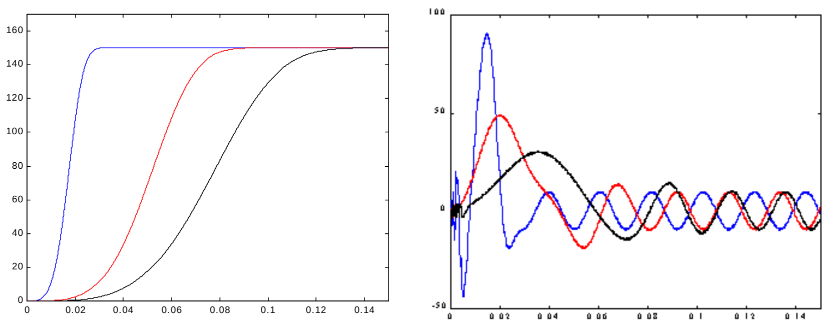

Figure 44: The effect of the reference speed slope on the current transient peaking

Rating power	$2.2kW$
Rating torque	$15Nm$
Rating speed	$1410rpm$
Pole pair	2
Inertia constant	$0.009kgm^2$
Damping coefficient	$0.005Ns$
Stator resistance	0.8533Ω
Stator leakage inductance	$0.005H$
Mutual inductance	$0.085H$
Rotor resistance	0.95Ω
Rotor leakage inductance	$0.005H$

Table I: IM Parameters and Ratings

7.5 Summary

A new approach for the variable structure control of IM drives, which combines first and second order sliding mode control strategies, is proposed in this paper. Robustness against parameter uncertainty and/or their variation is obtained, as evidenced by simulations. No acceleration observer must be implemented, therefore reducing the sensitivity to the load disturbance as well. Further investigations will be devoted to test the performances of its digital realization and to reduce the peaking of the currents, making it ready for experimental verifications of the good simulation results.

References

[Bartolini et al. '98a] G. Bartolini, A. Ferrara, E. Usai "Chattering Avoidance by Second Order Sliding Mode Control", *IEEE Trans. on Automatic Control*, vol. 43, no. 2, pp. 241–246, 1998.

[Bartolini et al. '99] G. Bartolini, A. Ferrara, A. Levant, E. Usai "On Second Order Sliding Mode Controllers", in "Variable Structure Systems, Sliding Mode and Nonlinear Control", K.D. Young and U. Ozguner eds., Lecture Notes in Control and Information Sciences, Springer-Verlag, vol. 247, pp. 329-350 , 1999.

[Bartolini et al. '98b] G. Bartolini, A. Ferrara, A. Pisano, E. Usai "Adaptive reduction of the control effort in chattering-free sliding mode control of uncertain nonlinear systems Sliding Mode Control", *J. Appl. Math and Computer Sci.*, vol. 8, no. 1, pp. 51–71, 1998.

[Benchaib et al. '99] A. Benchaib *et al.* "Real-Time Sliding-Mode Observer and Control of an Induction Motor", *IEEE Trans. on Ind. Electronics*, **46**, 128–137 (1999).

[Bose '86] B.K. Bose *Power Electronics and AC Drives*, Englewood Cliffs, NJ, Prentice Hall, (1986).

[Damiano et al. '99] A. Damiano, G. Gatto, I. Marongiu A. Pisano "Synthesis and Digital Implementation of a Reduced Order Rotor Flux Observer for IM drive", Proc. of the IEEE Int. Symp. on Industrial Eletronics ISIE 99, Bled, Slovenia, pp. 729–734 June 1999.

[Levant '93] A. Levant "Sliding order and sliding accuracy in sliding mode control", *International Journal of Control*, vol. 58, pp. 1247–1263, 1993.

[Marino et al. '99] R. Marino, S. Peresada, P. Tomei, "Global Adaptive Output Feedback Control of Induction Motors with Uncertain Rotor Resistance", *IEEE Trans. on Aut. Control*, **44**, 967–983 (1999).

[Espinoza-Perez and Ortega '95] G. Espinoza-Perez, R. Ortega, "An Output Feedback Globally Stable Controller for Induction Motors", *IEEE Trans. on Aut. Control*, **40**, 138–143 (1995).

[Sabanovic and Izosimov '81] A. Sabanovic, D. Izosimov, "Applications of Sliding Modes to Induction Motor Control", *IEEE Trans. on Industry Applications*, **17**, 41–49 (1981).

[Sangwongwanish et al. '90] S. Sangwongwanish et al., "Desing of Sliding Observers for Robust Estimation of Rotor Flux of Induction Motors " Proc. of the Int. Power Electr. Conf. IPEC 90, Tokyo, Japan, pp. 1235–1242, 1990.

[Utkin '92] V.I. Utkin *Sliding Modes In Control And Optimization*, Springer Verlag, Berlin, (1992).

[Utkin '93] V.I. Utkin "Sliding Modes Control Design Principles and Applications to Electric Drives", *IEEE Trans. on Ind. Electronics*, **40**, 23–35 (1993).

[Utkin et al. '99] V.I. Utkin et al. *Sliding Modes Control in Electromechanical Systems*, Taylor and Francis, London, 1999.

[Vas '92] P. Vas, *Vector Control of AC Machines*, Oxford Science Publications, (1992).

[Verghese and Sanders '88] G. Verghese, P. Sanders, "Observers for Flux Estimation in Induction Machines", *IEEE Trans. on Ind. Electronics*, **35**, 85–94 (1988).

8 Control of Container Cranes

8.1 Introduction

An interesting and challenging applicative test for advanced control techniques is constituted by the control of cranes. In many industrial as well as civil engineering environments, safety constraints and economical reasons require that the transfer of heavy loads over long distances is executed minimizing the load oscillation and the operation time.

Inspired from the behaviour of expert crane drivers, the control strategy has been often designed in two-stages: off-line path planning, in accordance with some optimization criteria, and on-line path tracking. In particular, optimal control techniques have been widely used to address the problem of the path planning [Auernig and Troger '87, 6, 10, 15]. The reference trajectories were chosen to minimize some specific indexes, linked to the swing angle and its derivative [15], or to the energy consumption, which is claimed to be meaningful with respect to system stresses such as oscillations and non-smooth motions [10]. Nevertheless, the high sensitivity of the resulting open-loop strategies to parameter mismatching and external disturbances has been pointed out in the literature [21].

A linear, parameter-varying, crane model can be obtained by means of a suitable time-scaling [18, 20], that allows for the use of adaptive pole-placement control techniques [19], gain-scheduling [7] or Lyapunov-equivalence-based observer/controller design [8].

The usual goal is to achieve zero swing only at the end of the transport. However, swing during transport may bee too large. In [14] this fundamental consideration was pointed out, and an effective approach to obtain the swing suppression also during load motion was presented, which requires the perfect knowledge of the system's parameters.

We address and solve the same problem assuming that the actual system parameters are uncertain but belonging to a known compact domain, and also that the control torque are generated by means of unmodeled actuators (DC drives with unknown parameters).

Due to model uncertainties, the use of robust control techniques is motivated. Variable structure systems are well known to be robust and easy to implement [17]. A suitable manifold in the state space is defined such that the system exhibits the desired behavior when constrained to evolve on such a manifold. A control action is defined by a worst-case analysis to drive the system onto the manifold despite of model uncertainties. As a result, the plant behavior becomes insensitive to (and independent from) any uncertainties or disturbances that do not steer the plant outside from the manifold

The actual case does not belong to the standard classes of problems dealt with by the sliding mode control methodology; indeed, the overall system is under-actuated, since there are three degrees of freedom (dof) to be controlled (the load coordinates and the swing angle) and only two control actions (the motor voltages). Each dof is represented by a proper system output, and the control objective is to make these outputs to exhibit the desired behaviour.

When the number of controlled dof is the same as the independent controls, a sliding manifold could be chosen so that, in the constrained motion, the dynamics of the relevant system outputs are decoupled. If we try to apply this logic to the problem under investigation, at least one dof dynamics would result in being uncontrollable.

In this paper we succeed in proving that:

1. it is possible to identify a suitable couple of sliding outputs, that involve the three controlled dof's, such that the associated zero-dynamics is asymptotically stable and satisfies the control objective.

2. it is possible to define a robust control scheme that steers the system motion on then chosen manifold in finite time despite of uncertainties.

The paper is organized as follows. In the next section the crane model is given and the control problem is formulated. In section 3, the sliding manifold is proposed, and the behaviour of the system when constrained on such manifold is analyzed. In the subsequent section 4, recent results on multi-input second-order sliding mode control (SMC) are applied to attain, in finite-time, a sliding motion on the desired manifold. In sections 5 the implementation issues are discussed and some experimental results are presented, while in the final section 6 some final conclusions are drawn.

8.2 Problem formulation

We consider a container crane as that depicted in Figure 45 , actuated by two DC motors generating the mechanical forces acting on the trolley and on the rope.

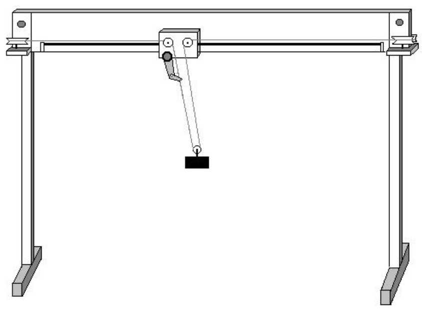

Figure 45: Overhead crane. A frontview.

By taking the trolley position x_t, the rope length l and the swing angle φ (and their time derivatives) as the state variables, assuming that the load can be regarded as a material point, and that the rope is always stretched (so that the swing angle can be uniquely defined) the equations of motion have been derived in [15] as

$$A_1\ddot{x}_t + B_1\ddot{l}\sin\varphi + B_1 l\ddot{\varphi}\cos\varphi + B_1(2\dot{l}\dot{\varphi}\cos\varphi - l\dot{\varphi}^2\sin\varphi) = t_1 \tag{334}$$

$$B_2\ddot{x}_t\sin\varphi + A_2\ddot{l} - B_2 l\dot{\varphi}^2 - B_2 g\cos\varphi = t_2 \tag{335}$$

$$\ddot{x}_t\cos\varphi + l\ddot{\varphi} + 2\dot{l}\dot{\varphi} + g\sin\varphi = 0 \tag{336}$$

where t_1 and t_2 are the applied trolley and hoisting torques, respectively, g is the gravity constant, and the positive constants A_1, A_2, B_1, B_2 are expressed as

$$\begin{aligned} A_1 &= [(J_1/b_1) + (M+m)b_1] \\ A_2 &= [(J_2/b_2) + Mb_2] \\ B_1 &= Mb_1 \\ B_2 &= Mb_2 \end{aligned} \tag{337}$$

in which M and m are the total masses of the container and of the trolley, respectively, J_1 and J_2 are the total inertia of brake, drum and reduction gears of the trolley motor (TM) and of the hoist motor (HM) drives, respectively, b_1 and b_2 represent the equivalent TM and HM drum radius, reduced to the motor side.

The actuator dynamics can be represented as

$$\Pi_1 \dot{\mathbf{t}} + \Pi_2 \mathbf{t} = \mathbf{v} - \Pi_3 \dot{\mathbf{r}} \tag{338}$$

where $\mathbf{v} = [v_1\ v_2]^T$ is the vector of the motor supply voltages, $\mathbf{t} = [t_1\ t_2]^T$, $\mathbf{r} = [x_t\ l\ ]^T$ and the diagonal matrixes Π_i, $i = 1, 2, 3$, are given by

$$\Pi_1 = \begin{bmatrix} l_1/k_{t1} & 0 \\ 0 & l_2/k_{t2} \end{bmatrix} \quad \Pi_2 = \begin{bmatrix} r_1/k_{t1} & 0 \\ 0 & r_2/k_{t2} \end{bmatrix} \quad \Pi_3 = \begin{bmatrix} k_{e1}/b_1 & 0 \\ 0 & k_{e2}/b_2 \end{bmatrix} \tag{339}$$

where r_1 (r_2) is the TM (HM) resistance, l_1 (l_2) is the TM (HM) inductance, k_{t1} (k_{t2}) is the TM (HM) torque constant and k_{e1} (k_{e2}) is the TM (HM) back-emf constant.

The control objective is to move the load along a pre-specified trajectory as faster as possible, while keeping the swing angle sufficiently small. Assume that the crane and motor parameters are uncertain but belonging to a known compact set.

The control problem is challenging for many reasons: the system is nonlinear, highly coupled, uncertain and underactuated (three output variables must be controlled by using two control actions). The goal is to move the load from the initial position (x_i, y_i) to a final, desired, location (x_f, y_f) along a pre-specified path, while keeping the load oscillation as small as possible.

As the rope is assumed always stretched, the load coordinates depend on the system's state as follows

$$\begin{aligned} x &= x_t + l sin\varphi \\ y &= l cos\varphi \end{aligned} \tag{340}$$

Often [15, 10] the overall loading and unloading motion of the suspended mass is divided in three different phases which are separately dealt with: the vertical motion (pure load hoisting and lowering), the transversal motion and the horizontal one (Fig. 2). Apart from the pure vertical motion, which does not cause load oscillations, any generic motion task can be characterized by load oscillation, which must be kept as small as possible during the load transport and suppressed at the end of the transfer.

We distinguish two phases: the "traveling phase", including the whole travel of the load toward the final location, and the "arrival phase", activated as soon as a suitable vicinity of the destination point is reached, in which the load must be stabilized on the final location.

We propose a control strategy that is able to guarantee, for each type of load movement, (transversal, horizontal and vertical) the robust tracking of the desired path and, at the same time, the active damping of the load oscillations.

Generally, in the previously quoted literature, the load is forced to track the desired path with an off-line designed velocity profile, with no feed-back on the swing angle. In the actual case, the swing suppression is obtained on-line by constraining the system's motion on a suitable manifold which involves both the desired path and the swing angle. Roughly speaking, the velocity is modified on-line, on the basis of the actual swing angle, to obtain the suppression of the oscillations not only at the end of the transport but during transfer as well.

8.3 Sliding manifold design for trajectory tracking and oscillation damping

The design of a sliding-mode control system consists of two-steps. The first step is the choice of a manifold in the state space such that, once the state trajectory is constrained on it, the system behaviour, described by its zero dynamics with respect to the corresponding sliding outputs, exhibits the desired performances. The second step consists of the design of control actions capable of forcing the system state, after a finite transient time to evolve on the chosen manifold (accordingly called sliding manifold).

In the actual case, since the control torques are not directly manipulable due to the actuator dynamics, *any* sliding output of the type

$$\mathbf{s}(\mathbf{q}) = 0 \tag{341}$$

where $\mathbf{q} = [x_t\ ,\ \dot{x}_t\ ,\ l\ ,\ \dot{l}\ ,\ \varphi\ ,\ \dot{\varphi}]^T$ is the crane state vector has *relative degree two*, since the actual control vector $\mathbf{v}$ acts on the *second* derivative of $\mathbf{s}$. On the basis of these considerations, the use of second order sliding modes appears to be sensible and motivated.

The present chapter deals with the first step of the control design procedure, i.e. the design of the sliding manifold and the stability analysis of the zero-dynamics, while the presentation of the control technique guaranteeing the attainment of the sliding motion is postponed to Section 4, in which recent results on multi-input second-order sliding mode control are recalled and applied to the actual control problem.

In the case under investigation, three dof must be controlled by using two independent control actions. Of course, independent tracking of the three associated system's outputs is impossible, but a mixed objective of tracking for two variables, and stabilization for the remaining one, can be attained in principle,

The choice of a suitable sliding manifold is the most critical point of the controller design. When constrained onto the manifold, the system dynamics (zero-dynamics, [9]) must exhibit the desired path tracking performance, while the stability of the swing dynamics must be guaranteed as well.

If the swing angle were not an issue, it would be possible to define the sliding output vector as

$$\mathbf{s}(\mathbf{q}) = \begin{bmatrix} s_1 \\ s_2 \end{bmatrix} = \begin{bmatrix} \dot{x}_t - \dot{x}_t^d + c_1(x_t - x_t^d) \\ \dot{l} - \dot{l}^{\,d} + c_2(l - l^{\,d}) \end{bmatrix} \tag{342}$$

where c_1, c_2 are positive constants and the superscript $'d'$ indicates the desired behaviour.

On the manifold $\mathbf{s} = 0$, the exponential tracking of the desired path is achieved.

As for the analysis of the system's zero dynamics, we refer to the approximate model suggested in [15], valid for small load oscillations. More precisely, we assume that the the load swing angle is so small that all terms containing $\varphi^\alpha \dot{\varphi}^\beta$ $(\alpha \geq 0, \beta \geq 0, \alpha + \beta \geq 2)$ can be neglected, and the approximations $\cos(\varphi) \approx 1$ and $\sin(\varphi) \approx \varphi$ hold.

The above approximations yield the following model

$$\ddot{x}_t = \delta_1 g \varphi + z_1 - \delta_1 \varphi z_2 \tag{343}$$

$$\ddot{l} = -\delta_2 \varphi z_1 + z_2 \tag{344}$$

$$\ddot{\varphi} \;=\; -\frac{1}{l}\left[(1+\delta_1)g\varphi + 2\dot{l}\dot{\varphi}\right] - \frac{1}{l}z_1 + \frac{\delta_1}{l}\,\varphi\, z_2 \tag{345}$$

where z_1 and z_2 are new control variables defined as

$$z_1 = \tfrac{b_1}{J_1+mb_1^2}t_1 \qquad\qquad z_2 = \tfrac{b_2(t_2+Mb_2g)}{J_2+Mb_2^2} \tag{346}$$

and δ_1, δ_2 are the positive constants

$$\delta_1 = \tfrac{Mb_1^2}{J_1+mb_1^2} \qquad\qquad \delta_2 = \tfrac{Mb_2^2}{J_2+Mb_2^2} \tag{347}$$

The zero-dynamics of the swing angle can be obtained substituting z_1 and z_2 in (345) with those keeping to zero the outputs s_1 and s_2. Intuitively, such input $\mathbf{z}_{eq} = [z_{1_{eq}}\ z_{1_{eq}}]$ (which is referred in the VSS community as "equivalent control") is the solution of the system

$$\dot{\mathbf{s}} = 0 \tag{348}$$

Differentiating (342), and considering (343)-(347) and (348), after some manipulations one obtains

$$\begin{cases} z_{1_{eq}} = -\delta_1(g-\ddot{l})\varphi + k\dot{\varphi} + \ddot{x}_t^d - c_1(\dot{x}_t - \dot{x}_t^d) \\ \\ z_{2_{eq}} = \delta_2[\ddot{x}_t^d - c_1(\dot{x}_t - \dot{x}_t^d)]\varphi \end{cases} \tag{349}$$

Accordingly, the swing angle zero-dynamics turns out to be given by

$$\ddot{\varphi} = -\frac{g}{l(t)}\varphi - \frac{2\dot{l}(t)}{l(t)}\dot{\varphi} - \frac{1}{l(t)}[\ddot{x}_t^d - c_1(\dot{x}_t - \dot{x}_t^d)] \tag{350}$$

The stability of the above time-varying dynamics is strongly affected by the operating conditions, and it is very difficult to predict the actual system's behaviour. Indeed, also the frozen models may be unstable, depending on the actual movement performed by the load. The above zero dynamics can be considered as uncontrollable, in the sense that its stability is influenced by the sign of $\dot{l}$ and no control action seems to be available to ensure it.

The main idea proposed in this paper is to add a swing-dependent term in the definition of s_1, i.e. we propose to define the following sliding outputs

$$\begin{array}{l} s_1 = \dot{x}_t - \dot{x}_t^d + c_1(x_t - x_t^d) - k\varphi \\ s_2 = \dot{l} - \dot{l}^{\,d} + c_2(l - l^{\,d}) \end{array} \tag{351}$$

where k is a positive constant.

It is not difficult to verify that the zero-dynamics turns out to be modified as follows

$$\ddot{\varphi} = -\frac{g}{l(t)}\varphi - \frac{k + 2\dot{l}(t)}{l(t)}\dot{\varphi} - \frac{1}{l(t)}[\ddot{x}_t^d - c_1(\dot{x}_t - \dot{x}_t^d)] \tag{352}$$

i.e. an artificial viscous damping proportional to $kl^{-1}(t)$ appears in the swing's zero dynamics. It is reasonable to argue that the increase of k could have a stabilizing effect on the zero dynamics, and this intuitive property is formalized in the next subsections.

8.3.1 The traveling phase

Let the desired path be expressed as

$$l^{\,d} = f(x_t) \tag{353}$$

In order to better explain our proposal, the procedure will be detailed making reference to a parabolic reference trajectory (Fig. 46), i.e.

$$l^{\,d} = l_0 + \Gamma x_t^2 \qquad |x_t| \leq X_M \tag{354}$$

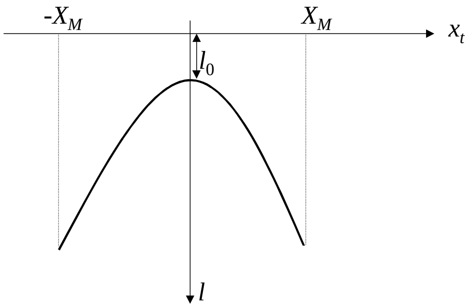

Figure 46: The parabolic reference path.

Consider the following two-dimensional sliding manifold

$$\begin{array}{l} s_1^{'} = \dot{x}_t - V_0 - k\varphi \\ s_2^{'} = \dot{l} - \dot{l}^d + c_2(l - f(x_t)) \end{array} \tag{355}$$

where V_0 is a positive constant that represents the desired horizontal speed, the desired rope velocity $\dot{l}^d$ can be obtained, by differentiating (354), as

$$\dot{l}^d = \frac{df}{dx_t}\dot{x}_t = 2\Gamma x_t \dot{x}_t \tag{356}$$

The requirements regarding the trolley position and the swing angle should be satisfied by keeping the equality $s_1^{'} = 0$. Note that $s_1^{'}$ contains both the trolley velocity and the swing angle.

The stabilizing effect of the k parameter (see (352)) can be first exploited to stabilize around the origin the nonlinear swing angle dynamics, so that the term φ in (355) vanishes, and, on $s_1^{'} = 0$, the trolley turns out to move with the desired velocity V_0.

The manifold $s_2^{'} = 0$ is designed to ensure that, for each current value of x_t, the rope length is adjusted in order to maintain the load on the desired trajectory $f(x_t)$.

In the actual case, when constrained onto the two-dimensional manifold $s_1^{'} = s_2^{'} = 0$, the original 6^{th}-order system is reduced to a 4^{th}-order plant, which must be proved to enjoy the desired properties of tracking and stability.

By considering (355) and (352), the actual system's zero-dynamics turns out to be

$$\begin{aligned} \dot{x}_t &= V_0 + k\varphi && (357) \\ \ddot{\varphi} &= -\frac{g}{l(t)}\varphi - \frac{k + 2\dot{l}(t)}{l(t)}\dot{\varphi} && (358) \\ \dot{l} &= \dot{l}^d - c_2(l - l^d) && (359) \end{aligned}$$

Note that the third equation is independent from the others, while the first two equations are coupled with the remaining ones.

In order to simplify the stability analysis, we regard the second order swing dynamics (358) as a linear, autonomous, parameter-varying, system, and our objective is to show that a suitably chosen k parameter guarantees the asymptotic stability.

Using the time-dependent Lyapunov-candidate function

$$V(\varphi, \dot{\varphi}, t) = \frac{1}{2}\frac{g}{l(t)}\varphi^2 + \frac{1}{2}\dot{\varphi}^2 \tag{360}$$

one obtains

$$\dot{V}(\cdot) = -\frac{k + 2\dot{l}(t)}{l(t)}\dot{\varphi}^2 - \frac{1}{2}\frac{g\dot{l}(t)}{l^2(t)}\varphi^2 \tag{361}$$

that, for any positive value of k, implies asymptotic stability if $\dot{l} > 0$ (i.e. when the rope is lenghtened). By virtue of the well known Barbalat's Lemma (see [16]), one can assess the swing angle asymptotic stability also if the rope length is kept constant ($\dot{l} = 0$, pure horizontal load motion).

To obtain a more general stability result, valid whatever the sign of $\dot{l}$ is, consider the following auxiliary variable

$$w = \dot{\varphi} + c\varphi \qquad c > 0 \tag{362}$$

where c is a positive arbitrary constant.

Note that on the manifold $s_2^{'} = 0$, after an exponential transient, the rope length and its derivative will coincide with the desired values in (354) and (356), so that, by considering (357) and (359), and neglecting, by assumption, the resulting term that contains $\varphi\dot{\varphi}$, (358) can be rewritten as

$$\ddot{\varphi} = -a(\xi)\varphi - b(\xi)\dot{\varphi} \tag{363}$$

where ξ represents the actual trolley position and

$$\begin{aligned} a(\xi) &= \frac{g}{l_0 + \Gamma\xi^2} && (364) \\ & \qquad\qquad |\xi| \le X_M && (365) \\ b(\xi) &= \frac{k + 4V_0\Gamma\xi}{l_0 + \Gamma\xi^2} && (366) \end{aligned}$$

In the new w-φ coordinates, (358) can be rewritten as

$$\begin{cases} \dot{\varphi} = -c\varphi + w \\ \dot{w} = -\left[b(\xi) - c\right] w + \left[\gamma(\xi) - a(\xi)\right] \varphi \end{cases} \tag{367}$$

where

$$\gamma(\xi) = c(b(\xi) - c) \tag{368}$$

Trivially, the asymptotic stability of system (367)-(368) implies that of system (358).

Define the following Lyapunov candidate function

$$V(\varphi, w) = \frac{1}{2}\varphi^2 + \frac{1}{2}w^2 \tag{369}$$

whose derivative $\dot{V}$ is a quadratic form of the type

$$\dot{V}(\cdot) = -[\varphi\ ,\ w]^T \mathbf{M}(\xi)[\varphi\ ,\ w] \tag{370}$$

where

$$\mathbf{M}(\xi) = \begin{bmatrix} c & -\frac{\gamma(\xi)-a(\xi)+1}{2} \\ -\frac{\gamma(\xi)-a(\xi)+1}{2} & b(\xi) - c \end{bmatrix} \tag{371}$$

In order to ensure that the matrix $\mathbf{M}(\xi)$ is positive definite, the inequality

$$4\gamma(\xi) > \left[\gamma(\xi) - a(\xi) + 1\right]^2 \tag{372}$$

must be verified for each admissible value of ξ.

Note that the parameter c is absolutely fictitious, as it appears only in the stability proof and does not affect in any way the structure of the sliding manifold and of the controller.

Moreover, note also that, thanks to the introduction of such artificial parameter, the stability analysis of the time-varying system (358) can be easily performed by means of a Lyapunov function that does not contain explicitly the time varying parameters.

After some algebraic manipulations, the solution of (372) can be derived as

$$g_1(\xi) < \gamma(\xi) < g_2(\xi) \tag{373}$$

where

$$\begin{aligned} g_1(\xi) &= a(\xi) + 1 - 2\sqrt{a(\xi)} \\ g_2(\xi) &= a(\xi) + 1 + 2\sqrt{a(\xi)} \end{aligned} \tag{374}$$

The limiting curves $g_1(\xi)$ and $g_2(\xi)$ (reported in fig. 5for $l_0 = 10cm$ and $\Gamma = 1m^{-2}$), depend only on the reference path, while the actual crane parameters do not enter in this stability test.

By acting on k and c, the curve $\gamma(\xi)$ must be "*shaped*" in order to lie within the limiting curves $g_1(\xi)$ and $g_2(\xi)$ in the domain of interest. Note that, as ξ tends to $\pm\infty$, $\gamma(\xi)$ tends to $-c^2$, while $g_1(\xi)$ and $g_2(\xi)$ tend to the unity. This means that the domain of stability will be always a finite open interval (fig. 5).

The product kc defines the shape of $\gamma(\xi)$ for "small" values of $|\xi|$, and by varying kc the curve moves in the vertical direction. In Fig. 47 it is shown that different curves $\gamma(\xi)$, obtained for different values of c and k while their product is kept constant, are almost coincident.

The effect on $\gamma(\xi)$ of reducing c, while keeping constant ck, is evident only far from the origin, and traduces in "pulling up" the curve. This can be used to enlarge the domain of solution of the inequality. The price to be payed is a reduced rate of decay for the swing angle.

As a design example, consider a desired path defined by $l_0 = .1m$, $\Gamma = 1m^{-1}$ and $X_M = 3$, and let the reference horizontal speed be $V_0 = 10cms^{-1}$.

First of all, we choose the product ck to place the maximum of $\gamma(\xi)$ (i.e. $\gamma(0)$) approximately at the medium between $g_1(0)$ and $g_2(0)$. Choosing $c = 0.6$ and $k = 16.65$ ($ck \approx 10$) one obtains the behaviour in Fig. 48 . Note that the actual curve $\gamma(\xi)$ is entirely contained between the limiting curves in the domain of interest $|\xi| \leq 3$.

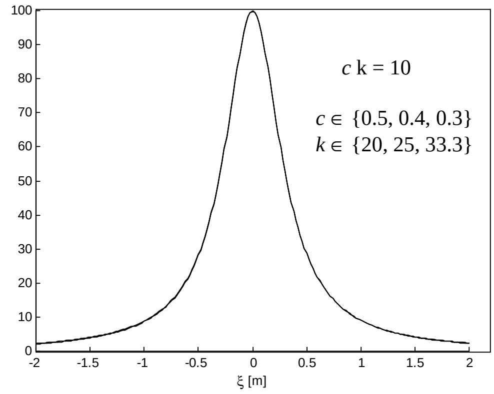

Figure 47: Different curves $\gamma(\xi)$ with the same value of the product ck.

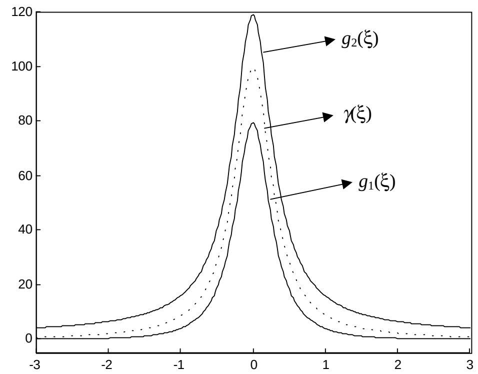

Figure 48: $c = 0.6$ and $ck = 10$. The actual curves.

8.3.2 The arrival phase

As for the stabilization of the load around the desired final location, we use a different sliding manifold, which is only devoted to a regulation task and relaxes any tracking objective.

Consider the following sliding outputs

$$\begin{array}{l} s_1^{''} = \dot{x}_t + c_1(x_t - x_f) - k_a\varphi \\ s_2^{''} = \dot{l} + c_2(l - y_f) \end{array} \tag{375}$$

where k, c_1 and c_2 are positive constants and x_f, y_f represent the final, desired, location. Following the same procedure as in the previous subsection 3.1, it is not difficult to derive the expression for the system zero dynamics as

$$\dot{x}_t = -c_1(x_t - x_f) + k_a\varphi \tag{376}$$

$$\dot{l} = -c_2(l - y_f) \tag{377}$$

$$\ddot{\varphi} = -\frac{g - c_1 k_a}{y_f}\varphi - \frac{k_a}{y_f}\dot{\varphi} \tag{378}$$

Around the final location, the swing dynamics is linear and stationary, and choosing

$$k_a \in (0, \frac{g}{c_1}) \tag{379}$$

the asymptotic stability is trivially guaranteed.

It would be desirable to keep constant the value of k in both the traveling and arrival phases. To this aim, one can choose k according to the stability requirements relevant to the traveling phase, and then it is sufficient to set c_1 sufficiently small to include the chosen k in the stability domain (379).

8.4 A multi-input second-order sliding mode controller

In this section it is shown that the problem of steering the system motion on the desired manifold can be solved, both in the travel phase and in the arrival phase, by means of a recently-proposed multi-input second order sliding-mode control strategy [5].

Let $\mathbf{q}_m = [x_t \ \dot{x}_t \ l \ \dot{l} \ \varphi \ \dot{\varphi}]$ the state vector for the mechanical subsystem, and let $\mathbf{q} = [q_m^T \ t^T]$ be the state vector for the whole electromechanical plant. Moreover, let $\mathbf{p}_m$ be the column vector containing the mechanical parameters and $\mathbf{p}_e$ that containing the electrical ones, and define $\mathbf{p} = [p_m^T \ p_e^T]$.

Successive differentiation of (355) and (375) yield

$$\begin{array}{ll} \textit{Travel phase} & \textit{Arrival phase} \\ \dot{\mathbf{s}}^{'} = \mathbf{F}_1^{'}(\mathbf{q}_m, \mathbf{p}_m) + \mathbf{G}(\mathbf{q}_m, \mathbf{p}_m)t & \dot{\mathbf{s}}^{''} = \mathbf{F}_1^{''}(\mathbf{q}_m, \mathbf{p}_m) + \mathbf{G}(\mathbf{q}_m, \mathbf{p}_m)t \\ \ddot{\mathbf{s}}^{'} = \mathbf{F}_2^{'}(\mathbf{q}, \mathbf{p}) + \Pi_1^{-1}\mathbf{G}(\mathbf{q}, \mathbf{p})v & \ddot{\mathbf{s}}^{''} = \mathbf{F}_2^{''}(\mathbf{q}, \mathbf{p}) + \Pi_1^{-1}\mathbf{G}(\mathbf{q}, \mathbf{p})v \end{array} \tag{380}$$

where $\mathbf{s}^{'} = [s_1^{'} \;\; s_2^{'}]^T$, $\mathbf{s}^{''} = [s_1^{''} \;\; s_2^{''}]^T$, $\mathbf{F}_i^{'}(\cdot)$ and $\mathbf{F}_i^{''}(\cdot)$, $i = 1, 2$, are uncertain vector fields and

$$\mathbf{G}(\mathbf{q}, \mathbf{p}) = \frac{1}{A_1 A_2 - Mb_1 - MJcos^2(\varphi)} \begin{bmatrix} A_2 & -Mb_2 sin(\varphi) \\ -Mb_1 sin(\varphi) & A_1 - Mb_2 cos^2(\varphi) \end{bmatrix} \tag{381}$$

is also uncertain but can be easily shown to be sufficiently dominant diagonal. This fact, according to [5], is sufficient to express the multi-input control problem in a set of suitable, almost decoupled, single-input second-order sliding mode control problems, without involving any observer.

Furthermore, it is not difficult to verify that, if the reference path is sufficiently smooth, the uncertain vectors $\mathbf{F}_i^{'}(\cdot)$ and $\mathbf{F}_i^{''}(\cdot)$ $(i = 1, 2)$ are norm-bounded in any bounded domain. This means that, given any compact domain of interest in the state space, constant upperbounds $\overline{F}_i^{'}$ and $\overline{F}_i^{''}$ can be found such that

$$\begin{array}{ll} \|\mathbf{F}_i^{'}(\cdot)\| \leq \overline{F}_i^{'} & i = 1, 2 \\ \|\mathbf{F}_i^{''}(\cdot)\| \leq \overline{F}_i^{''} & i = 1, 2 \end{array} \tag{382}$$

Therefore, both in the travel phase and in the arrival phase, the sliding variable dynamics can be stabilized by means of the sub-optimal second order sliding mode controller [1, 2].

The resulting control strategy consists of two stages, since the actual sliding manifold is modified after the final location has been sufficiently approached according to the stability conditions detailed in Sect. 3.1.

The control can be set as

$$v_i = -\beta_i^{'}(t) V_i^{'} \operatorname{sign}(s_i^{'}(t) - \frac{1}{2} s_i^{'}(T_{M_{ki}}^{'})) \qquad i = 1, 2 \tag{383}$$

until $|x_t - x_f| > \Sigma$, where the positive constant Σ represents the distance from the final position, $s_i^{'}$ is defined in (354)–(355), and $T_{M_{ki}}^{'}$ are the time instants at which $\dot{s}_i^{'}$, $(i = 1, 2)$, is zero, $V_i^{'}$, $(i = 1, 2)$, are proper constants [5] and

$$\beta_i^{'}(t) = \begin{cases} \beta_i^{'*} & if \;\; s_i^{'}(T_{M_{ki}}^{'})(s_i^{'}(t) - \frac{1}{2} s_i^{'}(T_{M_{ki}}^{'})) > 0 \\ 1 & if \;\; otherwise \end{cases} \tag{384}$$

where $\beta_i^{'*}$, $(i = 1, 2)$, are proper constants [5]. After the vicinity $|x_t - x_f| \leq \Sigma$ has been reached, the arrival phase is activated, and the definition of the sliding variable is modified according to (375), where the positive coefficient c_1 is chosen sufficiently small to include the actual value of k within the stability domain (379). The resulting control strategy has still the form (383)-(384), but considering $s_i^{''}(t)$, $V_i^{''}$, $\beta_i^{''}(t)$ and $T_{M_{ki}}^{''}$ instead of $s_i^{'}(t)$, $V_i^{'}$, $\beta_i^{'}(t)$ and $T_{M_{ki}}^{'}$, respectively.

The implementation of such controller guarantees the robust tracking of the desired path, and, at the same time, the damping of the load oscillations during the whole load travel.

8.5 Implementation Issues and Experimental Results

First of all refer to a picture of the crane prototype (Fig. 54) and to a schematic diagram of the digital experimental setup (Fig. 55).

The digital implementation of the proposed control scheme has been tested on a laboratory-sized prototype built for experimental investigations. The sub-optimal second order SMC algorithm has been shown to be robust against the sample-and-hold effect [3], so that the feasibility of the digital implementation of the control law does not require further investigations. A sampling period of $T_s = .002s$ was used, and the acquired data have been on-line stored in the memory of the PC and then off-line processed to make the graphics.

A load with mass of about 1 Kg is moved with a parabolic reference trajectory. The trolley and rope velocities have been estimated by using real-time numerical differentiators based on second order sliding modes [4]. A smooth transition between the travel phase and the arrival phase must be performed to preserve the sliding behaviour. In Figures 49 and 50 the actual load coordinates, and the swing angle versus time, are depicted, respectively. In a second experiment, an initial oscillation is intentionally introduced, and the proposed controller has been implemented usinf different values for the coefficient k, that corresponds to a "feedback gain" for the swing angle.

In particular, in a first test no-feedback action is performed on the swing angle ($k = 0$, see Figure 51). Note that the oscillations propagates through the whole transfer of the load until the destination point. Then, increasing values of k have been used and the oscillation is damped faster and faster until the stability bound defined in section 8.3.2 is overcame. Using $k = 80$, the actual trajectory remains close to the desired one, and the oscillation disappears before the vertex of the actual trajectory is reached ($k = 0$, see Figure 52). In Figure 53 (corresponding to the use of $k = 640$) it is evident the unstable behaviour of the swing angle in a vicinity of the destination point.

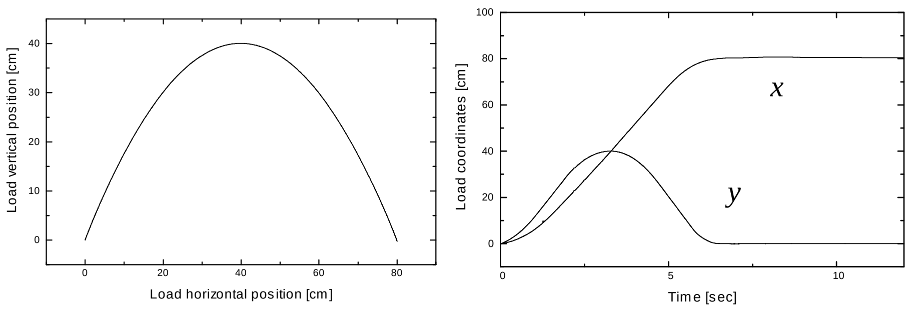

Figure 49: The actual and reference load coordinates.

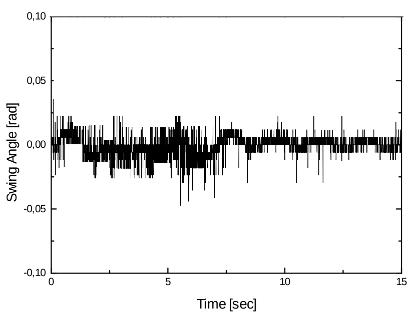

Figure 50: The actual swing angle.

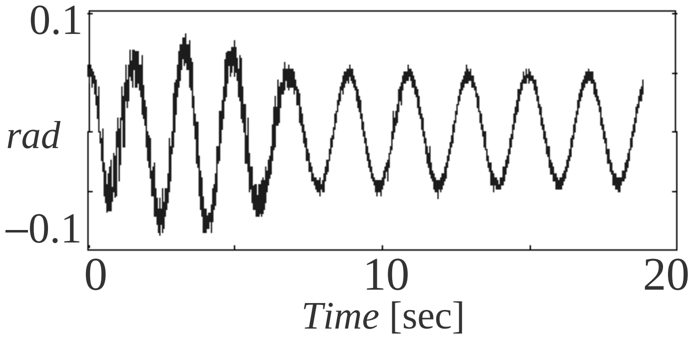

Figure 51: k=0. The propagation of the load oscillation.

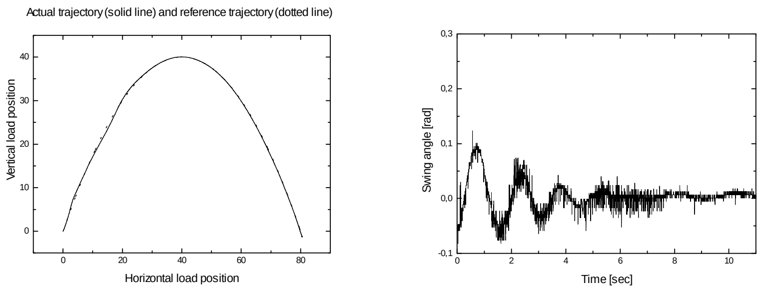

Figure 52: k=80. The actual and reference load coordinates and the load swing.

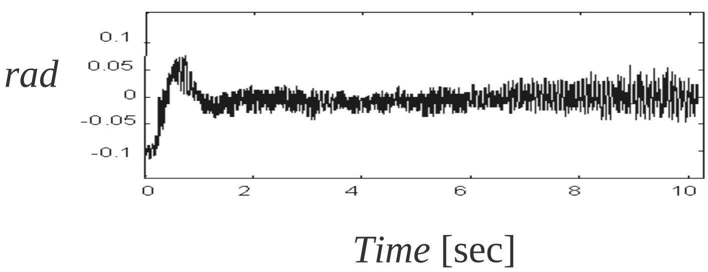

Figure 53: k=640. The unstable behaviour of the swing angle.

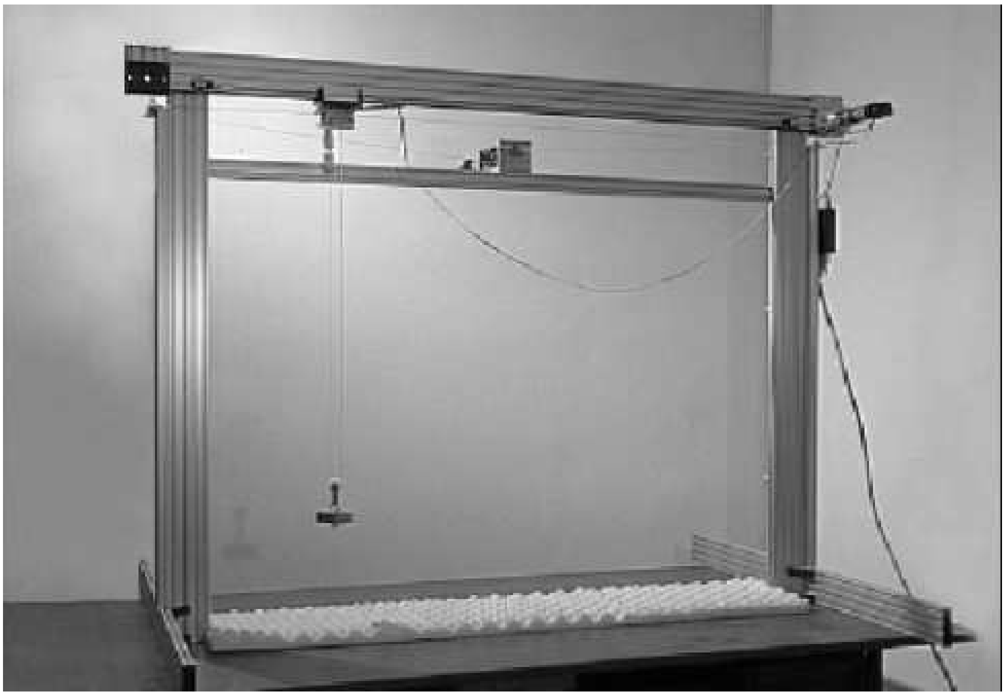

Figure 54: Picture of the crane prototype.

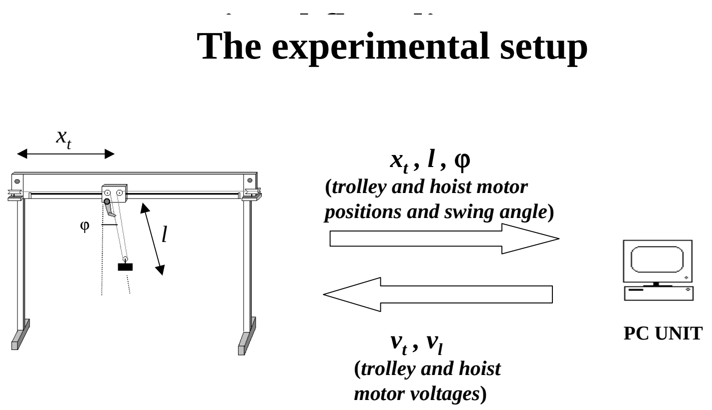

Figure 55: Schematic Diagram of the experimental setup

8.6 Conclusions

The problem of moving a suspended load using a container crane has been addressed and solved by sliding-mode techniques. A suitable sliding manifold has been defined such that the system motion, when constrained on such manifold, satisfy the control objectives, i.e. fast and accurate load transfer and damping of the swing, both during the movement and at the end of the transportation. The explicit dependence of the sliding manifold on the swing angle, that guarantees the stability of the system's zero dynamics, constitutes the main novelty of the present approach. The use of the second order SMC methodology allows to take into account the unmodeled actuator dynamics, often neglected by other methodologies. Experimental investigations confirm the good performance of the proposed method.

References

[Auernig and Troger '87] J.W. Auernig and H. Troger, "Time Optimal Control of Overhead Cranes with Hoisting of the Load" *Automatica*, 23, 3, 437-447, 1987.

[1] G. Bartolini, A. Ferrara and E. Usai, "Chattering Avoidance by Second Order Sliding Mode Control", *IEEE Trans. on Automatic Control*, vol. 43, no. 2, 241–246, 1998.

[2] G. Bartolini, A. Ferrara, A. Levant and E. Usai, "On Second Order Sliding Mode Controllers", in *Variable Structure Systems, Sliding Mode and Nonlinear Control*, K.D. Young and U. Ozguner (Eds.), Lecture Notes in Control and Information Sciences, Springer-Verlag, vol. 247, 329–350 , 1999.

[3] G. Bartolini, A. Pisano, E. Usai "Variable Structure Control of Nonlinear Sampled Data Systems by Second Order Sliding Modes", in *Variable Structure Systems, Sliding Mode and Nonlinear Control*, K.D. Young and U. Ozguner (Eds.), Lecture Notes in Control and Information Sciences, Springer-Verlag vol. 247, 43-68, (1999).

[4] G. Bartolini, A. Pisano and E. Usai, "First and Second Derivative Estimation by Sliding Mode Technique" Journal of Signal Processing, 4, 2, 167–176, 2000.

[5] G. Bartolini, A. Ferrara, E. Usai and V.I. Utkin "On Multi-input second order sliding mode control", *IEEE Trans. Aut. Contr.*, 45, 9, 1711-1717, 2000.

[6] J.W. Beeston, "Closed-loop time optimal control of a suspended load: a design study", *Proc. 4th IFAC World Congress*, pp. 85-99, 1969.

[7] G. Corriga, A. Giua and G. Usai, "An Implicit gain-Scheduling Controller for Cranes", *IEEE Trans. on Contr. Syst. Technology*, 6, 1, 15–20, 1998.

[8] A. Giua, C. Seatzu, G. Usai,"Observer-controller design for cranes via Lyapunov equivalence", *Automatica*, 35, 4, 669–678, 1999.

[9] A. Isidori, *Non Linear Control Systems*, Springer Verlag, Berlin, 1989.

[10] J.J. Hamalainen, A. Marttinen, L. Baharova and J. Virkkunen, "Optimal path planning for a trolley crane: fast and smooth transfer of the load". *IEE Proc. Control Theory Appl.*, 142, 1, 51–57, 1995.

[11] J. La Salle and S. Lefschetz, *Stability by Liapunov's Direct Method*, Academic Press, London, 1961.

[12] A. Levant, "Sliding order and sliding accuracy in sliding mode control", *Int. J. of Control*, vol. 58, pp. 1247–1263, 1993.

[13] J. Lévine, "Are there new industrial perspectives in the control of mechanical systems ?", *Advances in Control - Highlights of ECC99*, Paul M. Frank (Ed.), Springer-Verlag, London, 1999.

[14] K. Moustafa and A.M. Ebeid "Nonlinear Modeling and Control of Overhead Crane Load Sway", *J. of Dyn. Syst. Meas. and Contr., Trans. ASME*, vol. 110, pp. 266–271, 1988.

[15] A. Sakawa and Y. Shindo "Optimal Control of container cranes", *Automatica*, vol. 18, No.3, pp. 257–266, 1982.

[16] J.J.E.Slotine, W. Li *Applied Nonlinear Control*, Prentice–Hall International, Englewood Cliffs, New Jersey, 1991.

[17] V.I. Utkin, *Sliding Modes In Control And Optimization*, Springer Verlag, Berlin, 1992.

[18] J. Virkkunen et al., "Computer control of overhead and gantry cranes", *Proc. 11th IFAC world congress*, Tallinn, Estonia, USSR, 401–405, 1990.

[19] J. Virkkunen et al., "Adaptive pole-placement control of a pilot crane", *Proc. 11th IFAC world congress*, Tallinn, Estonia, USSR, 313-318, 1990.

[20] A.S.I. Zinober, "The self-adaptive control of overhead crane operations". *Proc. 5th IFAC Symp. On System Parameters Identification*, Darmstad, 1161–1167, 1979.

[21] A.S.I. Zinober and A.T. Fuller, "The sensitivity of nominally time-optimal control systems to parameter variation", *Int.J. of Control*, 17, 673-703, 1973.